DUBNA 2009

Tunneling in superconducting structures.

Yu.M.Shukrinov
BLTP, JINR, Dubna, , Russia

Plan of presentation:

- **Lecture 1.**
- **Tunneling in superconducting structures. Intrinsic Josephson effect. CCJJ and CCJJ+DC models.**

- **Lecture 2.**
- **Breakpoint in CVC of Layered Superconductors.**

- **Lecture 3.**
- **Fine Structure of the Breakpoint Region. Temperature Dependence of the Breakpoint Current**

Breakpoint in CVC

$$\frac{d^2}{dt^2}\varphi_l = (I - \sin\varphi_l - \beta\frac{d\varphi_l}{dt})$$

$$+\alpha(\sin\varphi_{l+1} + \sin\varphi_{l-1} - 2\sin\varphi_l)$$

$$+\alpha\beta(\frac{d\varphi_{l+1}}{dt} + \frac{d\varphi_{l-1}}{dt} - 2\frac{d\varphi_l}{dt})$$

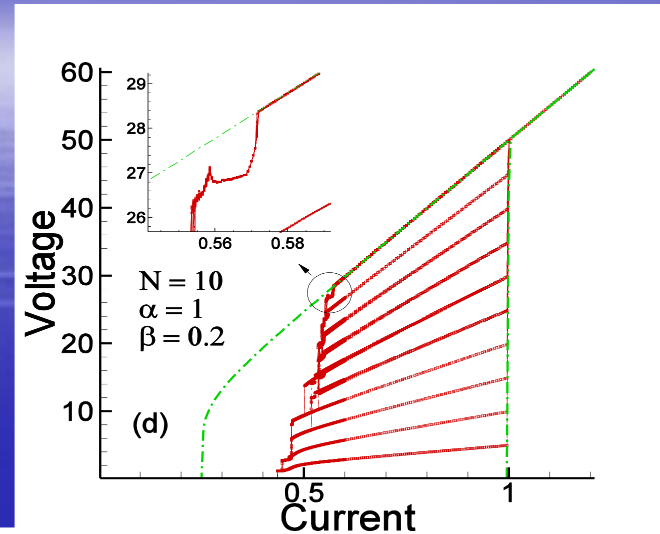

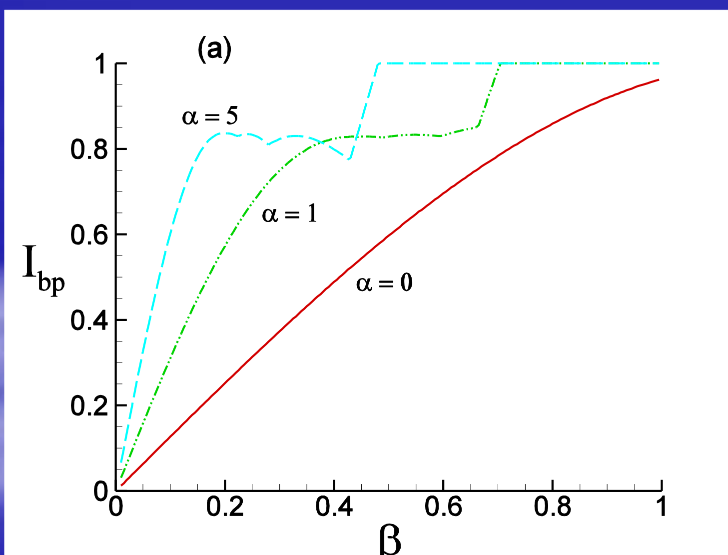

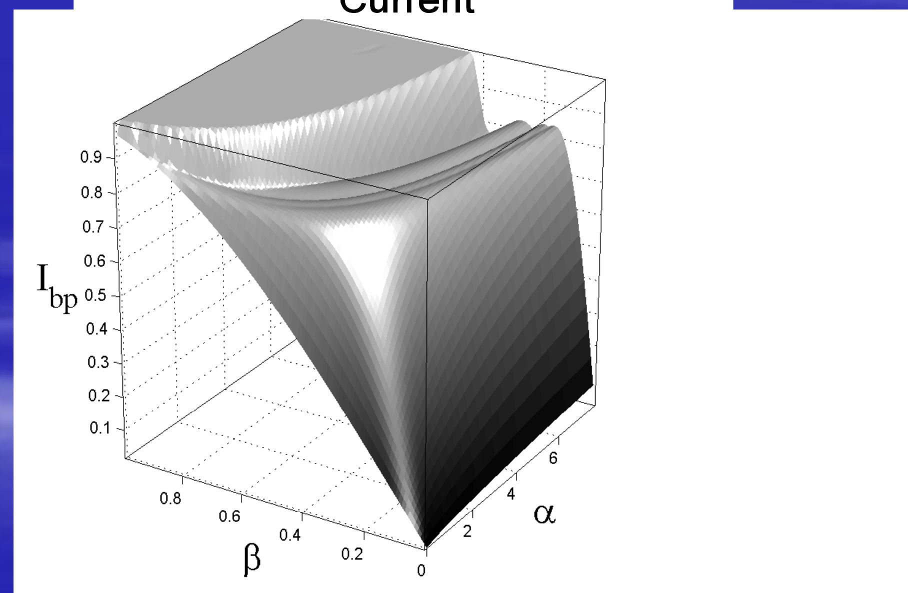

Shukrinov, F. Mahfouzi, PRL 98 (2007) 157001

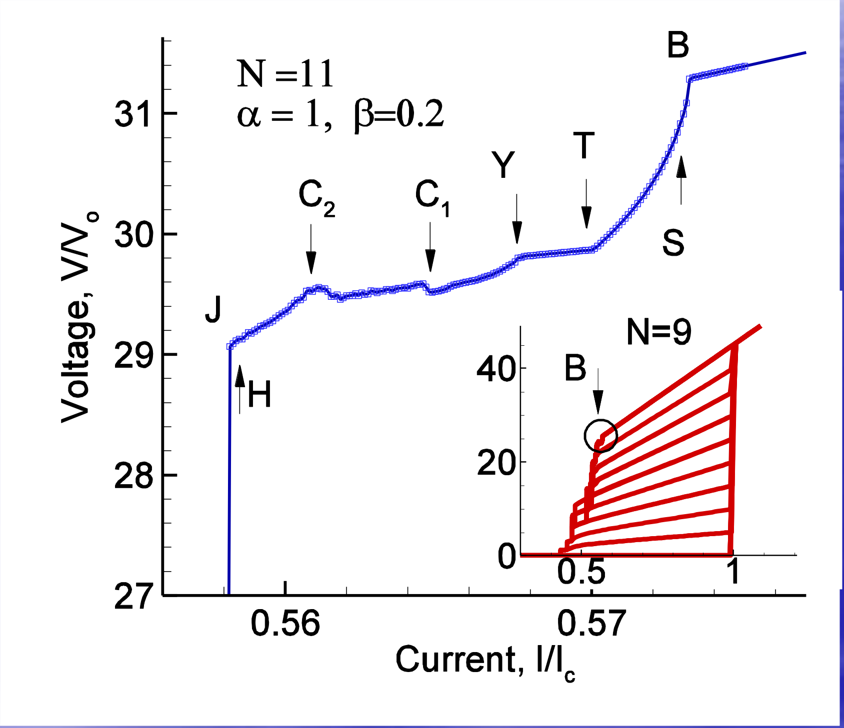

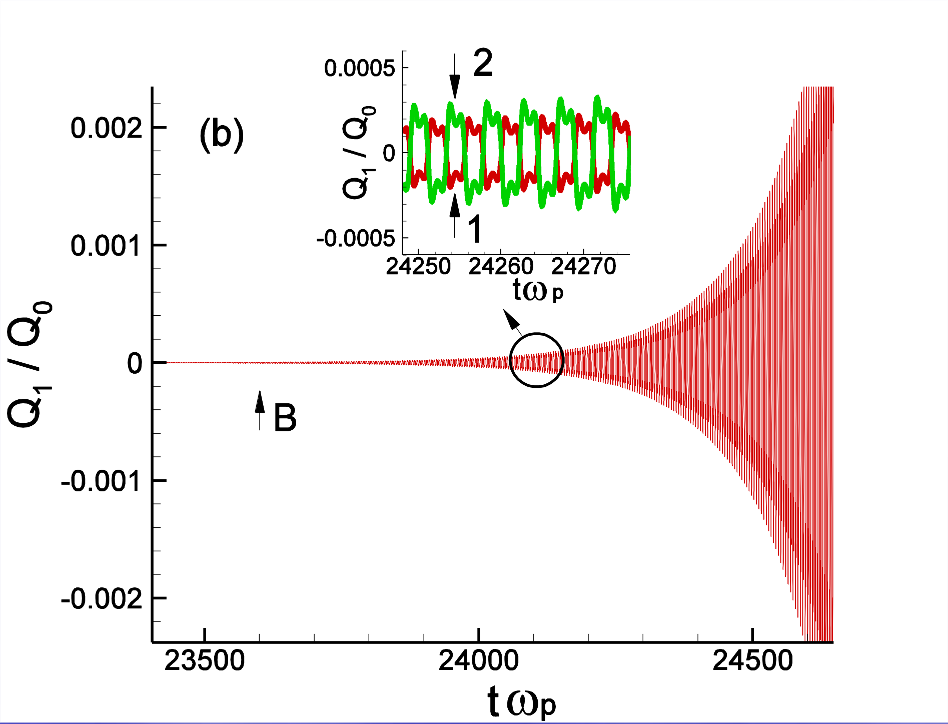

Yu.Shukrinov, F. Mahfouzi, M.Suzuki PRB 78 (2008) 134521

Layered $Bi_2Sr_2CaCu_2O_y$(Bi2212) single crystals represent natural stacks of atomic scale intrinsic Josephson junctions.

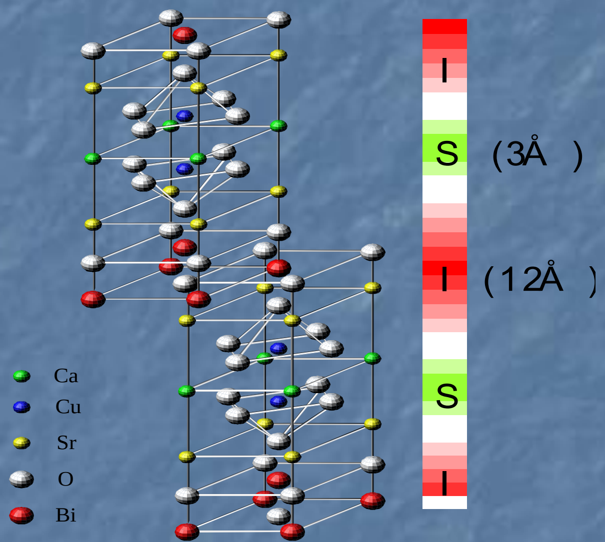

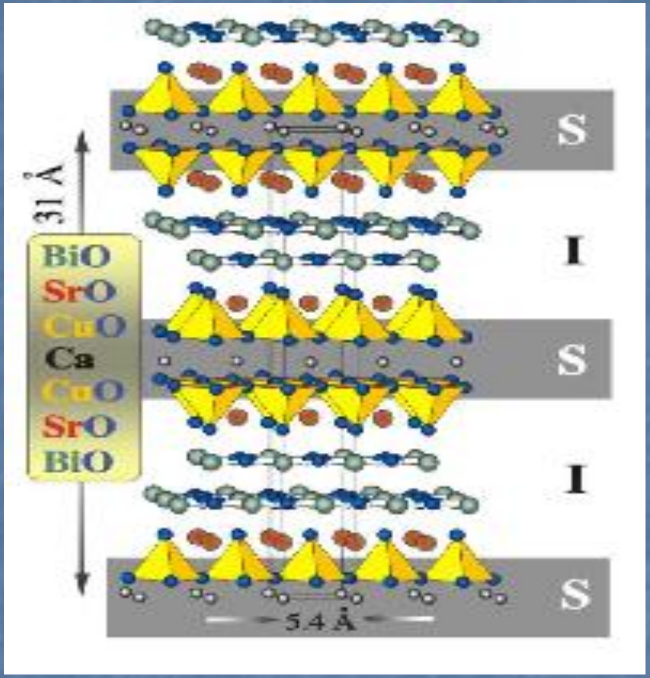

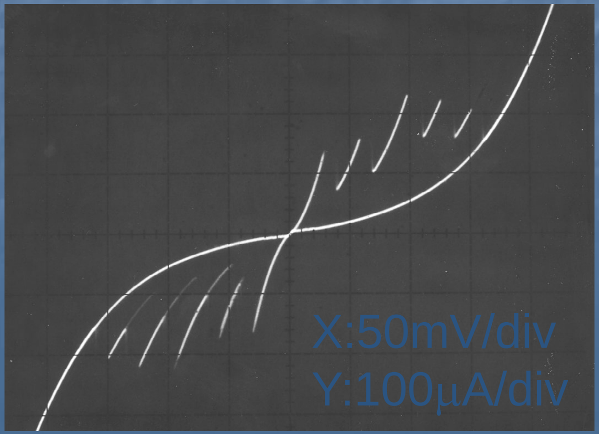

I-V characteristics

– Multi-branch structure
– large hysteresis
– Roughly equal spacing

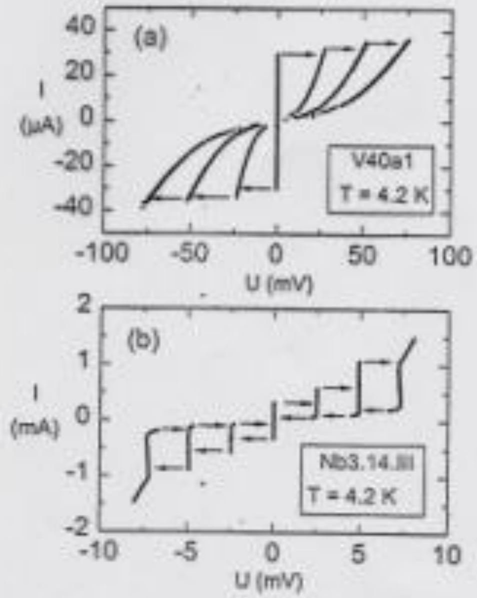

FIG. 2. (a) First three branches of the I-V characteristic of a $Tl_2Ba_2Ca_2Cu_3O_{10+\delta}$ step stack with a total number of 130 junctions: (b) I-V characteristics of an artificial three-junction Nb/Al-AlO_x/Nb stack. Arrows indicate voltage switching.

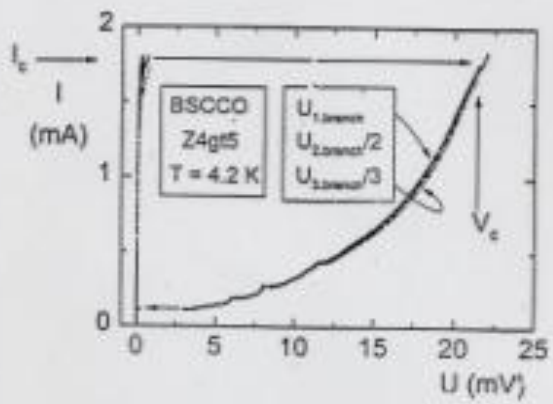

FIG. 3. Comparison of the first three branches of the I-V characteristic of a BSCCO mesa. The voltages of the second (third) branch have been divided by two (three).

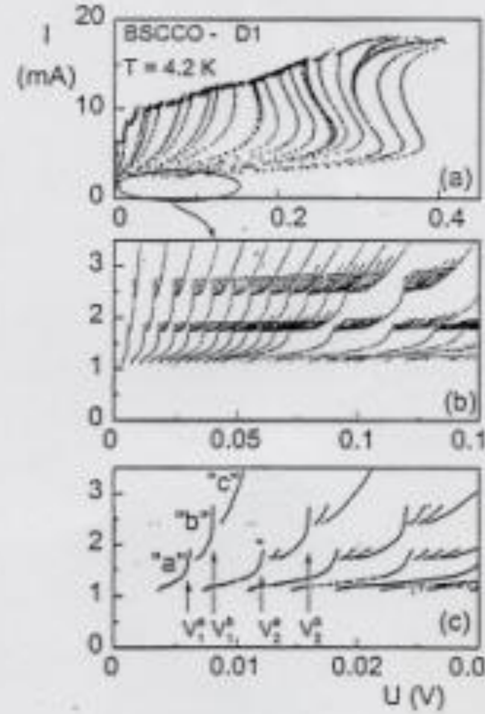

FIG. 10. (a) I-V characteristic of a BSCCO mesa at $T = 4.2$ K. Not all branches are traced out. With increasing number of resistive junctions, heating effects cause a backbending of the I-V curve. (b) Enlargement of the region indicated in (a) showing the extremely regular structures in all branches. (c) The same data on an expar scale with the sub-branch-s a, b, and c and the structure vo V_1^a, V_1^b, V_2^a, and V_2^b marked.

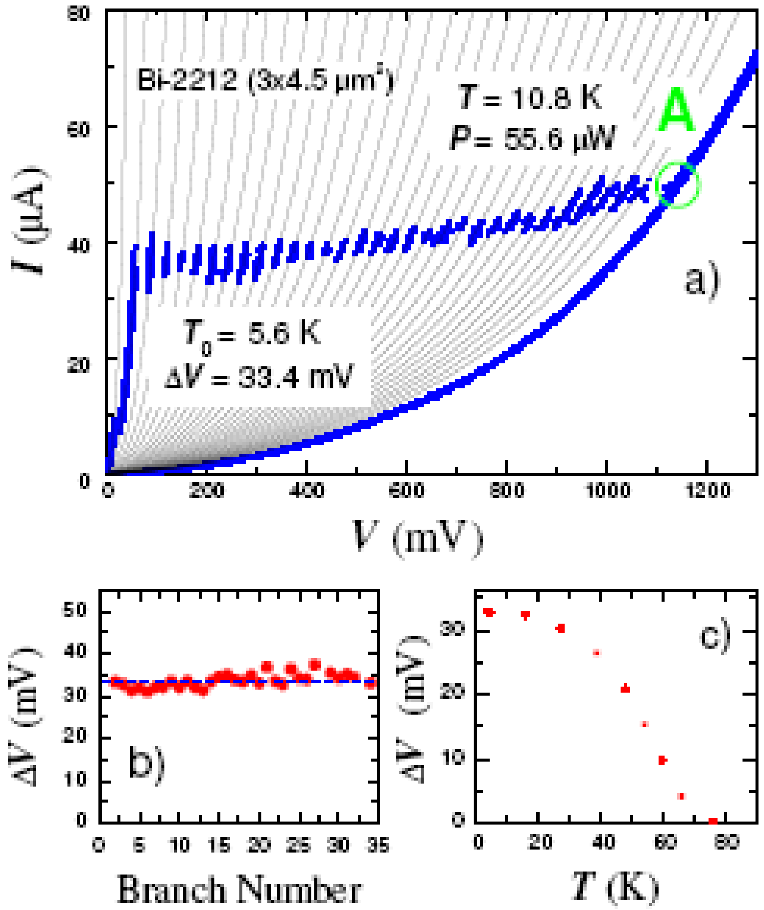

FIG. 2: (color) a) The IVC of a small underdoped Bi-2212 mesa at $T_0 = 5.6K$. Thin lines are multiple integers of the last branch divided by $N = 34$ and demonstrate perfect periodicity of the branches. Panels b) and c) show the voltage jumps between branches as a function of the branch number and the base temperature, respectively.

V.Krasnov, Phys.Rev.B 72 (2005) 094503

Pancake stacks

$Bi_2Sr_2CaCu_2O_{8+\delta}$
(BSCCO)
$T_c \approx 90$ K

Artemenko&Kruglov 1990, Buzdin&Feinberg 1990, Clem 1991

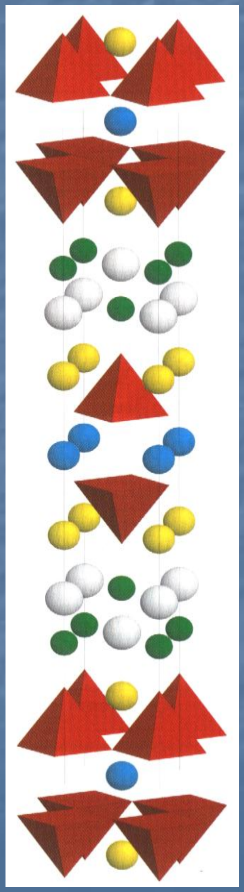

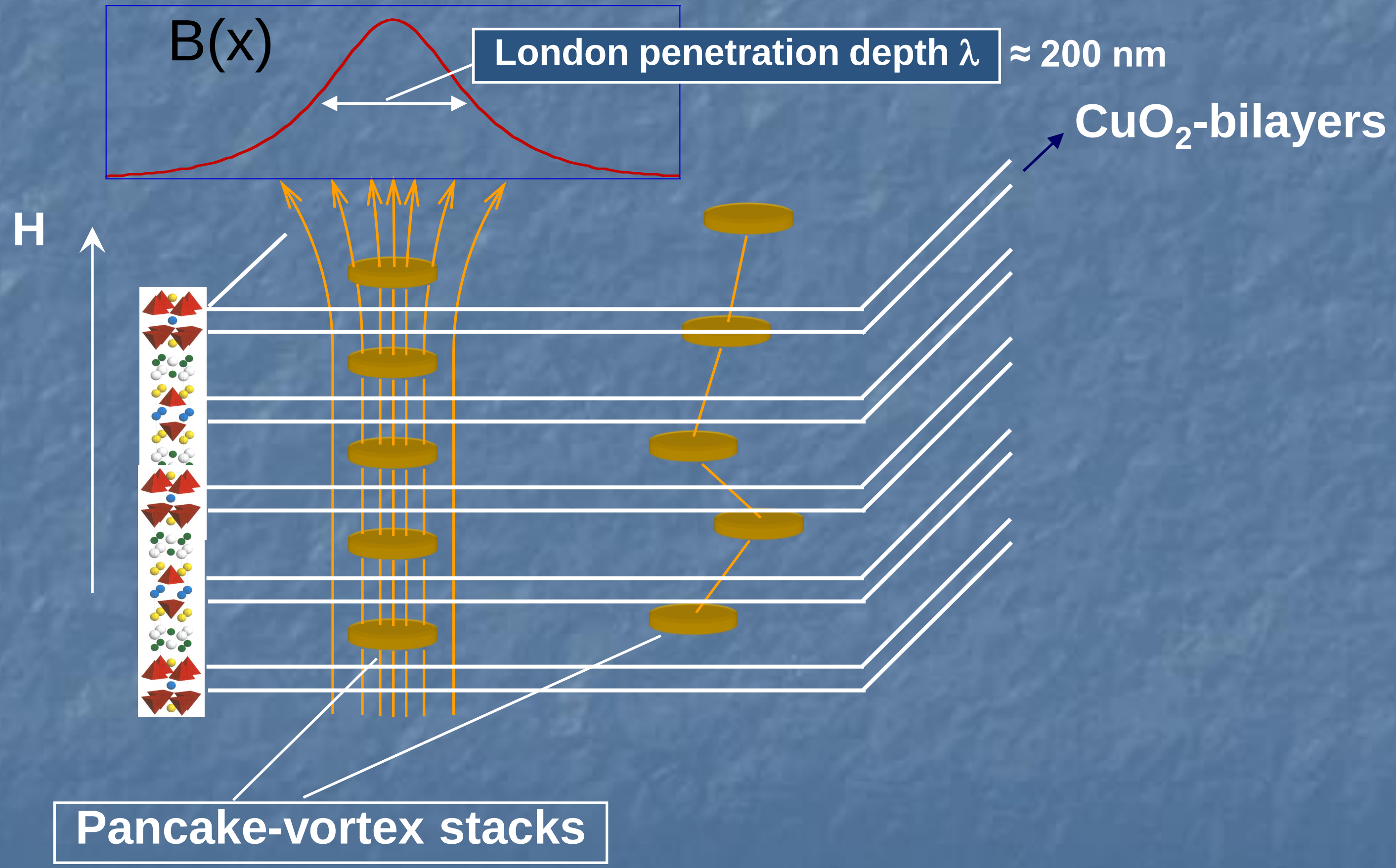

Fluxon in long junction

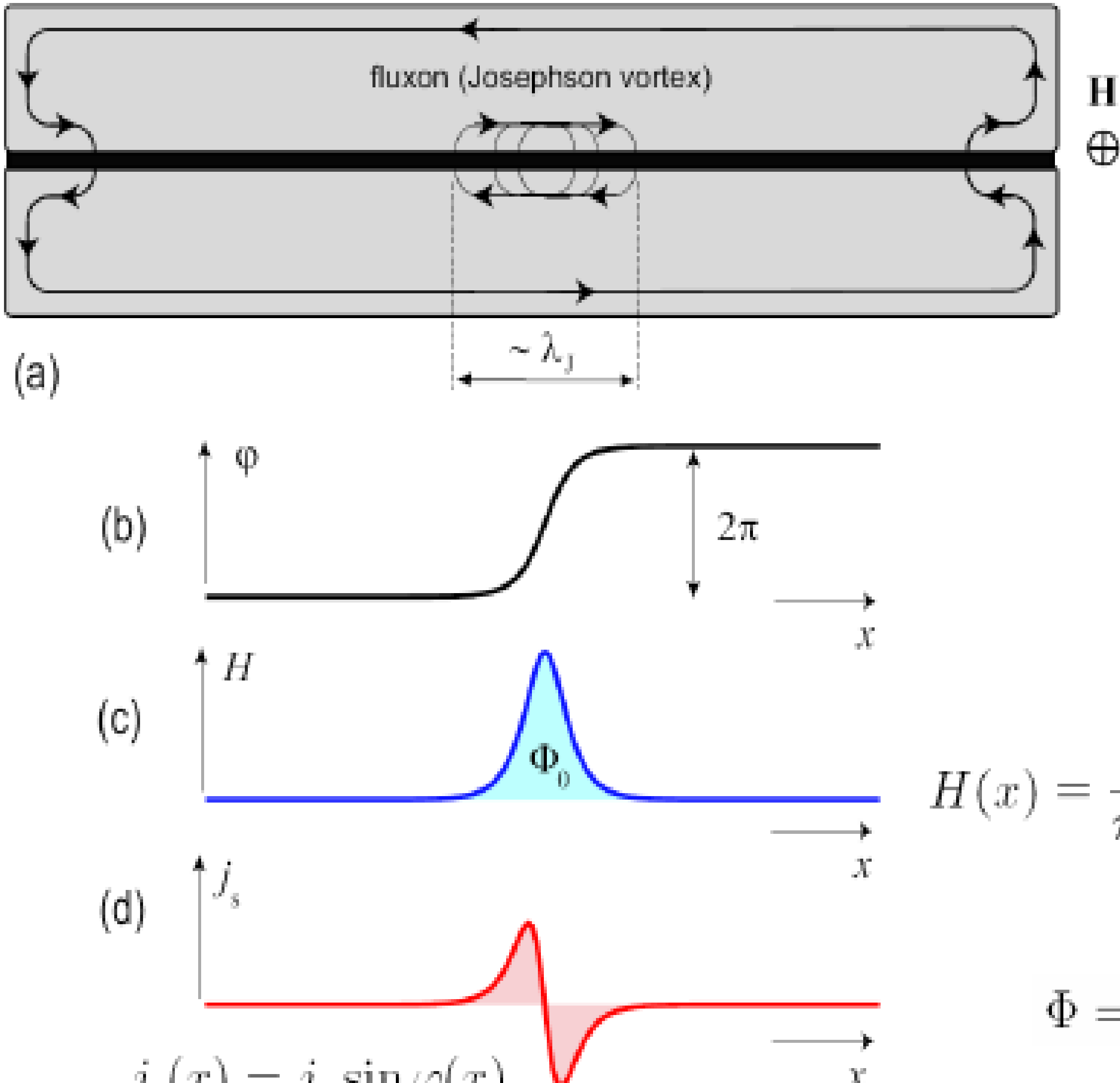

$$j_s(x) = j_c \sin\varphi(x)$$

$$\frac{d^2\varphi}{dx^2} = \frac{1}{\lambda_J^2}\sin\varphi$$

there is an exact solution

$$\varphi(x) = 4\arctan\left[\exp\frac{x - x_0}{\lambda_J}\right]$$

corresponding to a fluxon

$$H(x) = \frac{\Phi_0}{\pi\mu_0\Lambda\lambda_J}\,\frac{2\exp\left[(x - x_0)/\lambda_J\right]}{1 + \exp\left[2(x - x_0)/\lambda_J\right]}$$

$$\Phi = \frac{\Phi_0}{2\pi}\int_{-\infty}^{+\infty}\frac{d\varphi(x)}{dx}dx = \Phi_0$$

Macroscopic Quantum Tunneling

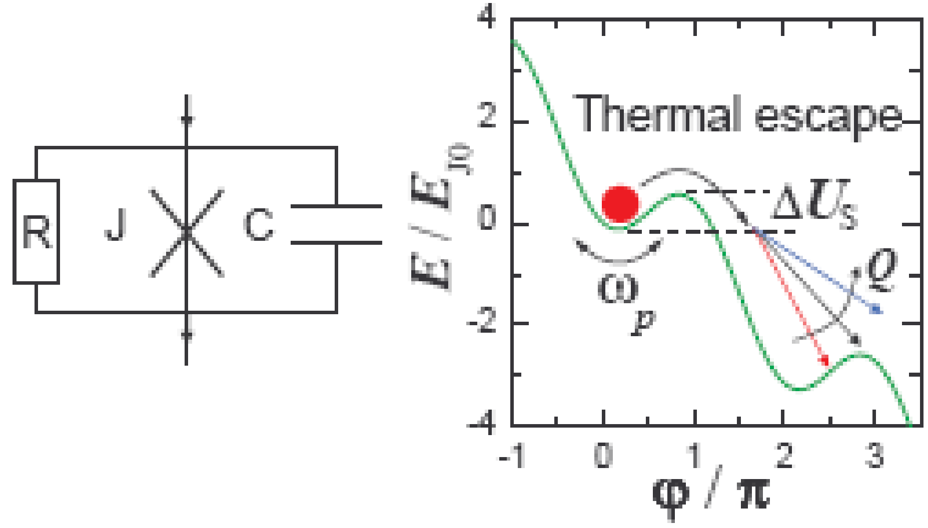

FIG. 1: (Color online). Left: the equivalent circuit of the RCSJ model. Right: the mechanical analog of the RCSJ model: the tilted wash board potential in the energy-phase space for $I = 0.5I_{c0}$. Arrows indicate three possible particle trajectories after thermal escape for different quality factors. For the lowest Q the particle get's retrapped in the next potential well, while for highest Q it will continue to roll down the potential, leading to switching of the JJ from the superconducting to the resistive state.

Macroscopic Quantum Tunneling

The TA escape rate

$$\Gamma_{TA} = a_t \frac{\omega_p(I)}{2\pi} \exp\left[-\frac{\Delta U_S(I)}{k_B T}\right]$$

$\Delta U_S \simeq (4\sqrt{2}/3) E_{J0} [1 - I/I_{c0}]^{3/2}$ where $E_{J0} = (\hbar/2e) I_{c0}$ is the Josephson energy.

$a_t = (1 + 1/4Q^2)^{1/2} - 1/2Q.$ $Q_0 = \omega_{p0} RC = \sqrt{2eI_{c0}R^2C/\hbar}.$

The MQT escape rate

$$\Gamma_{MQT} = \gamma(T) \frac{\omega_p}{2\pi} \left[\frac{\Delta U_S}{\hbar \omega_p}\right]^{1/2} \chi(Q) \exp\left[-\frac{\Delta U_S}{\hbar \omega_p} s(Q)\right]$$

Here $\gamma(T)$ is the thermal correction with the characteristic parabolic dependence $\ln\gamma \propto T^2$; and in the case of strong damping $\chi(Q) \simeq 2\pi\sqrt{3} Q^{7/2} [1 - Q^2(8ln(2Q) - 4.428)]$ and $s(Q) \simeq 3\pi[Q + Q^{-1}]$.

PRL 95, 107005 (2005) PHYSICAL REVIEW LETTERS week ending 2 SEPTEMBER 2005

Macroscopic Quantum Tunneling in a *d*-Wave High-T_C $Bi_2Sr_2CaCu_2O_{8+\delta}$ Superconductor

K. Inomata,[1,2,*] S. Sato,[1] Koji Nakajima,[1] A. Tanaka,[2] Y. Takano,[2] H. B. Wang,[2] M. Nagao,[2] H. Hatano,[2] and S. Kawabata[3]

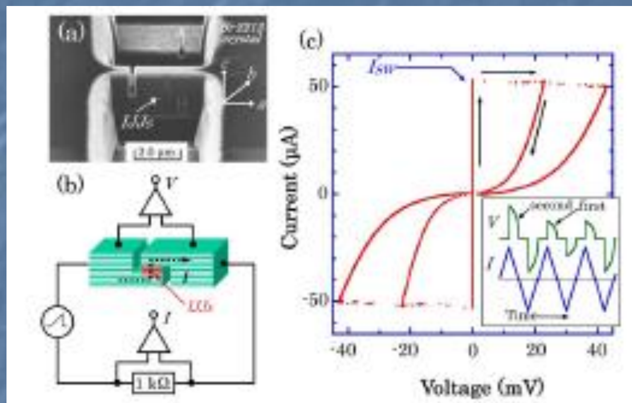

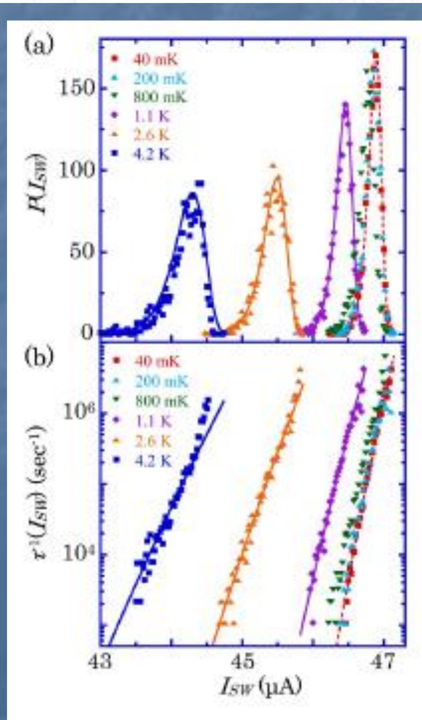

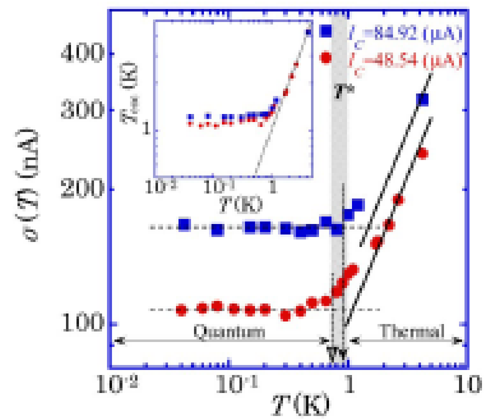

FIG. 3 (color online). Standard deviation $\sigma(T)$ of $P(I_{SW})$. $\sigma(T)$ were calculated by $\sigma = (\langle I_{SW}{}^2\rangle - \langle I_{SW}\rangle^2)^{1/2}$. The two sets of data were taken from the same sample by reducing the oxygen content. The solid lines show the theoretical fitting of the thermal region. $\sigma(T)$ starts to saturate below the crossover temperature T^* [12,27]. The experimental T^*'s of the measured samples are around 1 K, falling within the shaded crossover region calculated theoretically. The inset shows the escape temperature T_{esc} vs T. The dotted line corresponds to $T = T_{esc}$.

APPLIED PHYSICS

Filling the Terahertz Gap

A device made from a layered superconductor emits electromagnetic waves in a frequency range for which good radiation sources had been lacking.

Reinhold Kleiner

At almost every frequency, we have good methods to generate and detect electromagnetic radiation. One crucial exception is the low terahertz range, where despite intensive research there is a severe lack of devices such as oscillators and detectors. With better terahertz technology, researchers could develop new kinds of nondestructive imaging for materials testing and medical diagnosis, and carry out novel spectroscopic studies of materials and molecules.

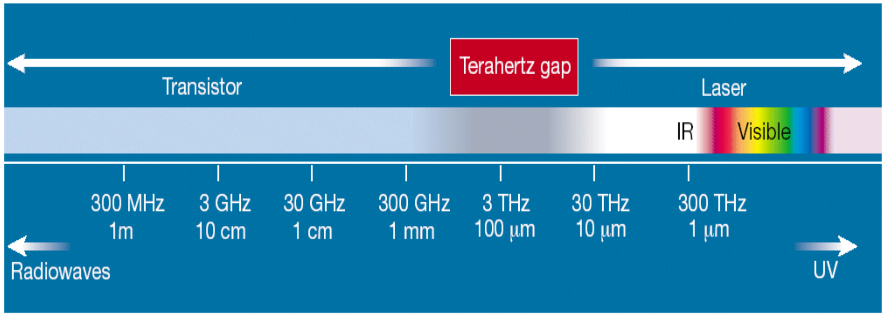

Figure 1 The terahertz gap. The gap, lying roughly between 300 GHz (0.3 THz) and 30 THz, exists because the frequencies generated by transistors and lasers, typical semiconductor devices, don't overlap. No current semiconductor technology can efficiently convert electrical power into electromagnetism in that range. But the 'heterostructure laser' produced by Köhler *et al.*[1] might, in due course, meet the demand for radiation sources at these terahertz wavelengths.

Emission of Coherent THz Radiation from Superconductors

L. Ozyuzer,[1,2] A. E. Koshelev,[2] C. Kurter,[2,3] N. Gopalsami,[4] Q. Li,[2] M. Tachiki,[5] K. Kadowaki,[6] T. Yamamoto,[6] H. Minami,[6] H. Yamaguchi,[6] T. Tachiki,[7] K. E. Gray,[2] W.-K. Kwok,[2] U. Welp[2*]

Emission of Coherent THz Radiation from Superconductors (1)

www.sciencemag.org SCIENCE VOL 318 23 NOVEMBER 2007 1291

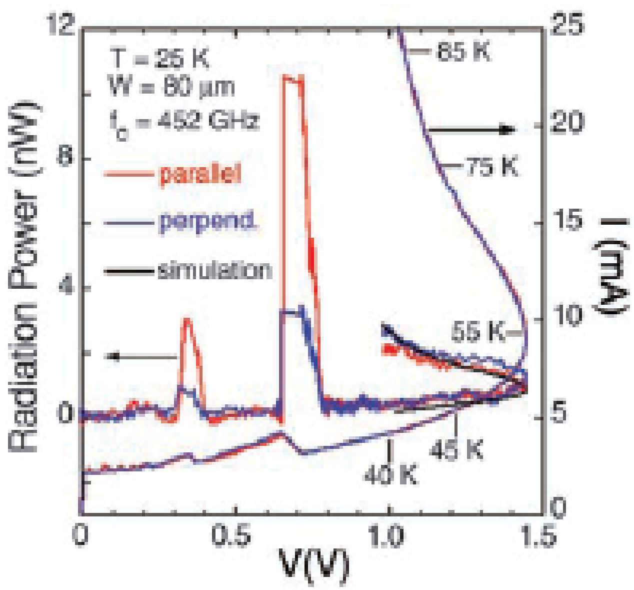

Fig. 2. Current-voltage characteristics and radiation power of the 80-μm mesa. The voltage dependence of the current (right *y*-axis) and of the radiation power (left *y*-axis) at 25 K for parallel and perpendicular settings of the filter with 0.452 THz cut-off frequency are shown for decreasing bias in zero applied magnetic field. Polarized Josephson emission occurs near 0.71 and 0.37 V, and unpolarized thermal radiation occurs at higher bias. The black solid line is a simulation of the thermal radiation (*22*).

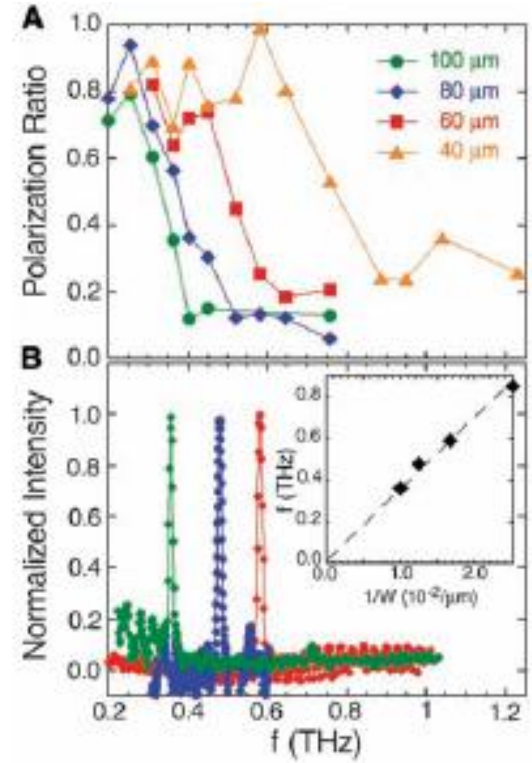

Fig. 3. Spectral characterization of the emission. **(A)** The polarization ratio—defined as the ratio the radiation power measured at perpendicular and at parallel filter settings—of the emission peaks is shown for four mesas as a function of cut-off frequency of the filters. The radiation frequency is estimated from the filter cut-off frequency at which the polarization ratio levels off at high frequencies (*22*). **(B)** Far-infrared spectra of the Josephson radiation. Sharp emission lines are clearly resolved. The observed line width of ~9 GHz (FWHM) is instrument-resolution limited. The scaling of the emission frequency with the inverse mesa width, shown in the inset, demonstrates that a cavity resonance on the width is excited.

Applied current, J

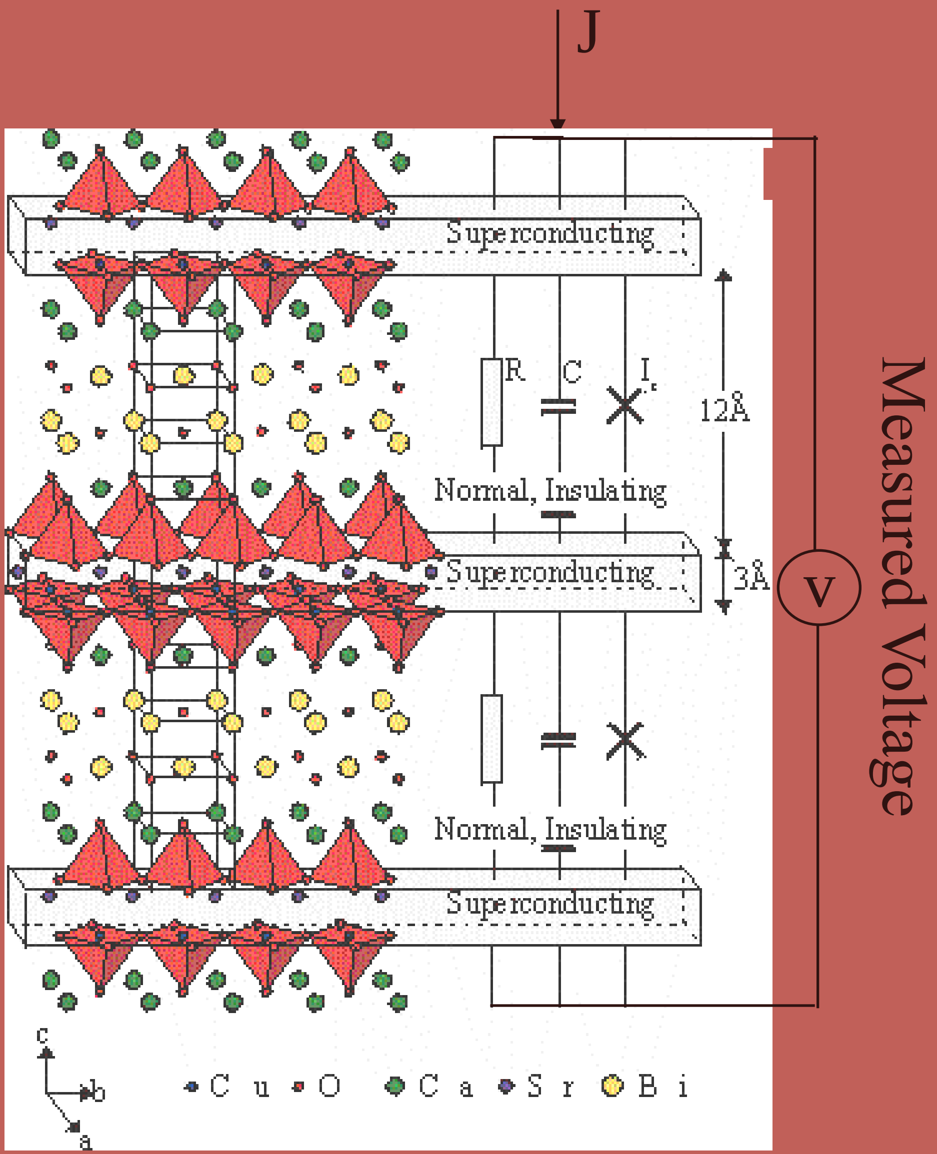

$$J = J^{d}_{l,l+1} + J^{s}_{l,l+1} + J^{qp}_{l,l+1}$$

$$J^{d}_{l,l+} = C\frac{dV_{l,l+1}}{dt}$$

$$J^{s}_{l,l+1} = J_c \sin(\varphi_{l,l+1})$$

$$J^{qp}_{l,l+1} = ?$$

Generalized Josephson Relation

Gauge invariant phase difference:

$$\varphi_{l,l+1}(t) = \theta_l(t) - \theta_{l+1}(t) - \frac{2e}{\hbar}\int_l^{l+1} dz\, A_z(z,t)$$

$$\rho_l = -\frac{\Phi_l}{4\pi\mu^2}; \qquad \Phi_l = \phi_l - \frac{\hbar}{2e}\frac{\partial\theta_l}{\partial t}; \qquad \alpha = \frac{\varepsilon\mu^2}{d_s d_I};$$

Generalized Josephson Relation :

$$\frac{\partial\varphi_{l,l+1}}{\partial t} = \frac{2e}{\hbar}V_{l,l+1} + \frac{2e}{\hbar}(\Phi_{l+1} - \Phi_l); \qquad V_{l,l+1} = \int_l^{l+1} dz E_z(z,t)$$

$$GJR: \quad \frac{\partial\varphi_{l,l+1}}{\partial t} = \frac{2e}{\hbar}V_{l,l+1} + \frac{2e}{\hbar}4\pi\mu^2(\rho_{l+1} - \rho_l)$$

$$div\,\varepsilon E = 4\pi\rho; \qquad E = \frac{V}{d_I} \qquad \rho_l = \frac{\varepsilon}{4\pi d_s d_I}(V_{l,l+1} - V_{l-1,l})$$

$$GJR: \quad \frac{\hbar}{2e}\frac{\partial\varphi_{l,l+1}}{\partial t} = V_{l,l+1} + \frac{\varepsilon\mu^2}{d_s d_I}(V_{l+2,l+1} + V_{l-1,l} - 2V_{l,l+1})$$

CCJJ model (Koyama, Tachiki, 1996)

$$I = C\partial V/\partial t + \frac{V}{R} + I_c \sin\varphi$$

$$\frac{\hbar}{2e}\dot{\varphi}_l = \sum_{l'=1}^{n} A_{ll'} V_{l'}$$

$$\partial^2 \varphi_l/\partial t^2 = \sum_{l'} A_{ll'}[I - \sin\varphi_{l'}] - \beta\partial\varphi_l/\partial t$$

$$\alpha = \frac{\mu^2 \varepsilon}{d_s d_I}$$

$$A = \begin{pmatrix} 1+\alpha G & -\alpha & 0 & \dots & & & \\ -\alpha & 1+2\alpha & -\alpha & 0 & \dots & & \\ 0 & -\alpha & 1+2\alpha & -\alpha & 0 & \dots & \\ \dots & \dots & \dots & \dots & \dots & \dots & \dots \\ & & & \dots & 0 & -\alpha & 1+\alpha G \end{pmatrix}$$

$$\tau = \omega_p t$$

$$\omega_p^2 = \frac{2eI_c}{\hbar C}$$

$$V_c = I_c R_N = \frac{\hbar\omega_c}{2e}$$

$$\beta = \frac{1}{\omega_p RC}$$

$$A = \begin{pmatrix} 1+2\alpha & -\alpha & 0 & \dots & & & -\alpha \\ -\alpha & 1+2\alpha & -\alpha & 0 & \dots & & \\ 0 & -\alpha & 1+2\alpha & -\alpha & 0 & \dots & \\ \dots & \dots & \dots & \dots & \dots & \dots & \dots \\ -\alpha & & & \dots & 0 & -\alpha & 1+2\alpha \end{pmatrix}$$

$$\beta^2 = \frac{1}{\beta_c}, \qquad \beta_c = \omega^2 R^2 C^2 = \frac{\omega_c^2}{\omega_p^2} = CR_N\omega_c$$

$$G = 1 + \gamma, \quad \gamma = d_s / d_{1,N}$$


Pringle

Resistively and Capacitively Shunted Junction Model

- The total current through JJ as sum of superconducting, quasiparticle and displacement currents
- $I=I_s+I_{qp}+I_d = I_c\sin\phi+V/R+C\,(dV/dt)$
- Josephson relation $(\sim/2e)(d\phi/dt)=V(t)$
- The dependence $I_{qp}(V)$ is nonlinear in general, but at small V we may consider $I_{qp}=V/R$.
- If C=0, then we have RSJ model.
- If $I_{qp}(V)$ is nonlinear, we call it as "Nonlinear RCSJ model".
- Equation
- $I=I_c\sin\phi+(\sim/2eR)/(d\phi/dt)+(C\sim/2e)(d^2\phi/dt^2)$
- is second order and nonlinear because of sin phi term.
- It can be solved numerically only.
- The analytical solution exists in the limit C=0.

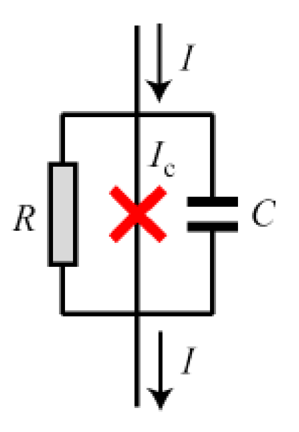

Collective Dynamics of Intrinsic Josephson Junctions in High-T_c Superconductors

Dmitry A. Ryndyk*

The key point of our theory is a nonequilibrium nature of the ac Josephson effect in layered superconductors [18,20–22]. It means that superconducting layers are in the nonstationary nonequilibrium state due to the injection of quasiparticles and Cooper pairs, and a nonzero invariant potential

$$\Phi_i(t) = \phi_i - (\hbar/2e)(\partial\theta_i/\partial t)$$

is generated inside them, where ϕ_i is the electrostatic potential and θ_i is the phase of superconducting condensate,

$$\rho_i = -2e^2 N(0)(\Phi_i - \Psi_i) = -\frac{1}{4\pi r_D^2}(\Phi_i - \Psi_i), \tag{2}$$

where Ψ_i is determined by the electron-hole charge imbalance

$$e\Psi_i = -\int_\Delta^\infty (n_\epsilon^i - n_{-\epsilon}^i)\,d\epsilon, \tag{3}$$

where we use the averaged-over-momentum-direction quasiparticle distribution function n_ϵ^i introduced by Eliashberg [26], which describes quasielectron (at $\epsilon > 0$) and quasihole (at $\epsilon < 0$) energy distributions, $|\epsilon|$ is the quasiparticle energy. In equilibrium $n_\epsilon^i = n_{-\epsilon}^i = n_\epsilon^{(0)} = 1/2[1 - th(|\epsilon|/2T)]$.

$$\beta \frac{d^2\varphi_{ij}}{d\tau^2} + \frac{d\varphi_{ij}}{d\tau} + (1-\kappa\psi_i^2)(1-\kappa\psi_j^2)\sin(\varphi_{ij}) + \psi_i - \psi_j + \beta\left(\frac{d\mu_i}{d\tau} - \frac{d\mu_j}{d\tau}\right) = j(t), \tag{8}$$

$$\alpha \frac{d\psi_i}{d\tau} + \psi_i + \eta(2\psi_i - \psi_{i-1} - \psi_{i+1}) = \eta\left(\frac{d\varphi_{i-1\,i}}{d\tau} - \frac{d\varphi_{i\,i+1}}{d\tau}\right), \tag{9}$$

$$\mu_i + \zeta(2\mu_i - \mu_{i-1} - \mu_{i+1}) = \psi_i + \zeta\left(\frac{d\varphi_{i-1\,i}}{d\tau} - \frac{d\varphi_{i\,i+1}}{d\tau}\right), \tag{10}$$

$$\sum_i \frac{d\varphi_{i-1\,i}}{d\tau} = v(t), \tag{11}$$

where $j(t)$ is the external current in J_c units, $v(t)$ is the external voltage in V_c units, $\mu(t) = \Phi(t)/V_c$, $\psi(t) = \Psi(t)/V_c$, and $\alpha = \tau_q\omega_c$, $\beta = \omega_c^2/\omega_p^2$, $\zeta = (\epsilon_0 r_D^2)/(d_0 d)$, $\omega_c = 2eRJ_c/\hbar$, $\omega_p^2 = (8\pi edJ_c)/(\hbar\epsilon_0 S)$, $\kappa = (eV_c/\Delta)^2$, $\tau = \omega_c t$. These equations may be considered as a good phenomenological approximation at all temperatures. In the limit $\eta \to 0$ the quasiparticle contribution can be neglected (if the voltage is less than 2Δ and pair braking is forbidden), so that $\psi = 0$ and we have the equations for φ and μ similar to that obtained in Ref. [20].

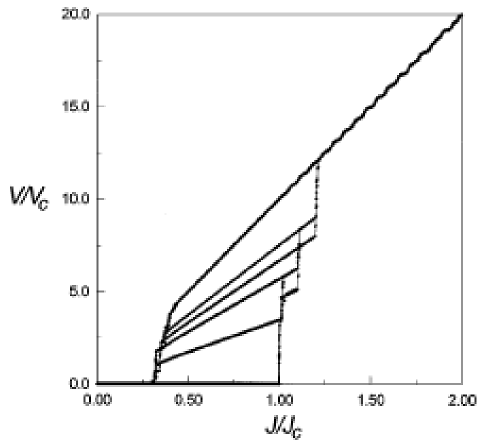

FIG. 1. The current-voltage characteristic of most anisotropic structure with $J_c/S \sim 10^3$ A/cm^2 ($\alpha = 100$, $\beta = 100$, $\eta = 0.1$, $\zeta = 2$). Multiple branches are clearly observed.

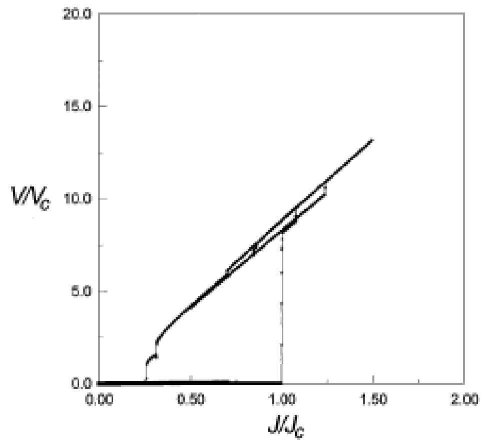

FIG. 2. The current-voltage characteristic of less anisotropic structure with $J_c/S \sim 10^4$ A/cm^2 ($\alpha = 100$, $\beta = 10$, $\eta = 10$, $\zeta = 2$). Collective switching takes place at $J = J_c$.

Переменный эффект Джозефсона

$$\partial\theta/\partial t = (2e/\hbar)V,$$

где $V = \varphi_1 - \varphi_2$. Если $V = \text{const}$, то разность фаз равна

$$\theta = \theta_0 + (2eV/\hbar)\,t.$$

$$j = j_c \sin[\theta_0 + (2eV/\hbar)\,t].$$

Частота, равная

$$\omega = 2eV/\hbar,$$

соответствует 10^{11} с$^{-1}$ для $V \sim 10^{-4}$ В.

$$j = j_c \sin\theta + (\hbar/2eR)\,\partial\theta/\partial t.$$

Интегрирование этого уравнения дает

$$\theta = 2\,\mathrm{arctg}\,\{[1-(j_c/j)^2]^{1/2}\,\mathrm{tg}\,[eRt\,(j^2-j_c^2)^{1/2}\,\hbar] + j_c/j\}.$$

$$V = (\hbar/2e)\,d\theta/dt$$

$$V(t) = Rj\,(j^2-j_c^2)/[j^2 + j_c^2\cos\omega t + j_c\,(j^2-j_c^2)^{1/2}\sin\omega t],$$

где

$$\omega = (2eR/\hbar)\,(j^2-j_c^2)^{1/2}.$$

Эту же формулу можно переписать в виде

$$V(t) = R\,(j^2-j_c^2)/[j + j_c\cos(\omega t - \theta_1)],$$

где $\theta_1 = \arccos(j_c/j)$. При $j \to \infty$ $V \to Rj$,

$$\overline{V} = (2\pi)^{-1}\int_0^{2\pi} V(t)\,d(\omega t) = R\,(j^2-j_c^2) = \frac{\omega\hbar}{2e}.$$

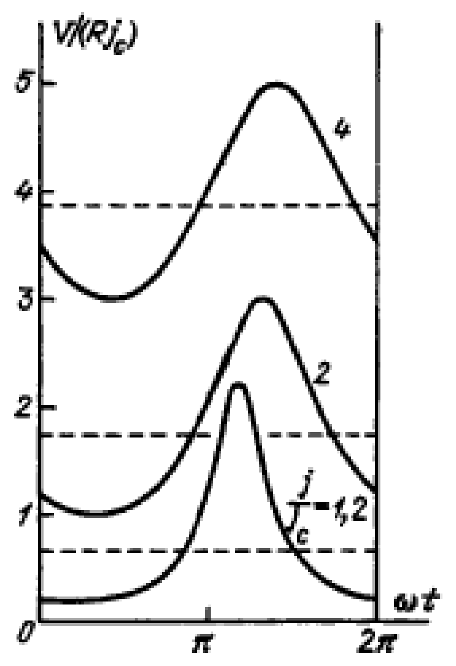

Numerical Procedure

$$\frac{d^2}{dt^2}\varphi_l = (I - \sin\varphi_l - \beta\frac{d\varphi_l}{dt}) +$$

$$\alpha(\sin\varphi_{l+1} + \sin\varphi_{l-1} - 2\sin\varphi_l)$$

$$\bar{V}_l = \frac{1}{T_{\max} - T_{\min}}\int_{T_{\min}}^{T_{\max}} V_l\,dt \qquad V = \sum_{l=1}^{N}\bar{V}_l$$

$$R - state: \quad <\frac{\partial\varphi}{\partial t}>= const, <\sin\varphi>= 0$$

$$O - state: \quad <\frac{\partial\varphi}{\partial t}>= 0, <\sin\varphi>= const$$

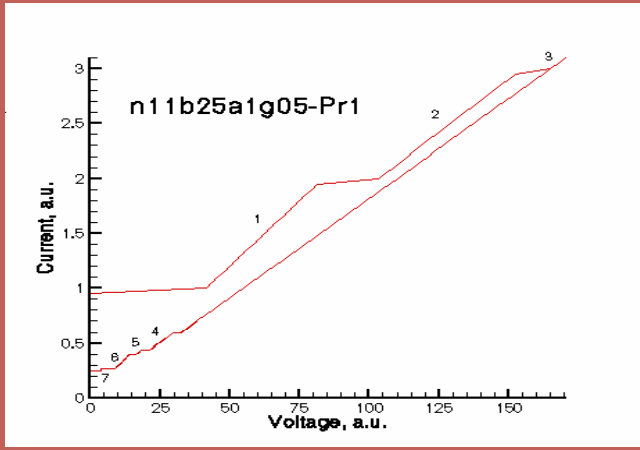

$$S => R_1[1,4,6,8,11] => R_2[5^-,7^-] => R_3 => R_4[3^-,6^-,9^-] =>$$
$$=> R_5[1,2,4,8,10,11] => R_6[1,4,8,11] => R_7[1,11] => S$$

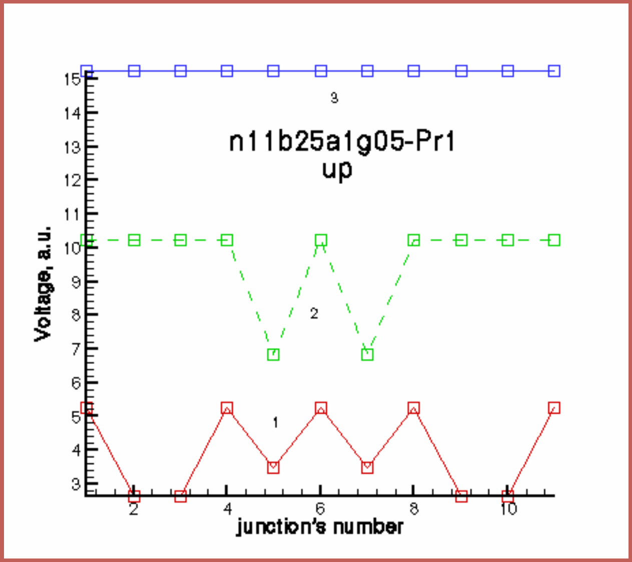

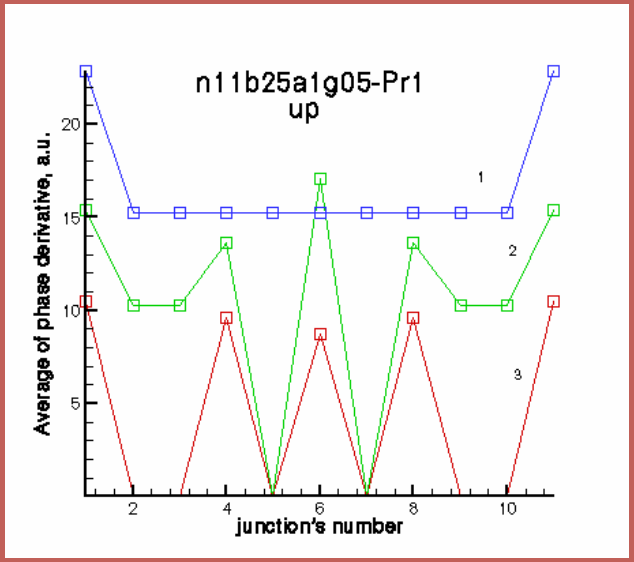

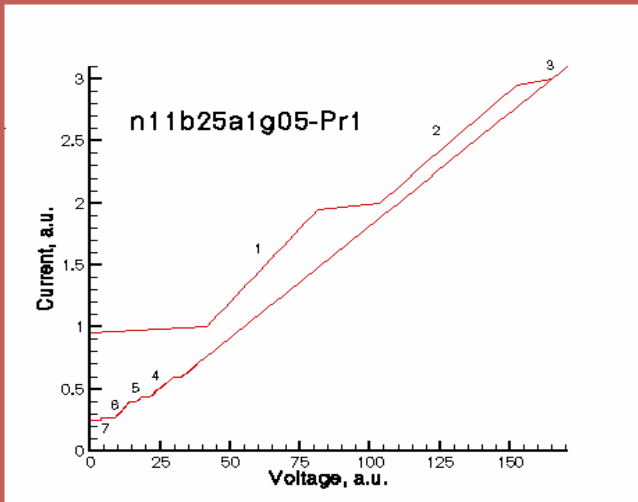

$$S => R_1[1,4,6,8,11] => R_2[5^-,7^-] => R_3 => R_4[3^-,6^-,9^-] =>$$
$$=> R_5[1,2,4,8,10,11] => R_6[1,4,8,11] => R_7[1,11] => S$$

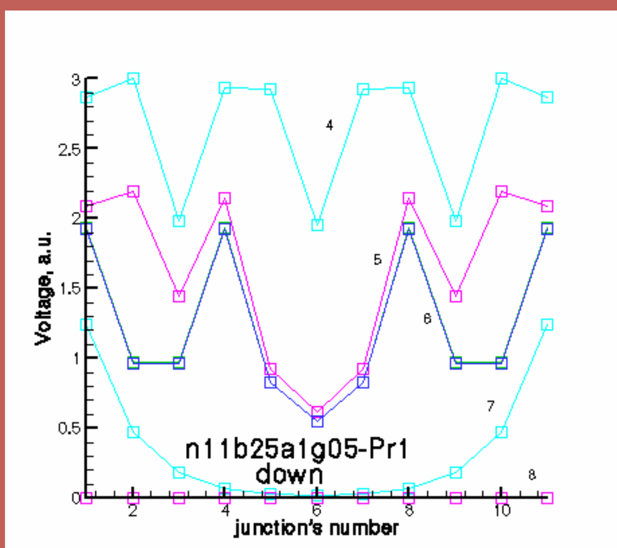

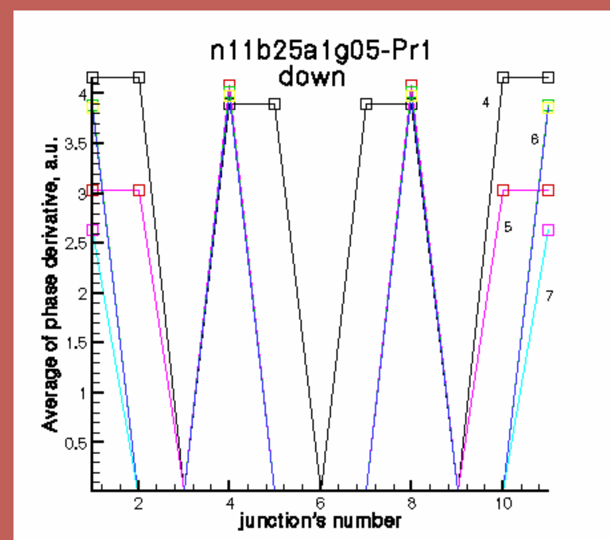

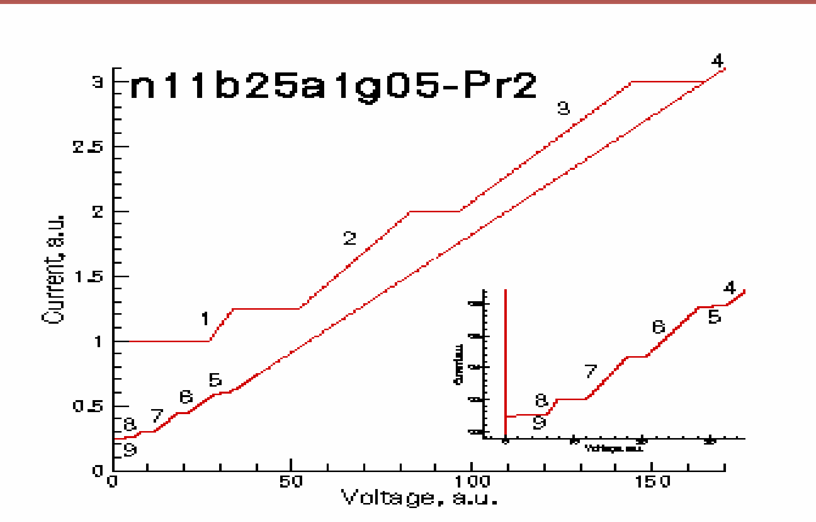

$$S \Rightarrow R_1[1,6,11] \Rightarrow R_2[1,4,6,8,11] \Rightarrow R_3[2^-,5^-,7^-,10^-] \Rightarrow$$
$$\Rightarrow R_4 \Rightarrow R_5[5^-,7^-] \Rightarrow R_6[2^-,5^-,7^-,10^-] \Rightarrow R_7[1,3,6,9,11] \Longrightarrow$$
$$\Rightarrow R_8[1,6,11] \Rightarrow R_9[1,11] \Rightarrow S$$

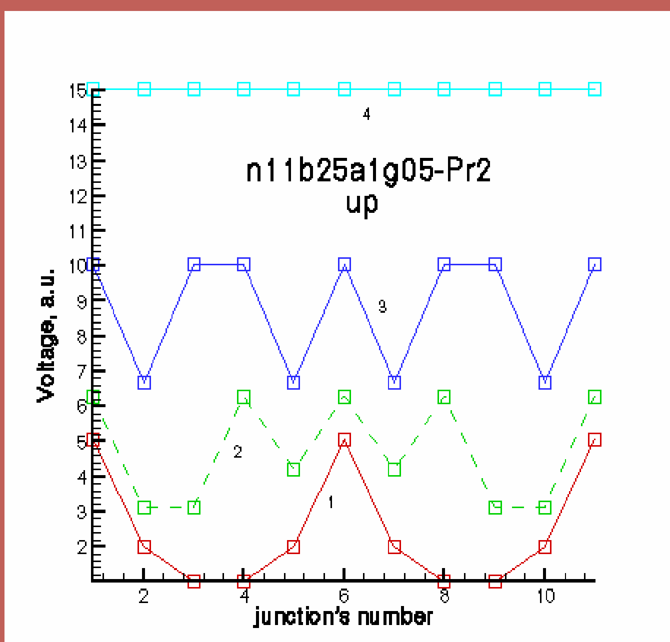

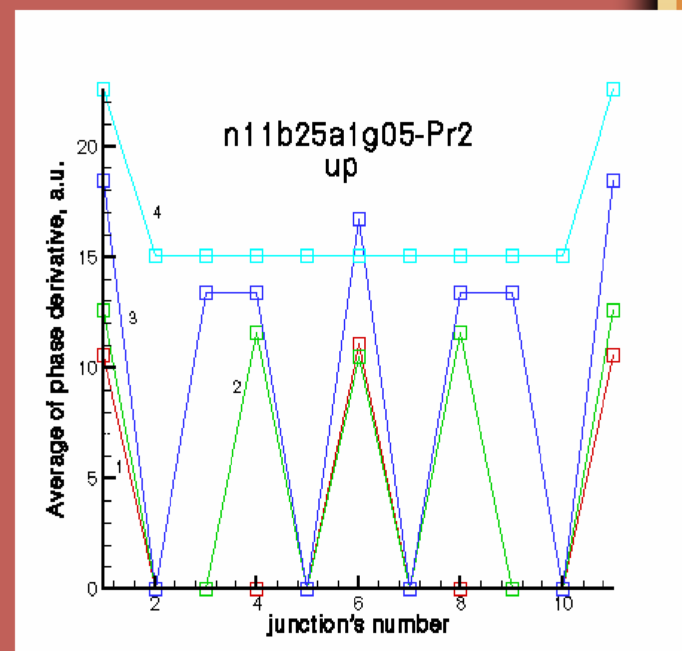

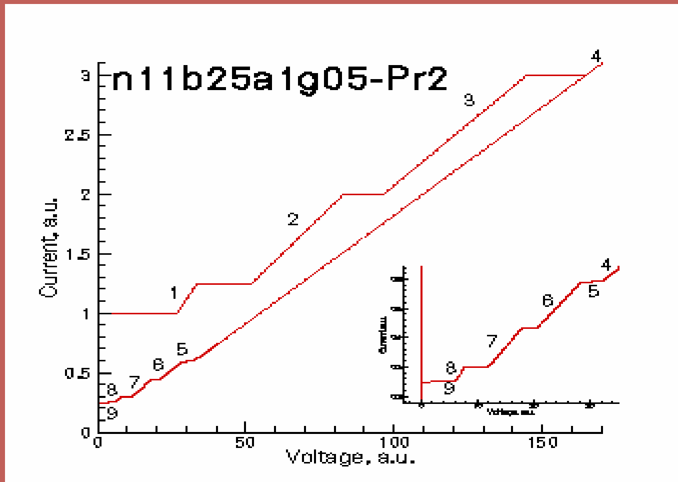

$$S => R_1[1,6,11] => R_2[1,4,6,8,11] => R_3[2^-,5^-,7^-,10^-] =>$$
$$=> R_4 => R_5[5^-,7^-] => R_6[2^-,5^-,7^-,10^-] => R_7[1,3,6,9,11] ==>$$
$$=> R_8[1,6,11] => R_9[1,11] => S$$

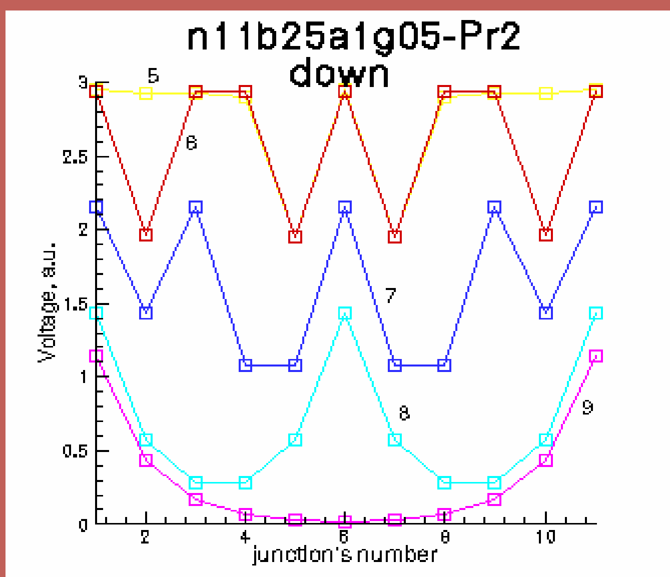

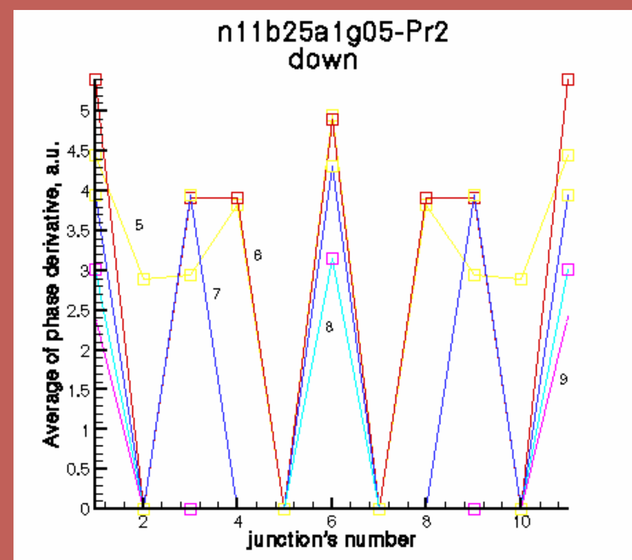

M.Machida, T.Koyama

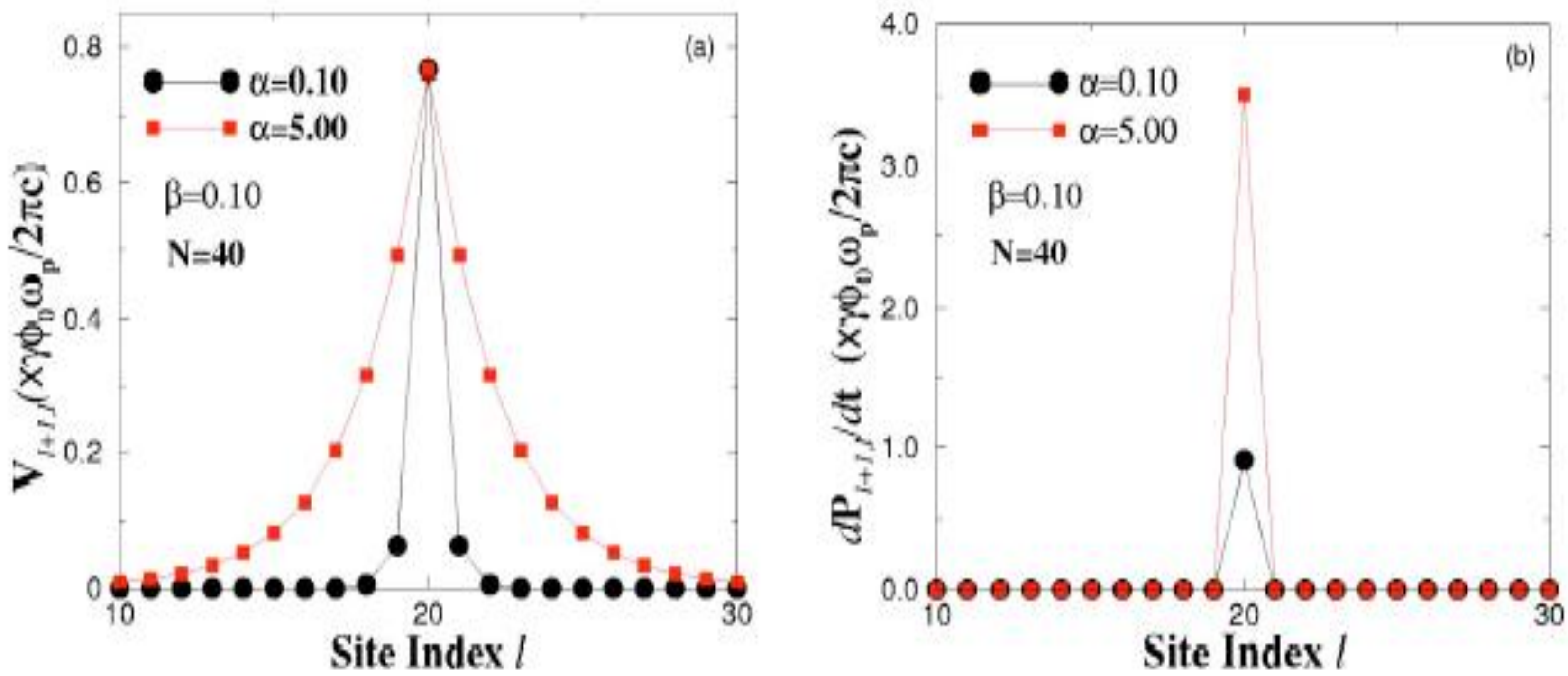

FIG. 3. (Color online) (a) Voltage distribution (Ref. 21) in the first branch for α=0.10 and α=5.00. The periodic boundary condition is imposed on the system with N=40; (b) distribution of $dP_{\ell+1,\ell}/(dt)$.

Result of calculation

$$\frac{d^2\varphi_{l,l+1}}{d\tau^2} = (1 - \alpha\nabla^{(2)})(J/J_c - \sin(\varphi_{l,l+1})) - \beta\frac{d\varphi_{l,l+1}}{d\tau}$$

$$\frac{\hbar}{2e}\dot{\varphi}_{l,l+1} = (1 - \alpha\nabla^{(2)})V_{l,l+1}$$

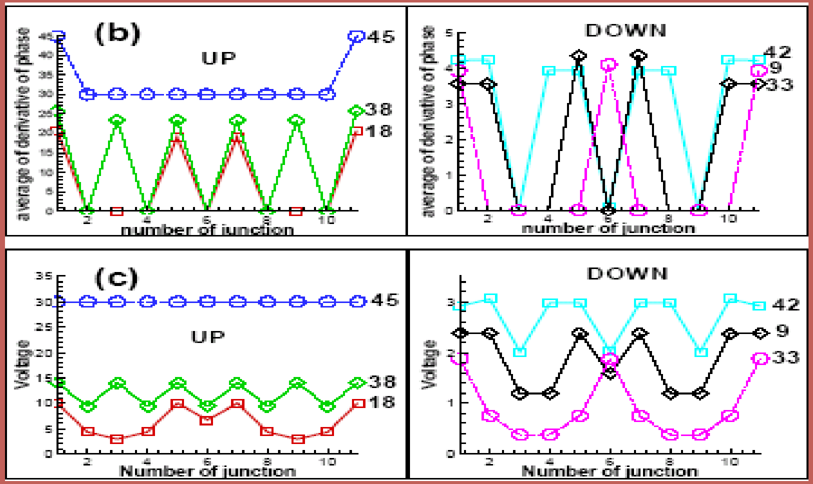

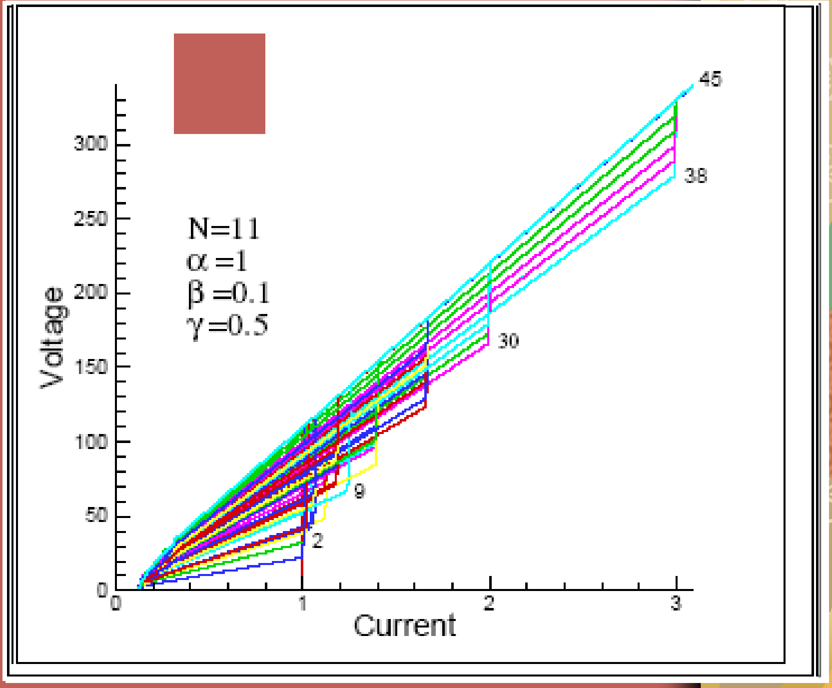

TABLE I: Branch's number, slopes and corresponding states for IVC of 11 IJJ in CCJJ model at $\alpha = 1, \beta = 0.1$ and $\gamma = 0.5$.

branch	*state*	*slope*	*branch*	*state*	*slope*
0 :	S	0	29 :	$R(3,4,5,6,7,8,9)$	80.77
1 :	$R(6)$	22.27	30 :	$R(1,3,6,9,11)$	83.33
2 :	$R(1,11)$	32.36	30 :	$R(1,4,6,8,11)$	83.33
3 :	$R(5,7)$	38.80	31 :	$R(2,4,6,8,10)$	84.67
4 :	$R(2,10)$	40.34	32 :	$O(3,5,6,7,9)$	84.76
5 :	$R(5,6,7)$	42.13	32 :	$O(2,5,6,7,10)$	84.76
6 :	$R(3,9)$	42.99	33 :	$O(3,4,6,8,9)$	86.67
7 :	$R(4,8)$	43.19	33 :	$O(2,3,6,9,10)$	86.67
8 :	$R(1,2,10,11)$	52.34	34 :	$O(1,4,6,8,11)$	88.00
9 :	$R(1,6,11)$	54.00	34 :	$O(1,3,6,9,11)$	88.00
10 :	$R(4,6,8)$	55.10	35 :	$O(4,5,7,8)$	90.00
11 :	$R(4,5,7,8)$	58.43	35 :	$O(3,4,8,9)$	90.00
12 :	$R(2,3,9,10)$	60.22	35 :	$O(2,3,9,10)$	90.00
13 :	$R(3,6,9)$	60.77	36 :	$O(1,5,7,11)$	91.33
14 :	$R(2,6,10)$	60.86	36 :	$O(1,4,8,11)$	91.33
15 :	$R(4,5,6,7,8)$	61.76	36 :	$O(1,5,7,11)$	91.33
16 :	$R(3,4,8,9)$	62.20	37 :	$O(5,6,7)$	91.43
17 :	$R(1,3,9,11)$	65.56	38 :	$O(2,4,8,10)$	93.33
18 :	$R(1,5,7,11)$	69.523	39 :	$O(1,6,11)$	94.67
19 :	$R(3,5,7,9)$	70.77	40 :	$O(3,5,7,9)$	96.67
20 :	$R(1,4,8,11)$	71.43	40 :	$O(2,5,7,10)$	96.67
21 :	$R(1,2,3,9,10,11)$	72.22	40 :	$O(3,5,7,9)$	96.67
22 :	$R(2,4,8,10)$	72.76	41 :	$O(1,11)$	98.000
23 :	$R(1,2,6,10,11)$	72.86	42 :	$O(4,6,8)$	100.00
23 :	$R(1,5,6,7,11)$	72.86	42 :	$O(3,6,9)$	100.00
24 :	$R(3,4,6,8,9)$	74.10	42 :	$O(4,6,8)$	100.00
24 :	$R(3,5,6,7,9)$	74.10	43 :	$O(5,7)$	103.33
25 :	$R(2,5,7,10)$	74.67	43 :	$O(4,8)$	103.33
26 :	$R(3,4,5,7,8,9)$	77.44	43 :	$O(3,9)$	103.33
27 :	$R(2,3,6,9,10)$	78.00	43 :	$O(5,7)$	103.33
27 :	$R(2,5,6,7,10)$	78.00	44 :	$O(6)$	106.67
28 :	$R(2,3,4,8,9,10)$	79.43	45 :	R	110.00

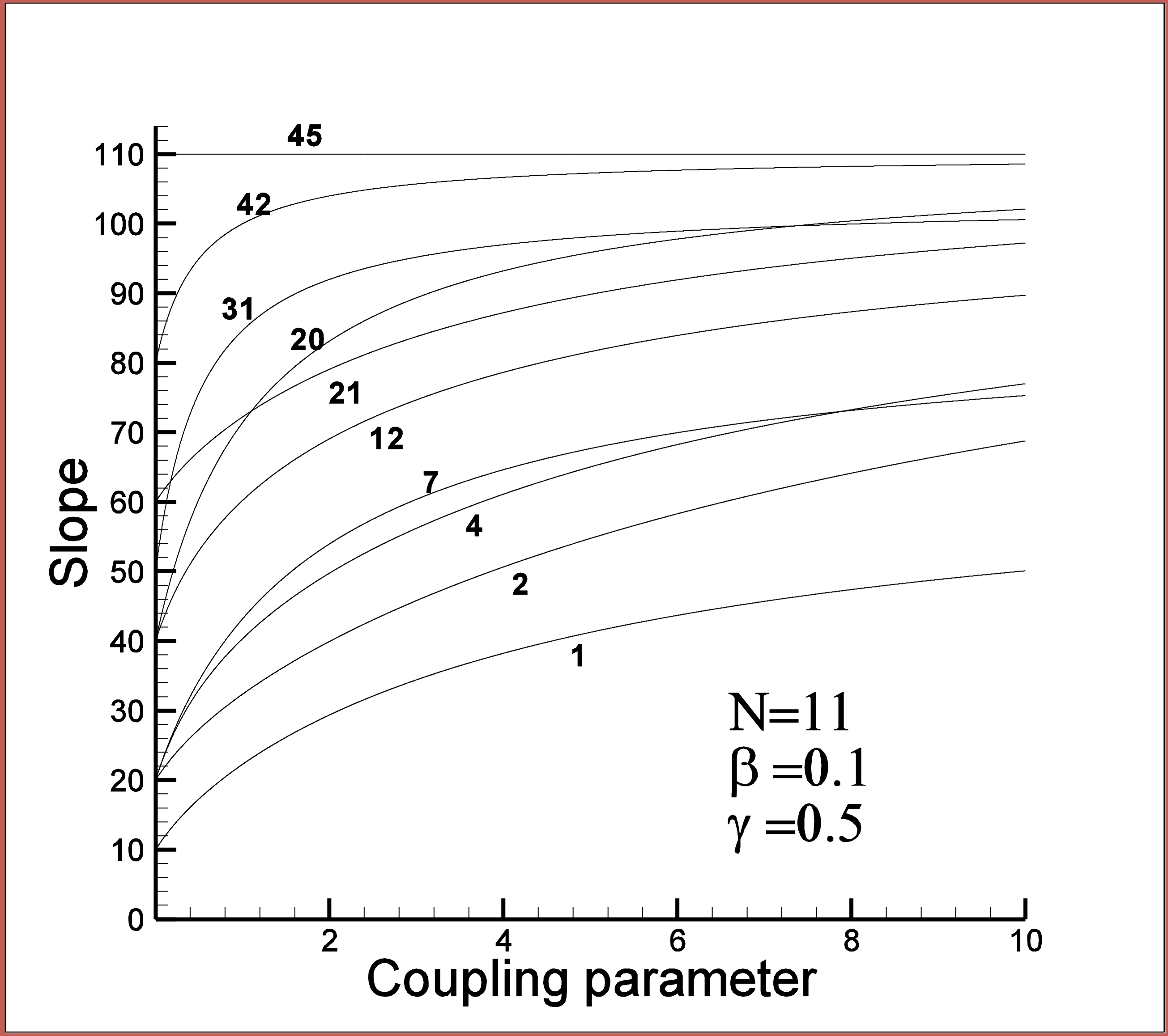
45
42
31
20
21
12
7
4
2
1
N=11
β =0.1
γ =0.5
Slope
Coupling parameter
0
10
20
30
40
50
60
70
80
90
100
110
2
4
6
8
10

CCJJ model

2

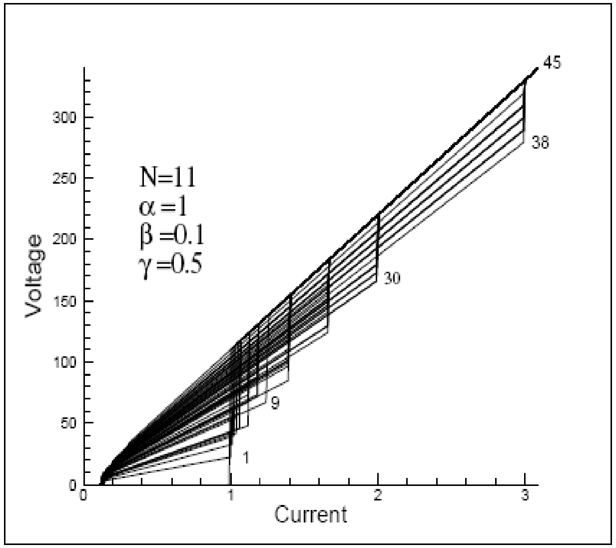

FIG. 1: The total branch structure in the IVC of IJJ. The branch's numbers correspond to the states shown in Table of Ref.[13].

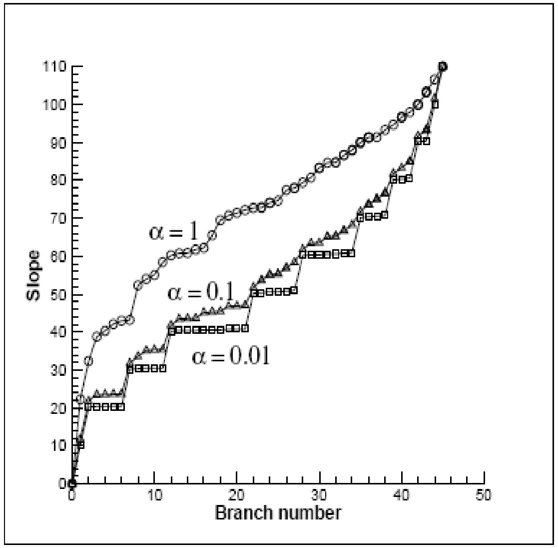

FIG. 2: The dependence of the slope versus branch number at different values of coupling parameter.

Shukrinov, F. Mahfouzi, Physica C 434 (2006) 6-12.

CCJJ+DC model

$$J = C\partial V/\partial t + V/R + J_C \sin\varphi \qquad J_D^l = -\frac{\Phi_l - \Phi_{l+1}}{R}$$

$$J = C\partial V/\partial t + J_C \sin\varphi + \frac{\hbar}{2eR}\partial\varphi/\partial t$$

$$\partial^2\varphi_l/\partial t^2 = \sum_{l'=1}^{N} A_{ll'}[J/J_c - \sin\varphi_{l'} - \beta\partial\varphi_{l'}/\partial t]$$

CCJJ+DC model

$$\frac{d^2}{dt^2}\varphi_l = (I - \sin\varphi_l - \beta\frac{d\varphi_l}{dt})$$

$$+\alpha(\sin\varphi_{l+1} + \sin\varphi_{l-1} - 2\sin\varphi_l)$$

$$+\alpha\beta(\frac{d\varphi_{l+1}}{dt} + \frac{d\varphi_{l-1}}{dt} - 2\frac{d\varphi_l}{dt})$$

The branch structure in IVC in CCJJ+DC model at different boundary conditions

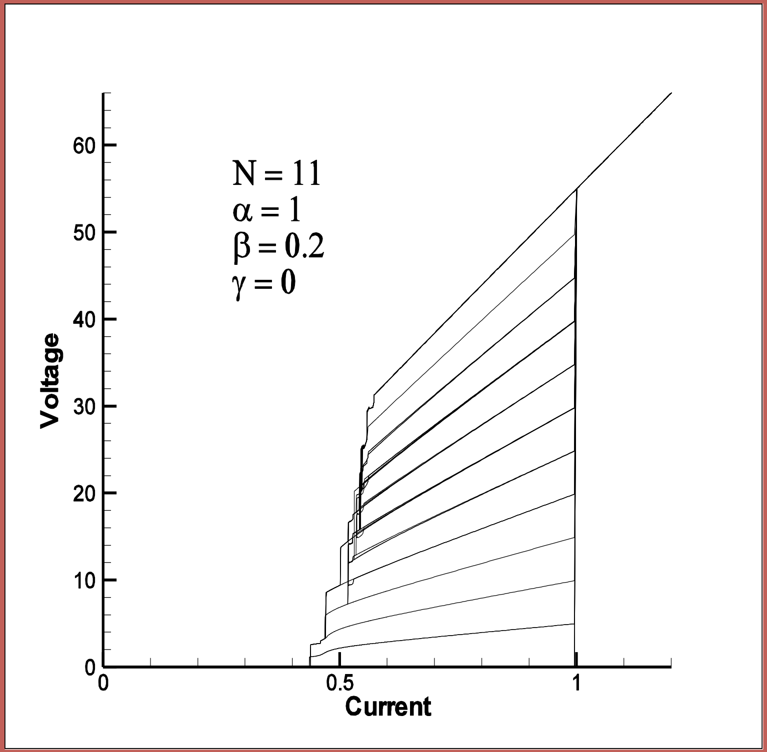

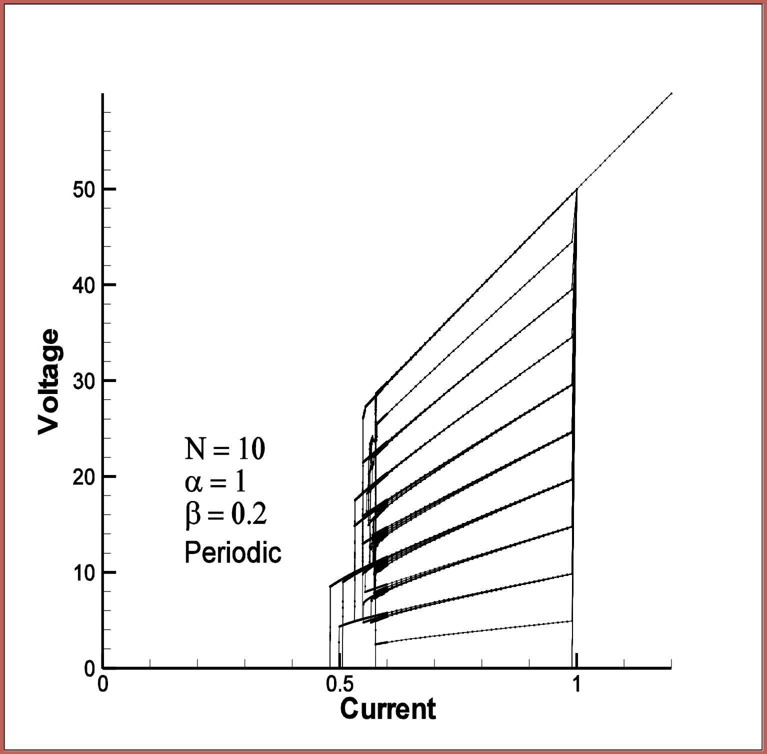

The branch structure in IVC in CCJJ+DC model at different beta

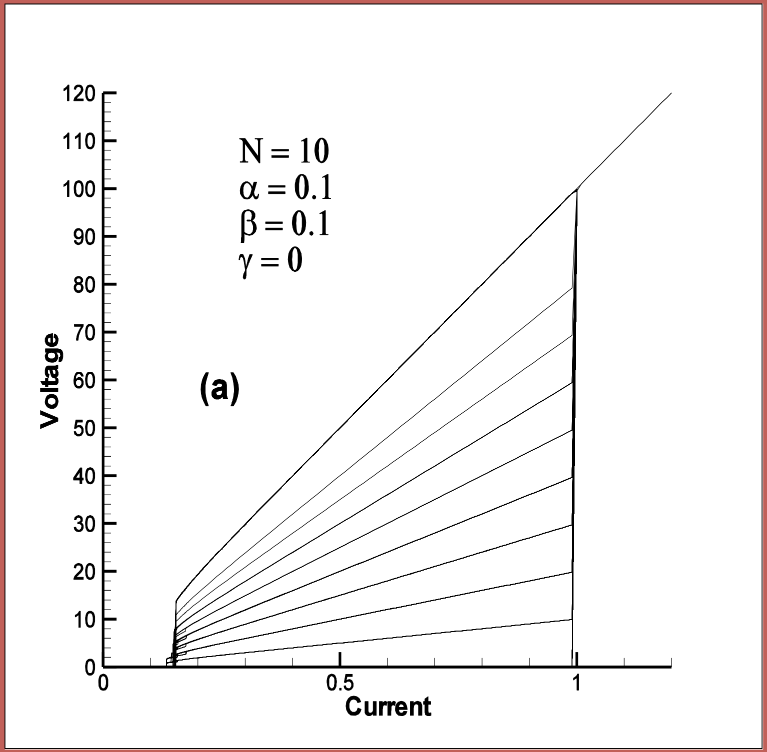

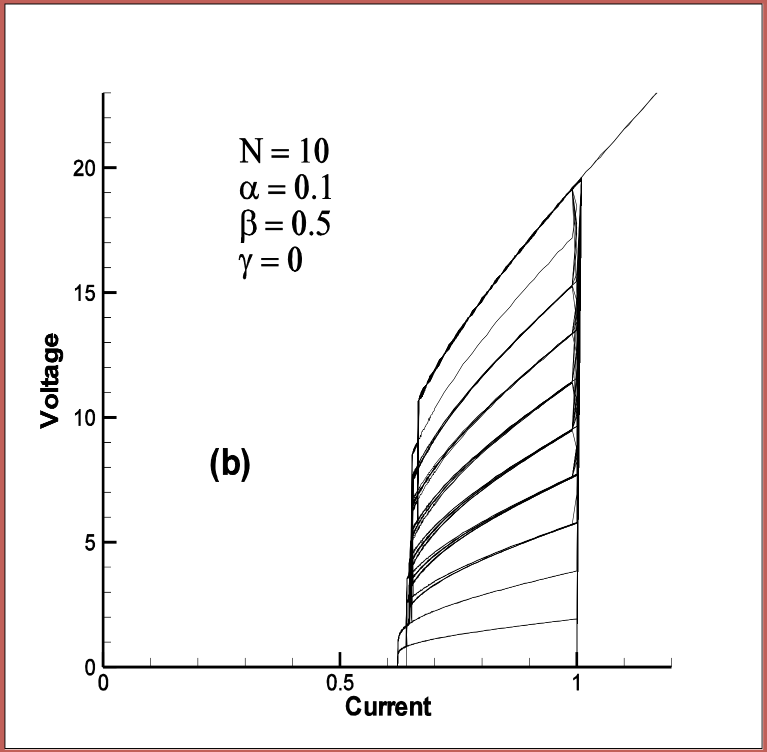

CCJJ+DC model

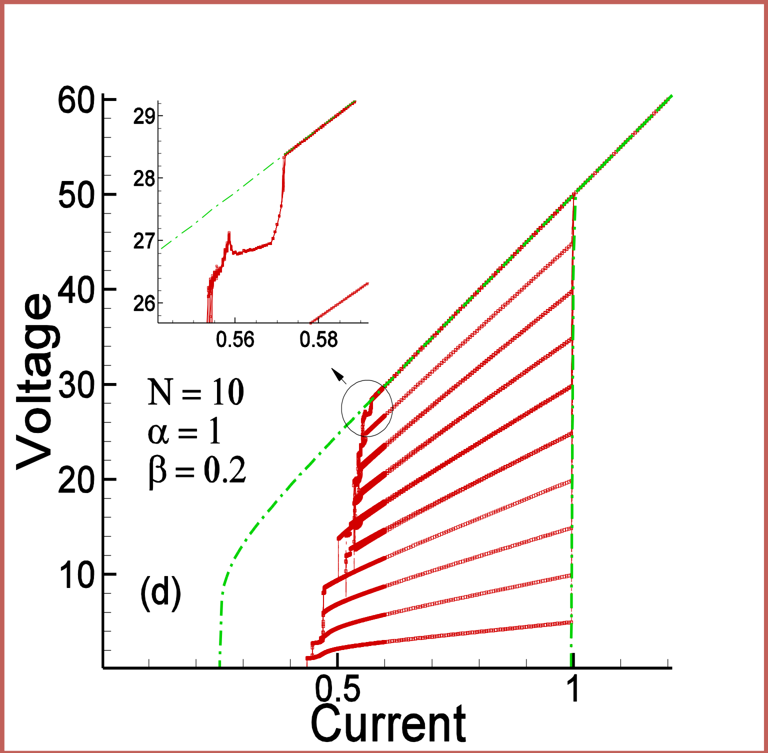

Yu.M.Shukrinov, F.Mahfouzi.- Supercond.Sci.Technol. 20 (2007) S38-S42

Lecture 2

Breakpoint in CVC of Layered Superconductors

Yu.M.Shukrinov
BLTP, JINR, Dubna, , Russia

CCJJ+DC model

$$J = C\partial V/\partial t + V/R + J_C \sin\varphi$$

$$J_D^l = -\frac{\Phi_l - \Phi_{l+1}}{R}$$

$$J = C\frac{dV_l}{dt} + J_c^l \sin(\varphi_l) + \frac{\hbar}{2eR}\dot{\varphi}_l$$

$$\ddot{\varphi}_l = \sum_{l'=1}^{n} A_{ll'}\left[\frac{J}{J_c} - \sin(\varphi_{l'}) - \beta\dot{\varphi}_{l'}\right]$$

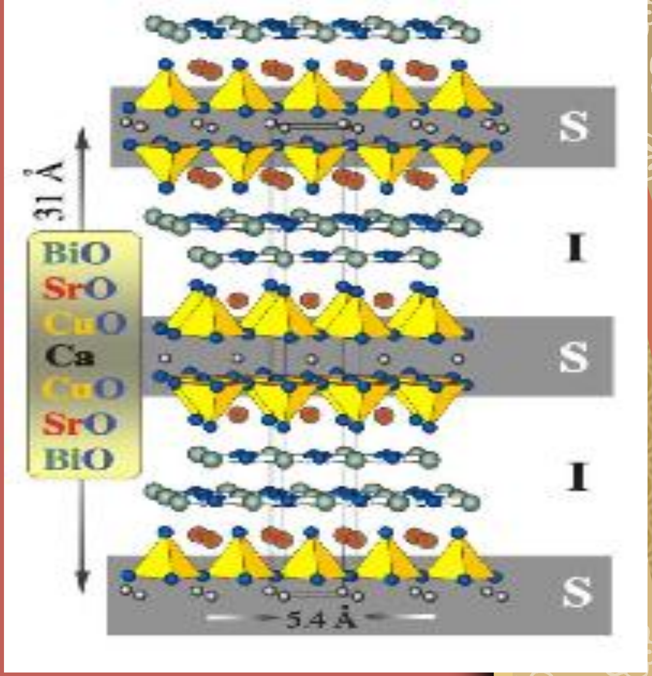

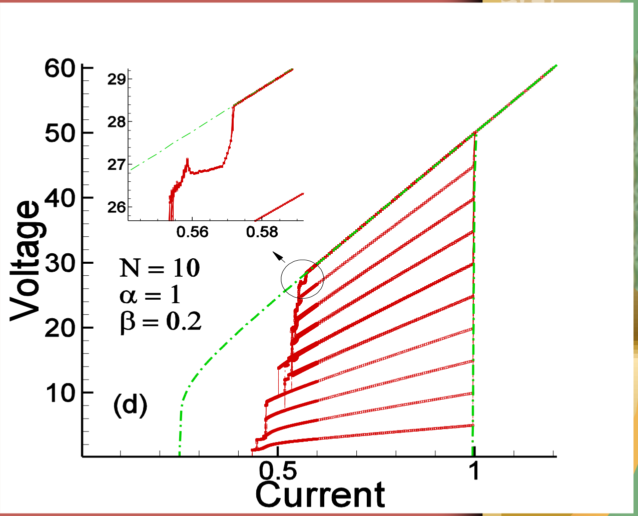

M. Machida, T. Koyama, and M. Tachiki, Phys. Rev. Lett. 83, 4816 (1999).
D. A. Ryndyk, Phys. Rev. Lett. 80, 3376 (1998).

- $\mathrm{div}\,(\varepsilon\varepsilon_0 E) = \rho$

$$Q_l = Q_0\,\alpha\,(V_{l+1} - V_l)$$

$$Q_0 = \varepsilon\,\varepsilon_0\,V_0/r_D^2$$

t – Tm*Io/dI

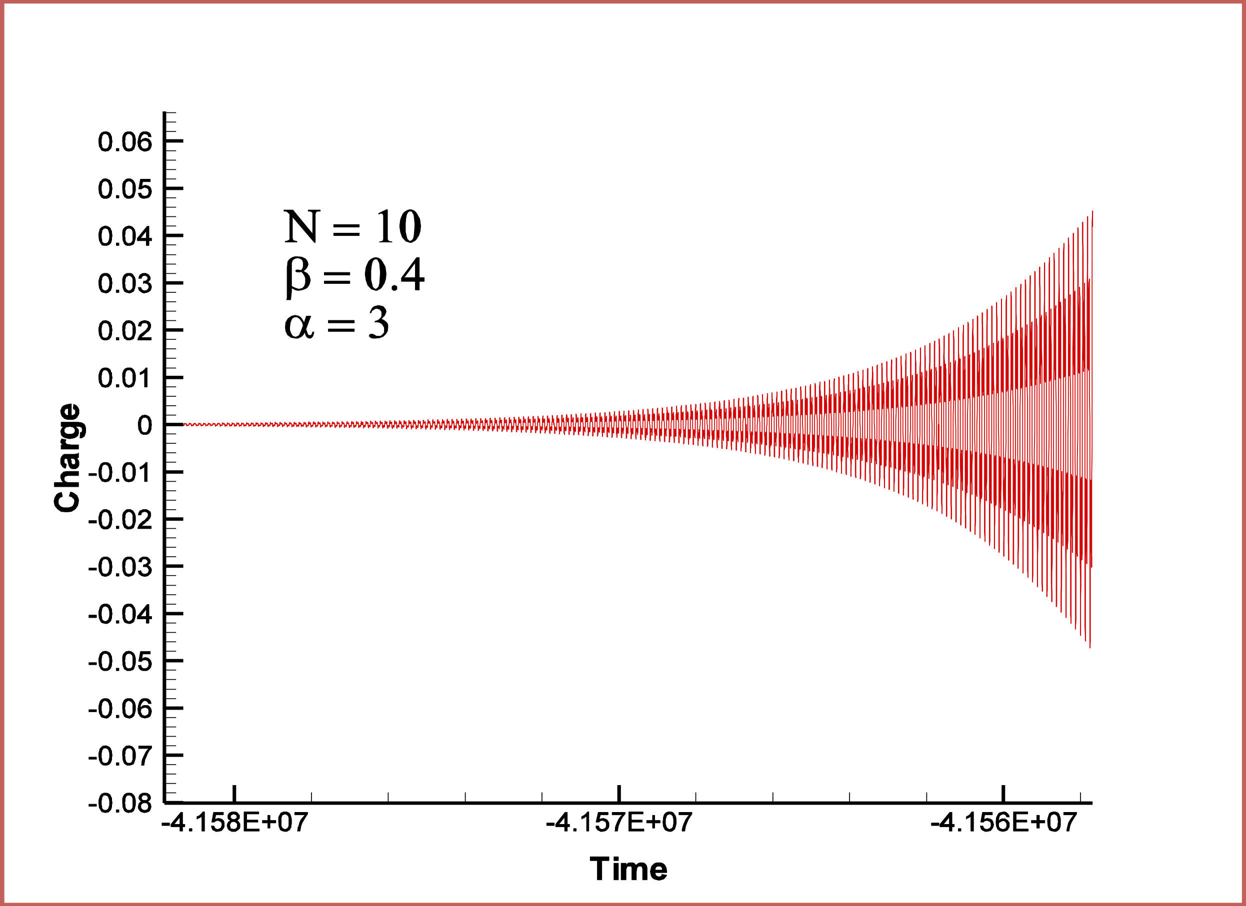

N = 10
β = 0.4
α = 3
Charge
0.06
0.05
0.04
0.03
0.02
0.01
0
-0.01
-0.02
-0.03
-0.04
-0.05
-0.06
-0.07
-0.08
-4.158E+07
-4.157E+07
-4.156E+07
Time

Time dependence of charge oscillation on the layers at periodic boundary condition at I = 0.575 (breakpoint)

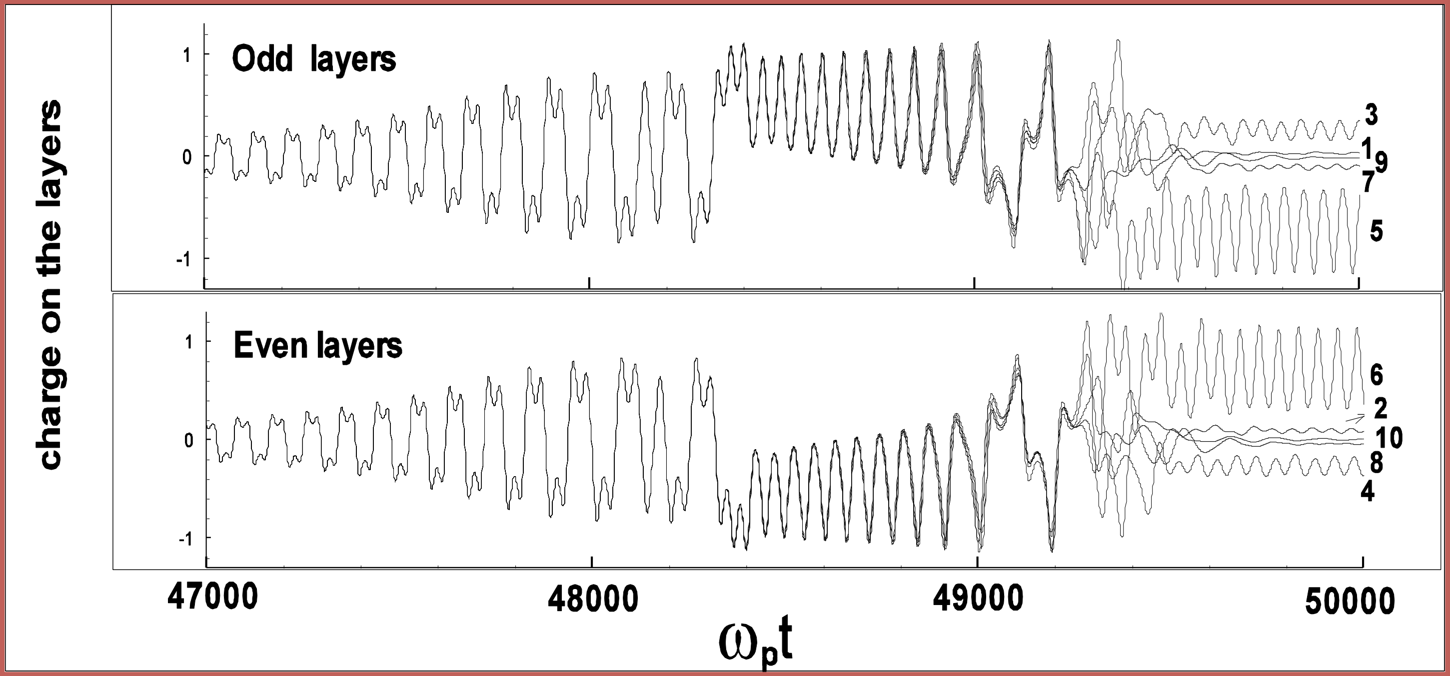

IVC of the outermost branch for the stacks with different number N of IJJ at γ=0 and at PBC

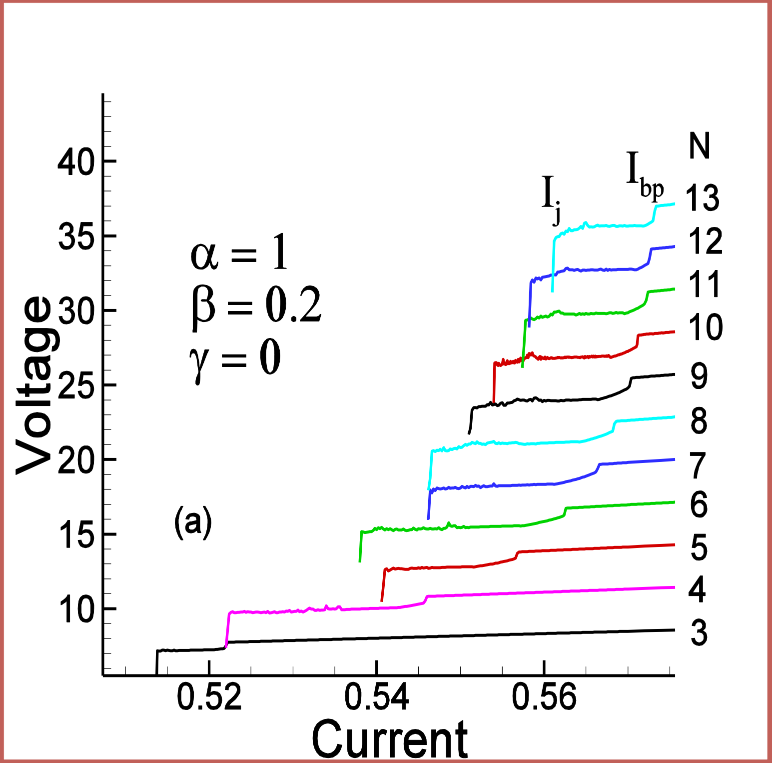

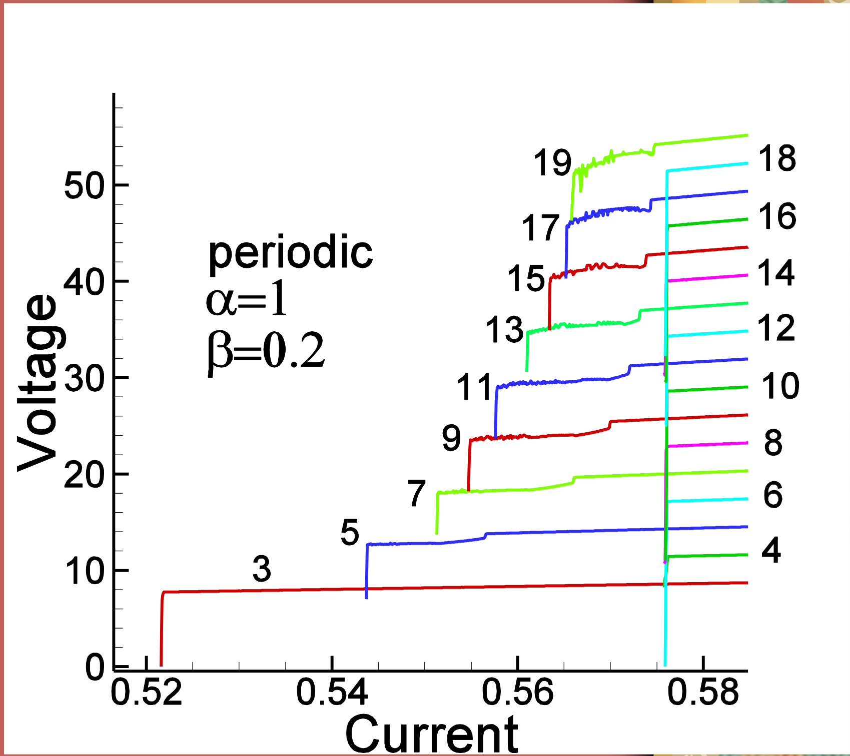

$$k = \pi \quad k = (N-1)\pi / N$$

Yu.M.Shukrinov, F.Mahfouzi, N.F.Pedersen. Phys.Rev.B 75, 104508 (2007).

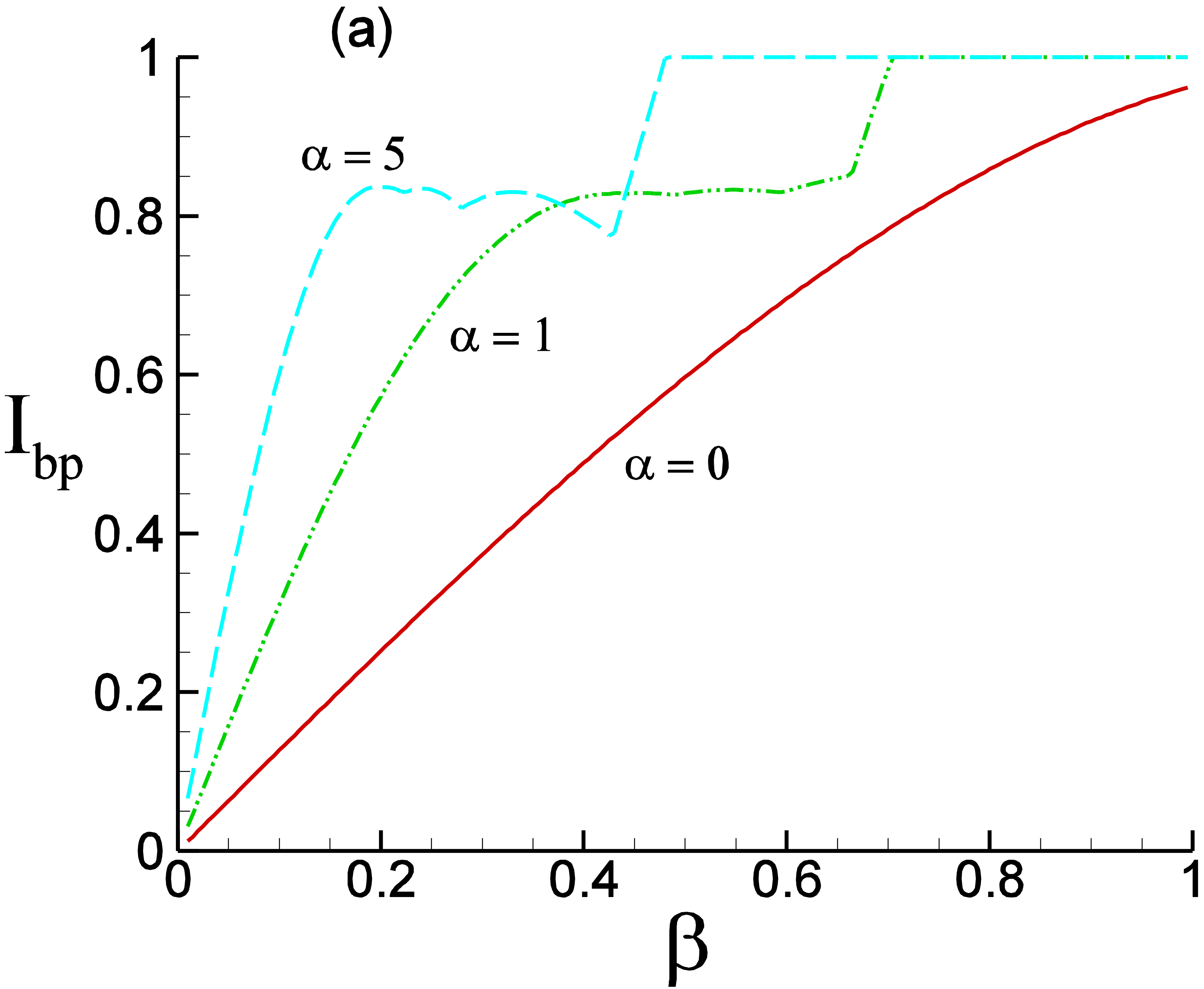
(a)
$\alpha = 5$
$\alpha = 1$
$\alpha = 0$
I_{bp}
β
0
0.2
0.4
0.6
0.8
1

The $\alpha\beta$–dependence of the BPC of the outermost branch of IVC for stack of 10 IJJ at PBC.

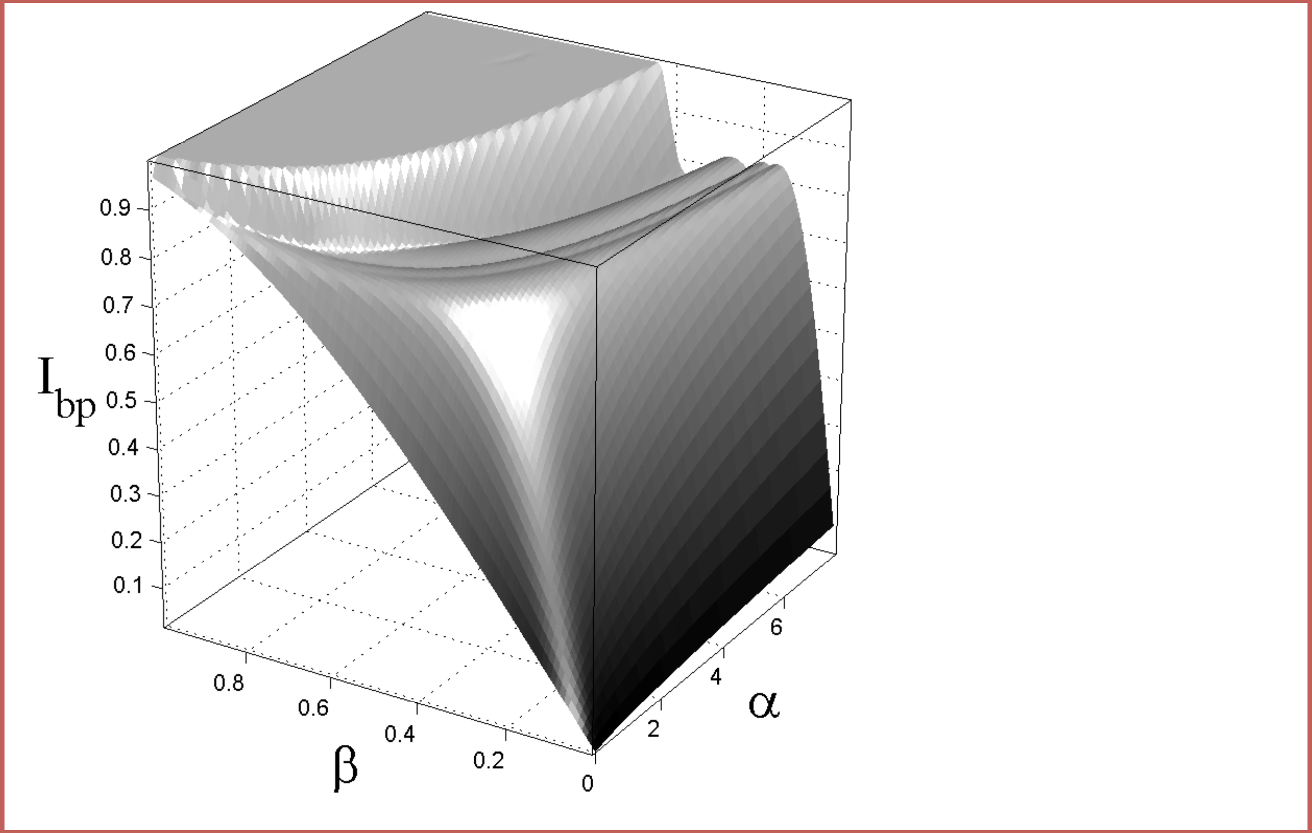

Yu.M.Shukrinov, F.Mahfouzi. Phys.Rev.Lett, 98, 157001 (2007)

(a,b) - The α – and β–dependence of the BPC at PBC.
(c) - Charge distribution among the junctions in the stack for different plasma modes

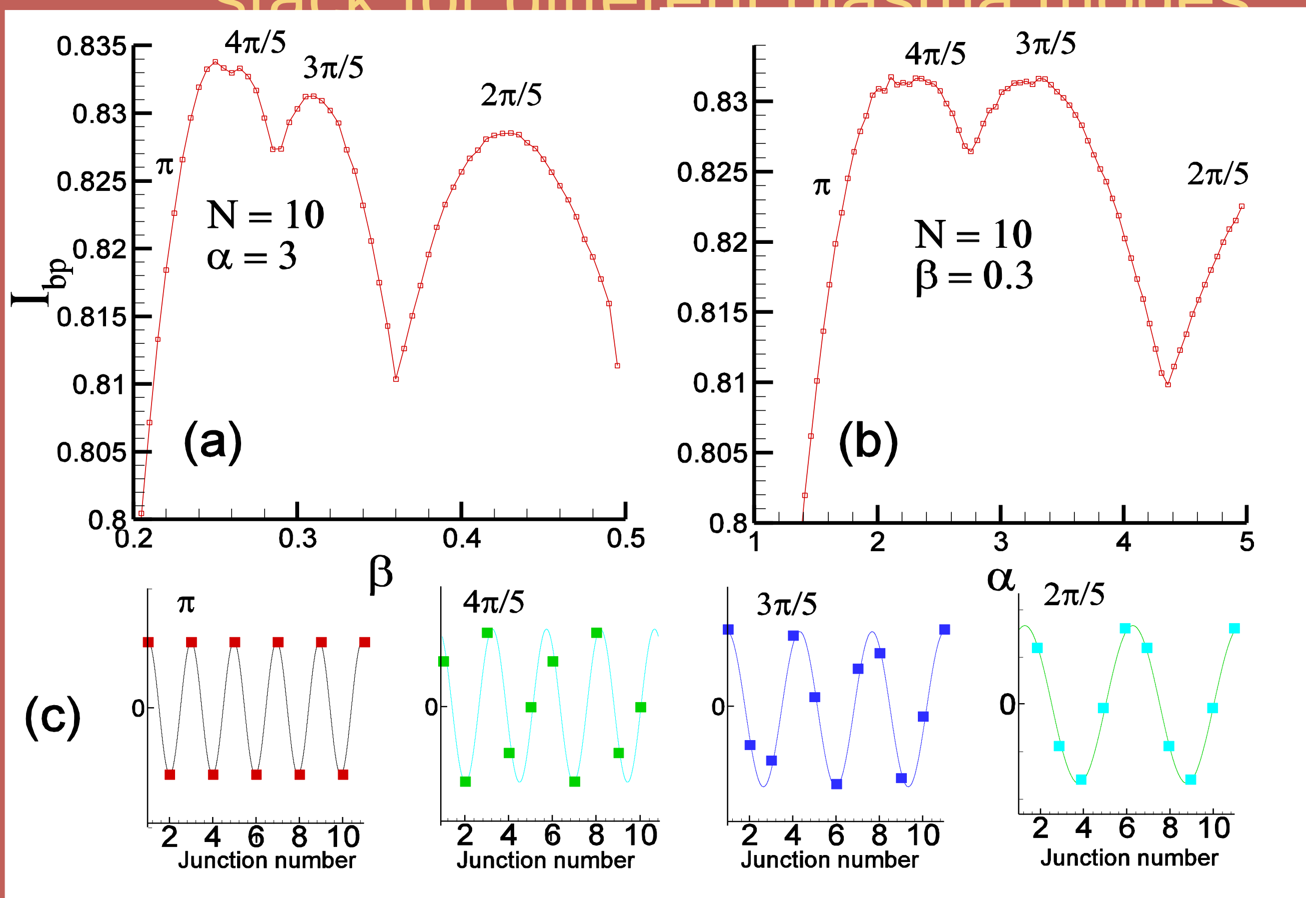

$\beta = 0.24$

$\beta = 0.27$

$\beta = 0.3$

$\beta = 0.4$

Yu.M.Shukrinov, F.Mahfouzi. Phys.Rev.Lett, 98, 157001 (2007)

Equation for difference of phase differences

By subtracting equation (1) for $(l)th$ and $(l-1)th$ junctions we have

$$(\ddot{\varphi}_l - \ddot{\varphi}_{l-1}) + (1 - \alpha\nabla^{(2)})\{\sin(\varphi_l) - \sin(\varphi_{l-1}) + \beta(\dot{\varphi}_l - \dot{\varphi}_{l-1})\} = 0$$

In linear approximation for difference of phase differences, $\delta_l = \varphi_l - \varphi_{l-1}$, we obtain

$$\ddot{\delta}_l + (1 - \alpha\nabla^{(2)})(\cos(\varphi)\delta_l + \beta\dot{\delta}_l) = 0$$

Expanding $\delta_l(t)$ in the Fourier series

$$\delta_l(t) = \sum_k \delta_k e^{ikl}$$

and taking into account, that

$$\nabla^{(2)} e^{ikl} = 2(\cos(k) - 1)e^{ikl}$$

we get

$$\ddot{\delta}_k + (1 + 2\alpha(1 - \cos(k)))(\beta\dot{\delta}_k + \cos(\varphi)\delta_k) = 0.$$

Equation for difference of phase differences

We consider that in rotating state $\varphi \simeq \Omega t = \frac{1}{N} V t$.
Introducing new dimensionless parameters,

$$\tau = \omega_p(k) t$$

$$\omega_p(k) = \omega_p \sqrt{1 + 2\alpha(1 - \cos(k))}$$

$$\beta(k) = \beta \sqrt{1 + 2\alpha(1 - \cos(k))}$$

$$\Omega(k) = \Omega \frac{1}{\sqrt{1 + 2\alpha(1 - \cos(k))}}$$

equation (9) can be written as

$$\ddot{\delta}_k + \beta(k)\dot{\delta}_k + \cos(\Omega(k)\tau)\delta_k = 0.$$

Parametric resonance region of the equation

$$\ddot{\delta}_k + \beta(k)\dot{\delta}_k + \cos(\Omega(k)\tau)\delta_k = 0$$

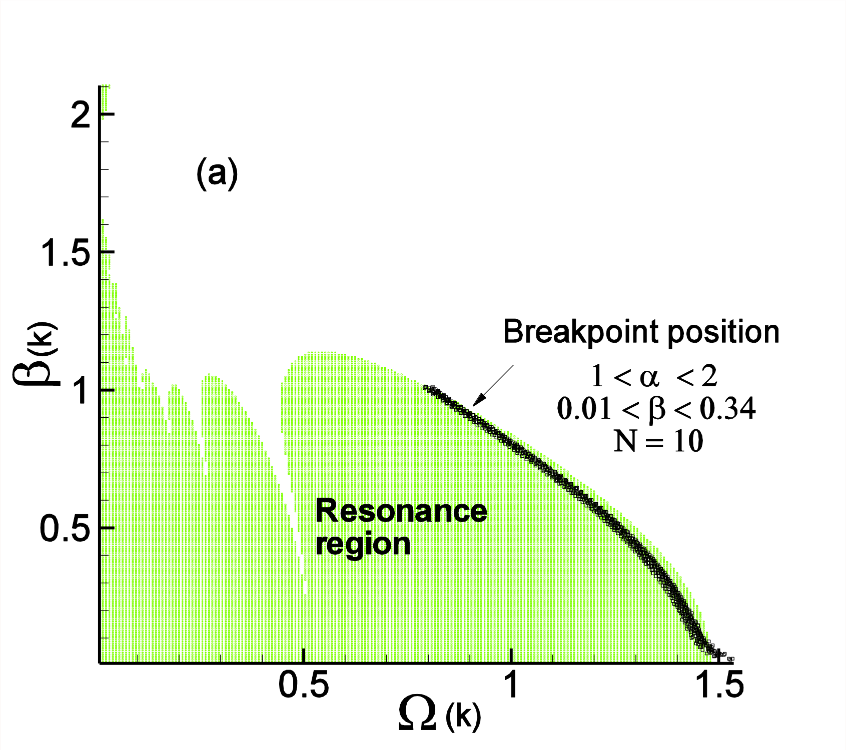

$$\varphi = \Omega t = \frac{1}{N} V t$$

$$\tau = \omega_p(k) t$$

$$\omega_p(k) = \omega_p \sqrt{1 + 2\alpha(1 - \cos k)}$$

$$\beta(k) = \beta \sqrt{1 + 2\alpha(1 - \cos k)}$$

$$\Omega(k) = \frac{\Omega}{\sqrt{1 + 2\alpha(1 - \cos k)}}$$

(a)-Parametric resonance region; (b) - Modeling of the BPC for plasma modes with k = π and k = $2\pi/5$ for stack of 10 IJJ at PBC; (c), (d)- Modeling of the BPC from resonance region.

$$I_{bp} = \beta\sqrt{1+2\alpha(1-\cos k)}\,\Omega_{bp}(k,\beta)$$

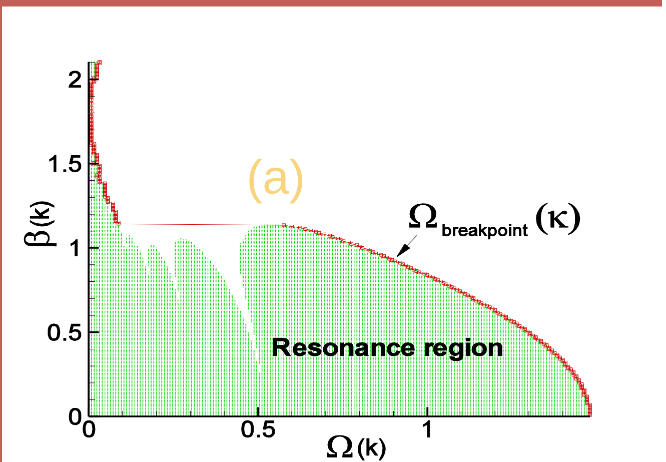

$$V_{bp} / N = I_{bp} / \beta$$

$$\Omega_{bp} = V_{bp} / \left[N\sqrt{1+2\alpha(1-\cos k)} \right]$$

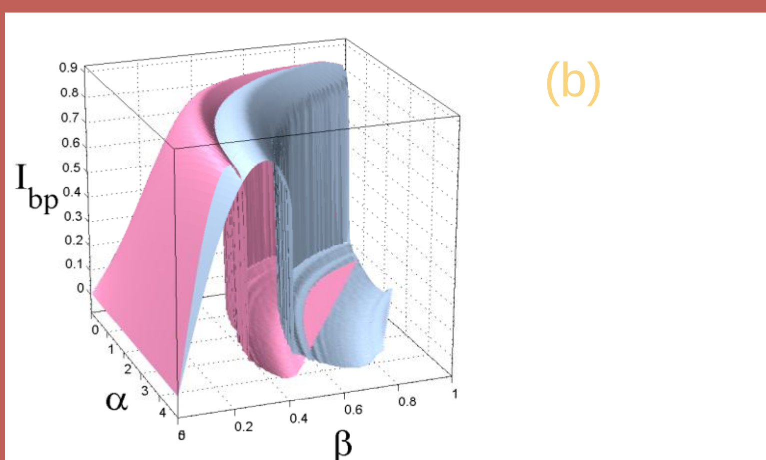

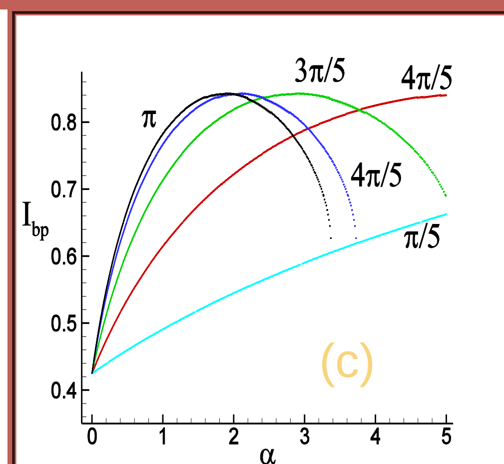

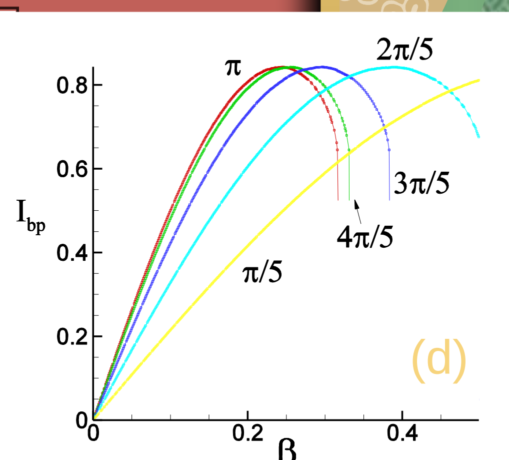

Yu.M.Shukrinov, F.Mahfouzi. Phys.Rev.Lett, 98, 157001 (2007)

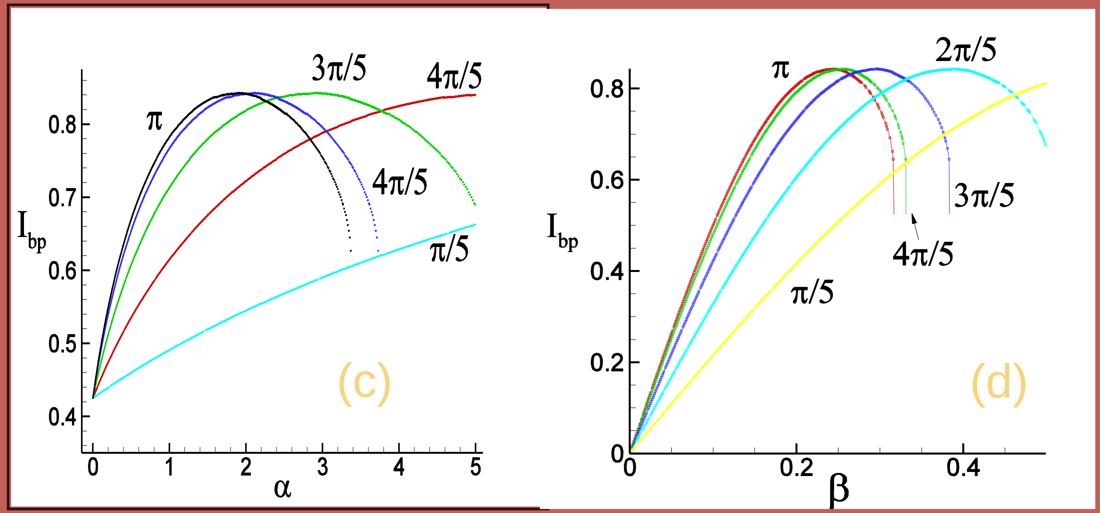

I_{bp}
α
π
$3\pi/5$
$4\pi/5$
$4\pi/5$
$\pi/5$
(c)
0.4
0.5
0.6
0.7
0.8
0 1 2 3 4 5
I_{bp}
β
π
$2\pi/5$
$3\pi/5$
$4\pi/5$
$\pi/5$
(d)
0 0.2 0.4 0.6 0.8
0 0.2 0.4

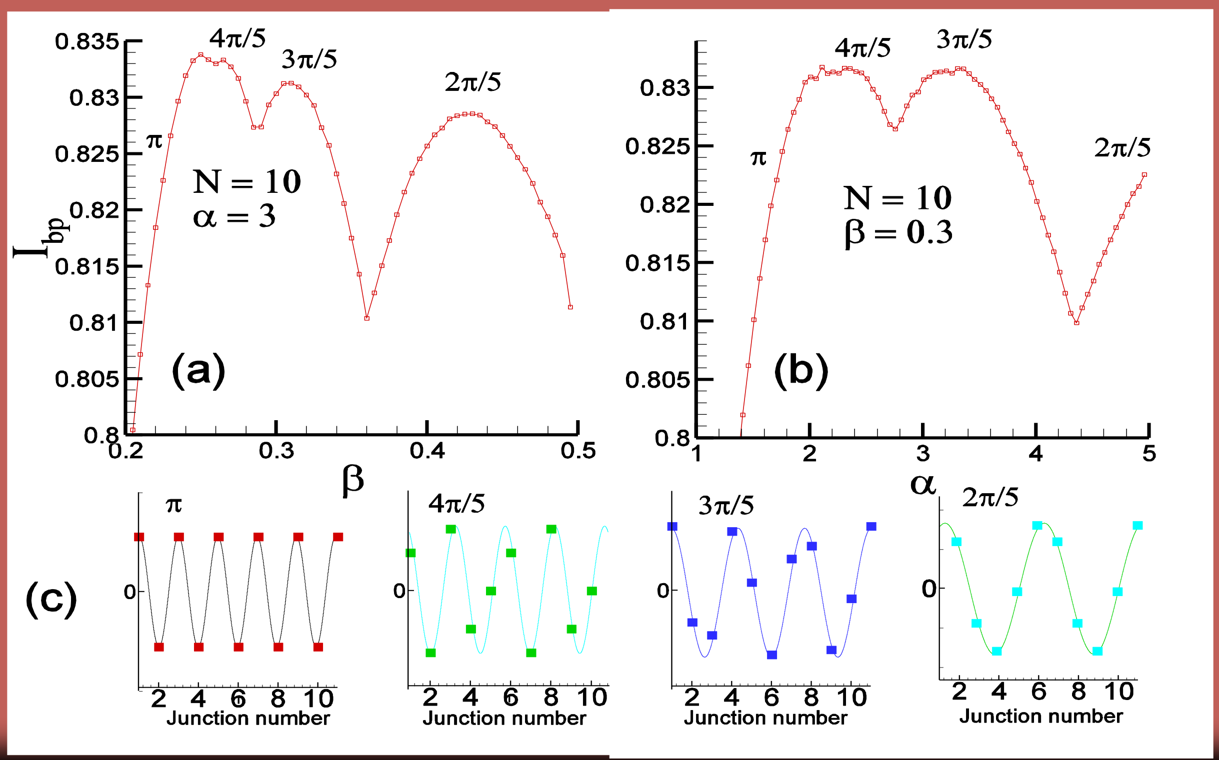

I_{bp}
β
π
$4\pi/5$
$3\pi/5$
$2\pi/5$
N = 10
$\alpha = 3$
(a)
0.8 0.805 0.81 0.815 0.82 0.825 0.83 0.835
0.2 0.3 0.4 0.5
α
π
$4\pi/5$
$3\pi/5$
$2\pi/5$
N = 10
$\beta = 0.3$
(b)
0.8 0.805 0.81 0.815 0.82 0.825 0.83
1 2 3 4 5
(c)
π
$4\pi/5$
$3\pi/5$
$2\pi/5$
0
2 4 6 8 10
Junction number

Modeled and calculated $\alpha\beta$– dependence of the BPC

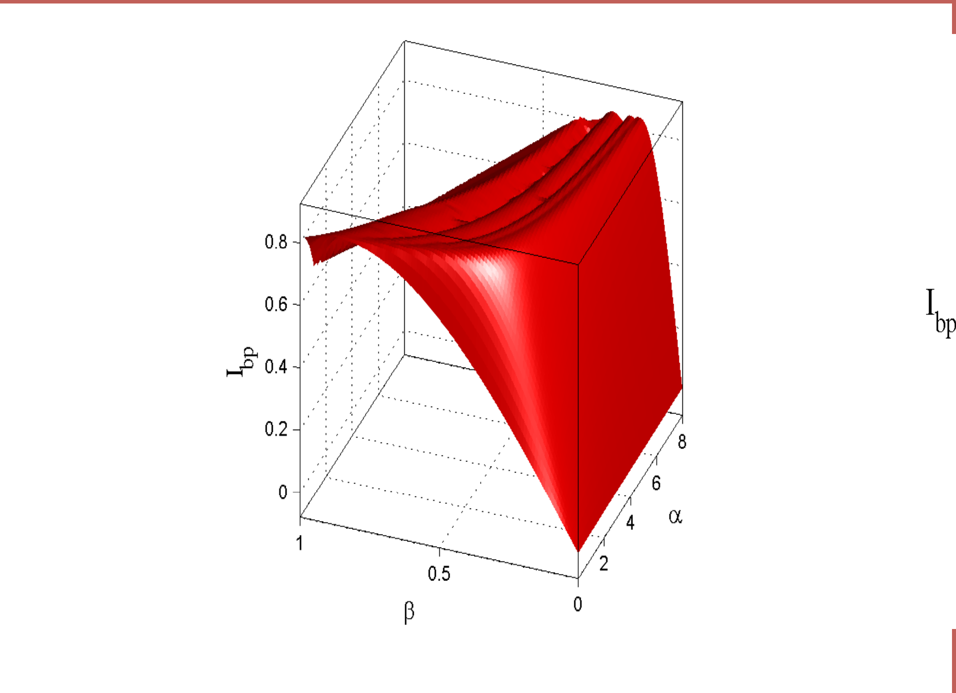

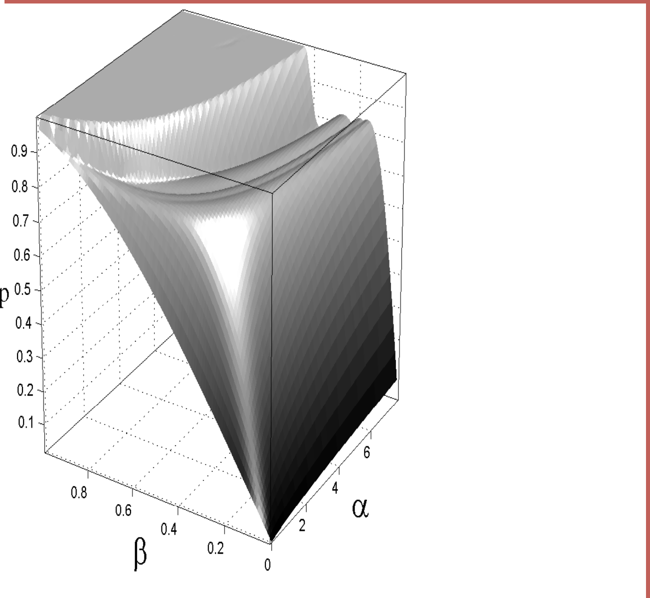

IVC of the stack of 11 IJJ and beta dependence of the

BPC

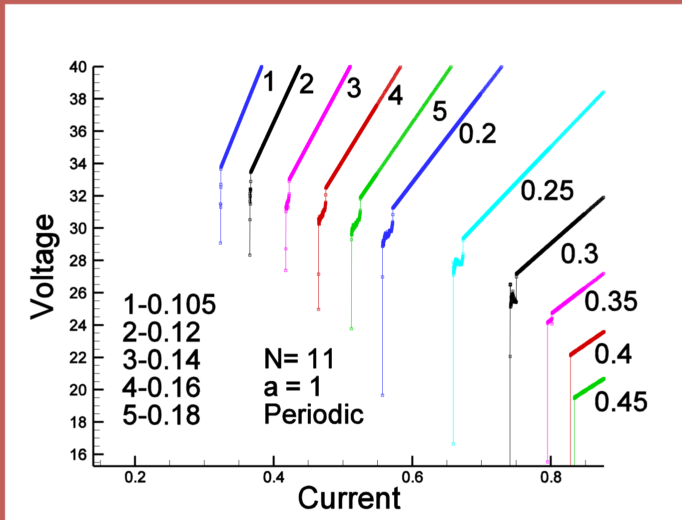

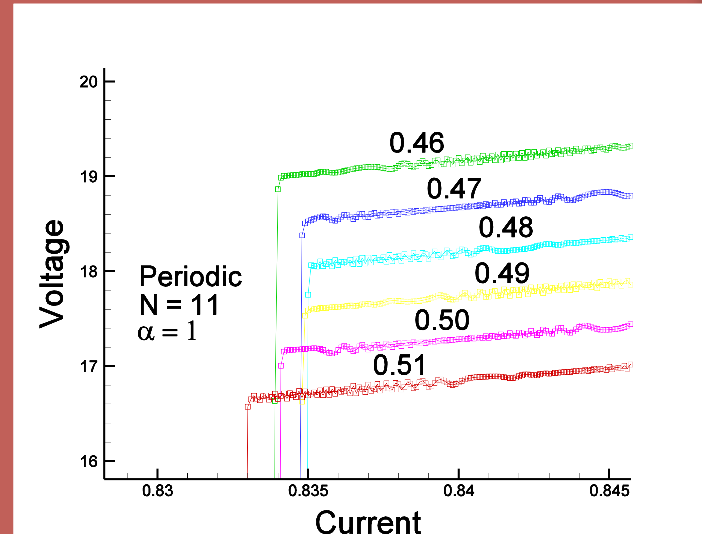

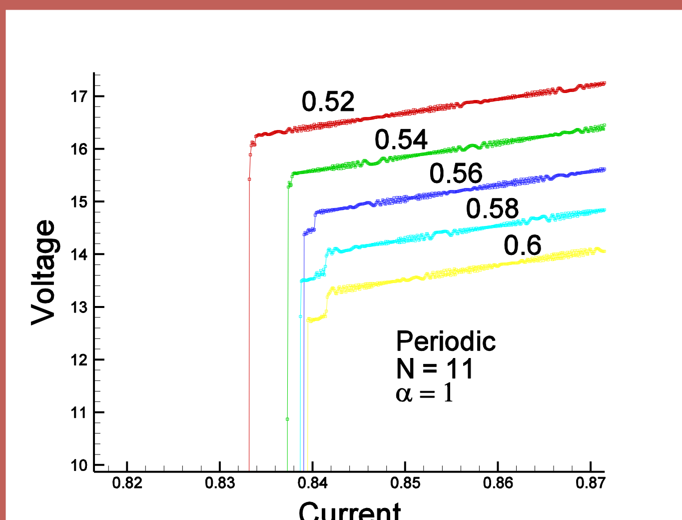

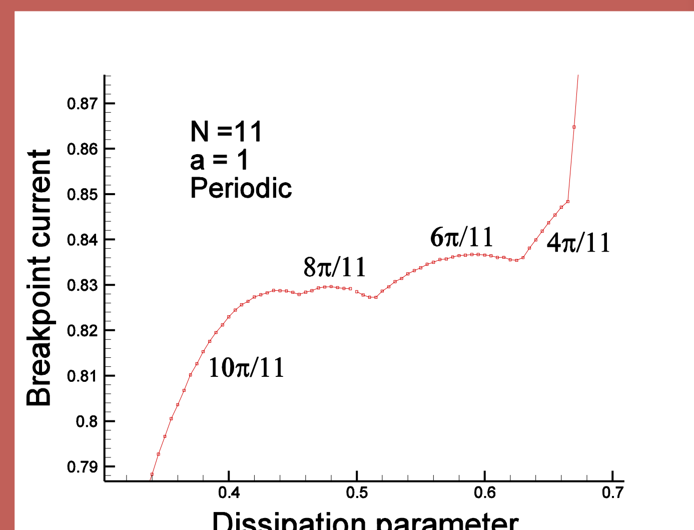

The simulated IVC of the outermost branch in the stack with different number of junctions

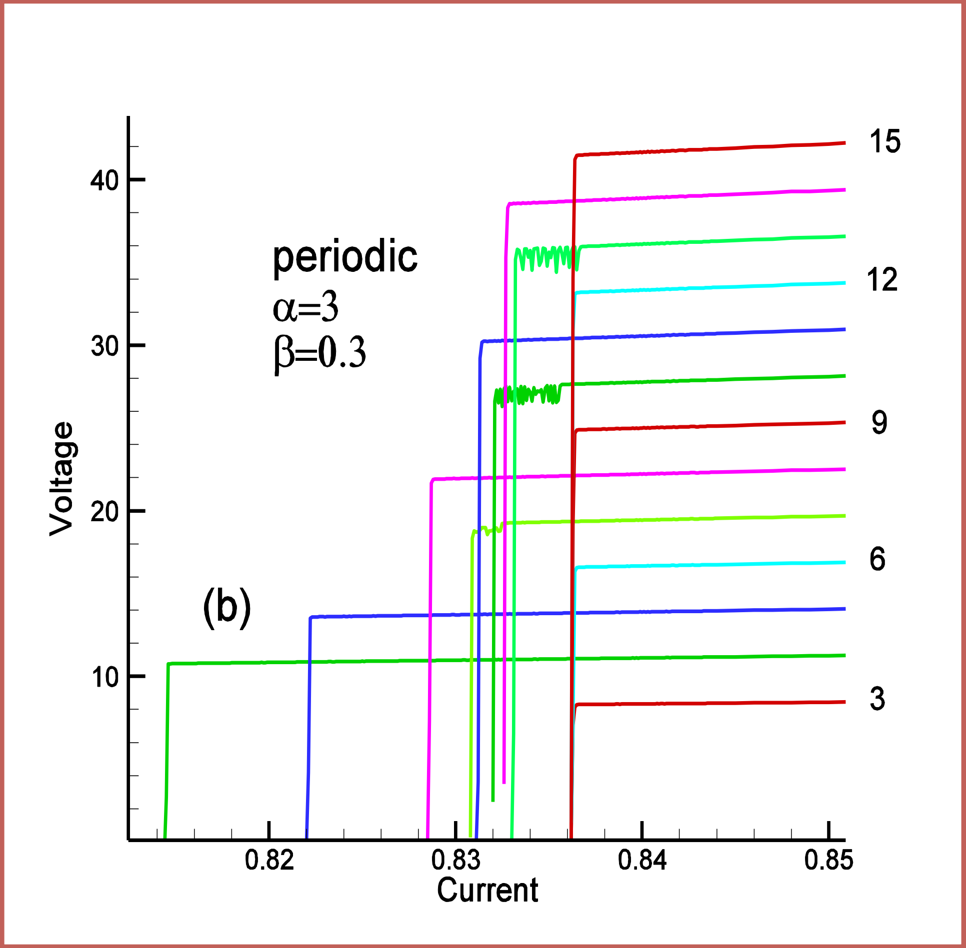

The β–dependence of the BPC for the stacks with different number of IJJ.

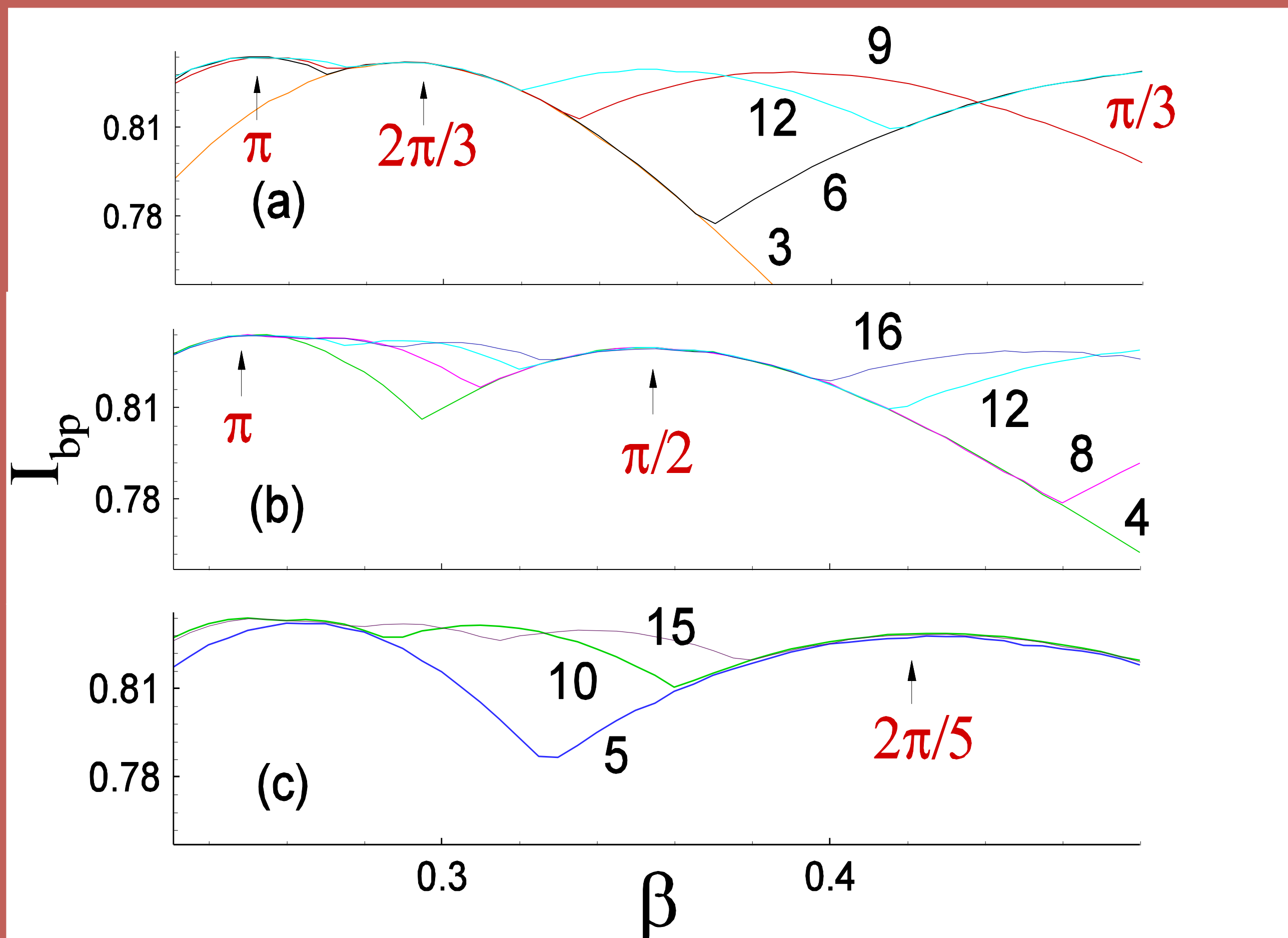

The simulated IVC of the outermost branch in the stacks with different number of junctions

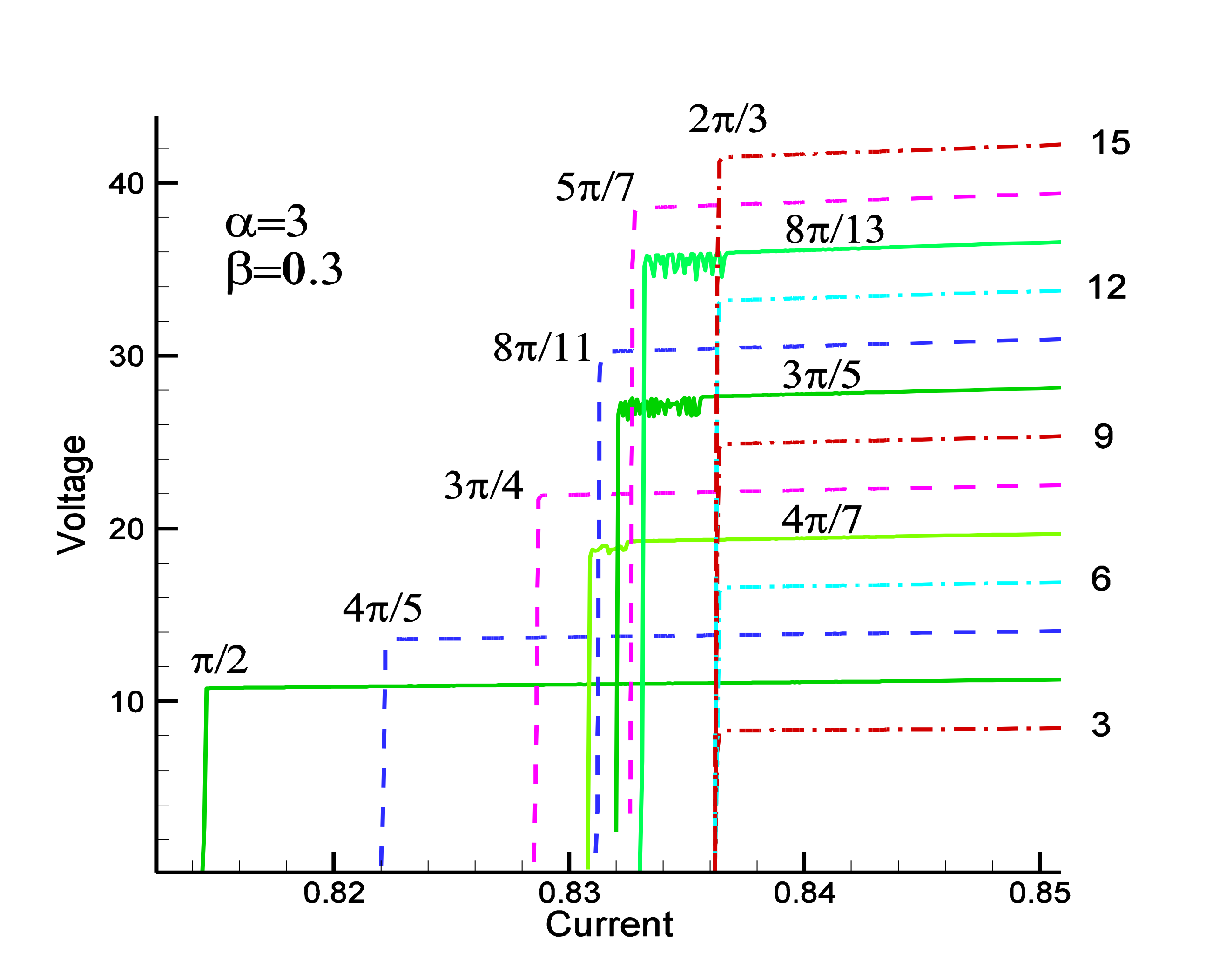

$$N = 3n, \quad k = \frac{2\pi}{3} \qquad N = 3n+1, \quad k = \frac{2(N-1)\pi}{3N} \qquad N = 3n+2, \quad k = \frac{2(N+1)\pi}{3N}$$

Experimental IVC of BSCCO-2212 (Sample Ea, 10K) :Kyoto university, Japan

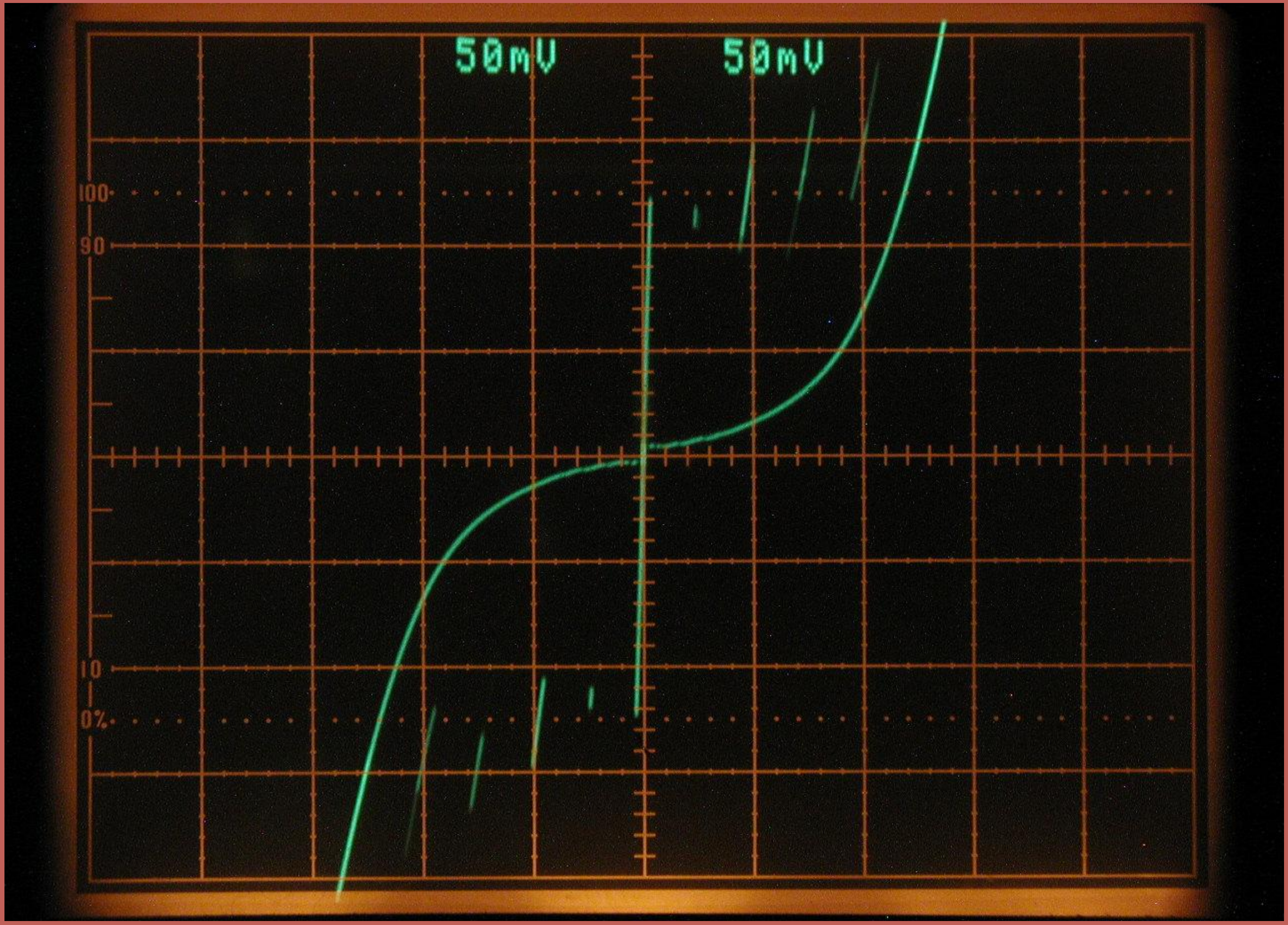

Experimental IVC of BSCCO-2212 (Sample Eb, 35K) :Kyoto university, Japan

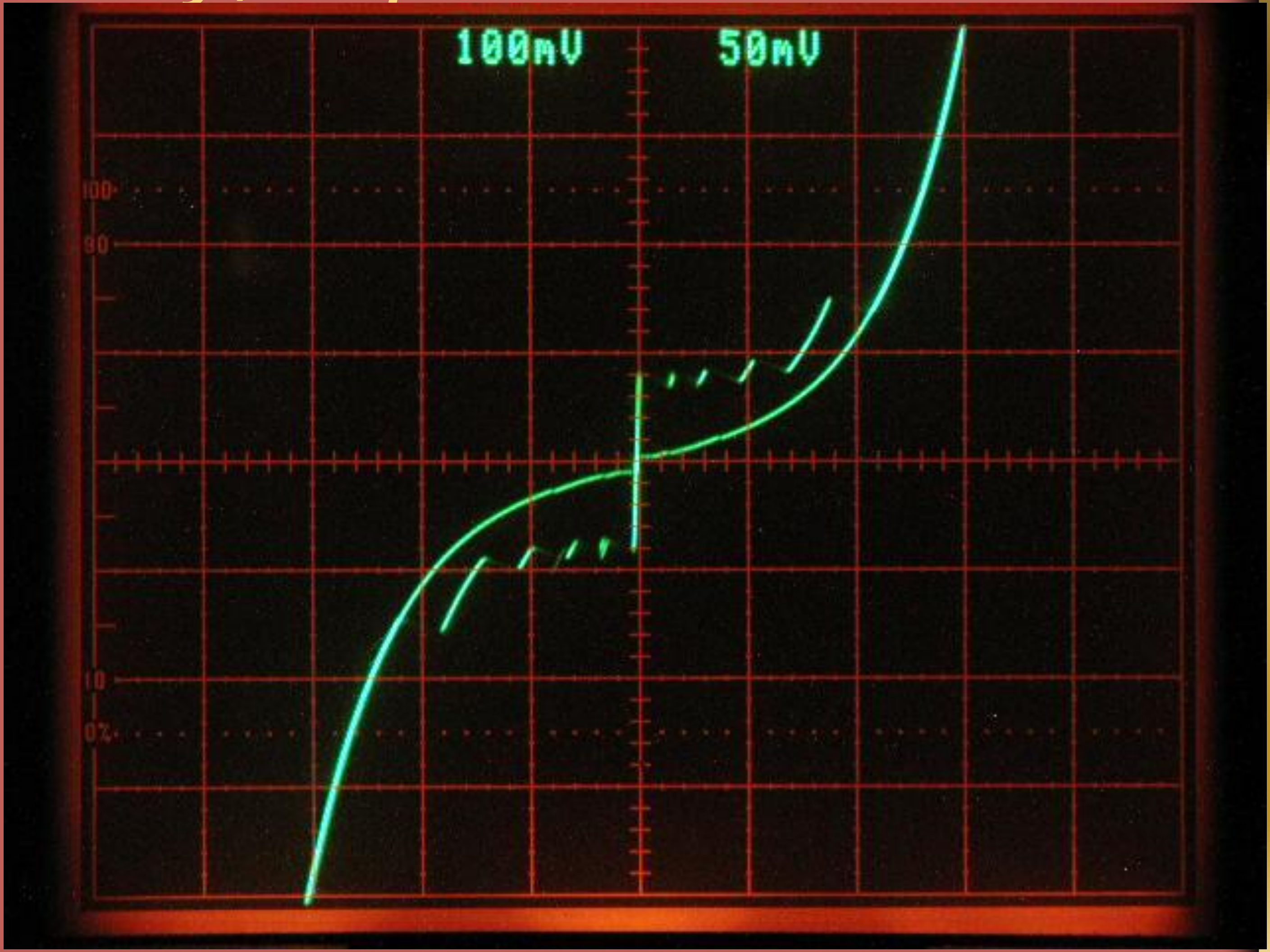

Breakpoint current I_{bp}

Sample:Nm1- 11

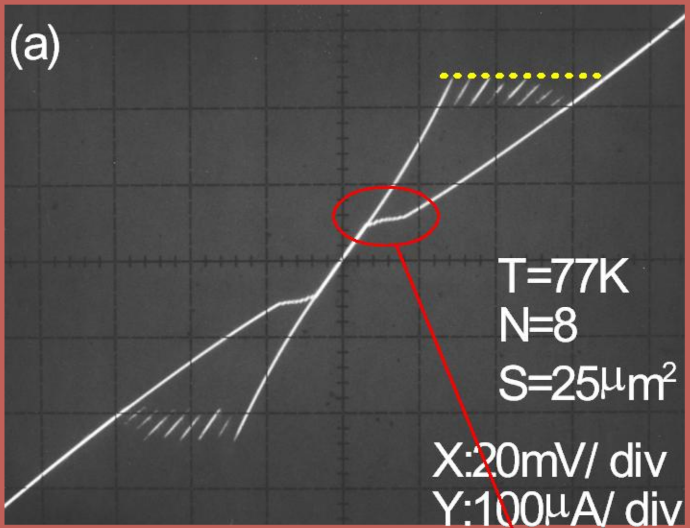

I_c=240μA
I_r=45μA
I_{bp}=54μA
ΔV=39.1mV

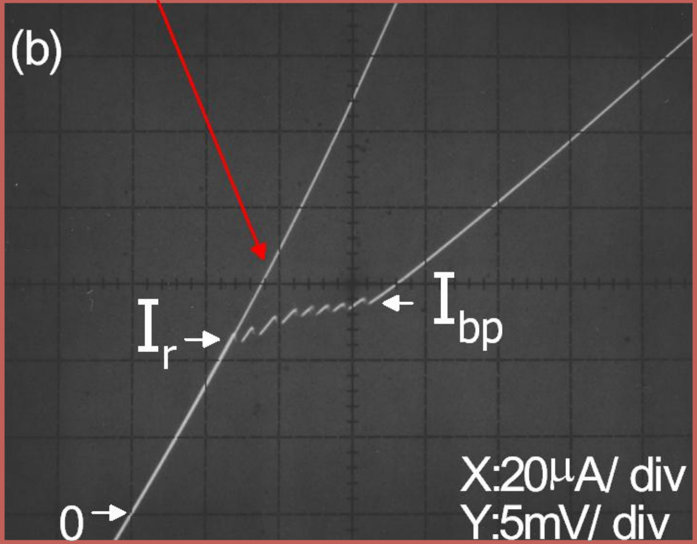

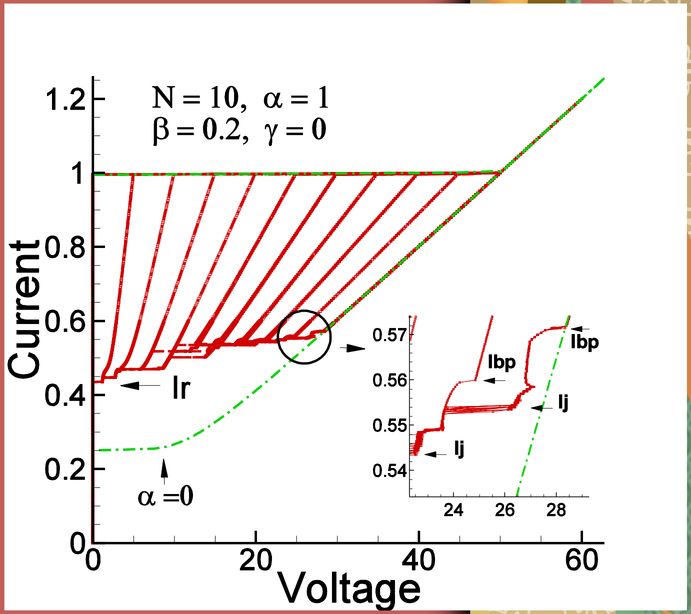

Experimental results:
Utsunomiya university

Breakpoint region

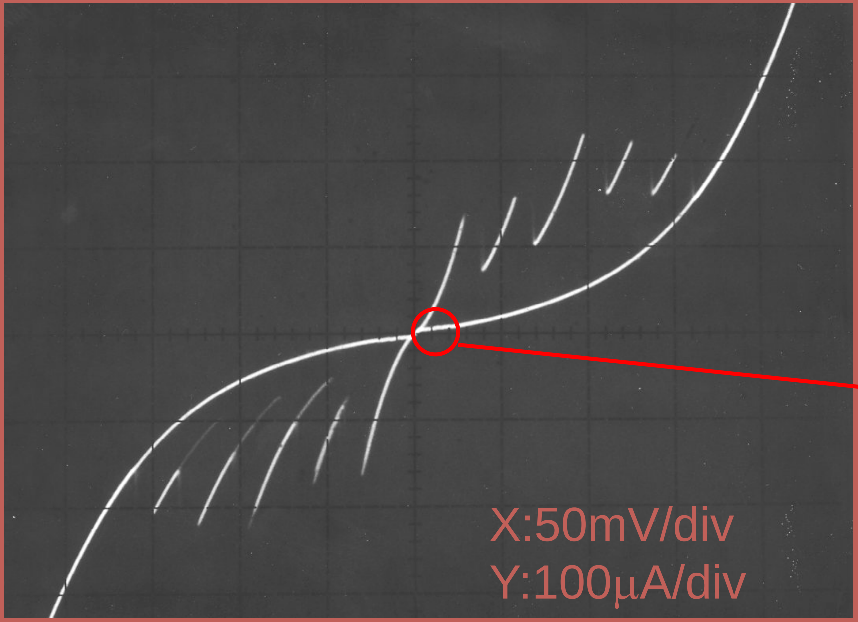

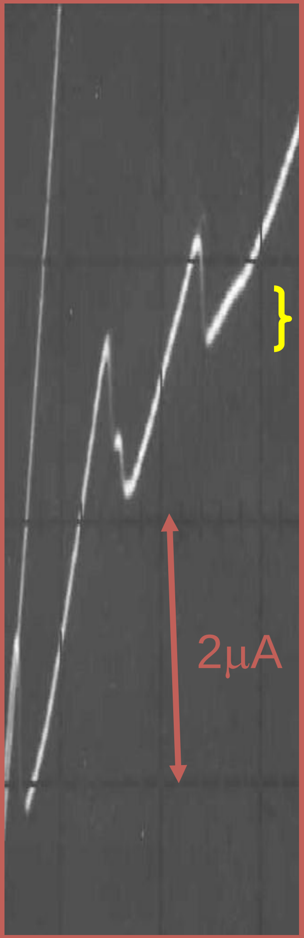

} Breakpoint region

$\Delta I = \sim 0.5 \mu A$

The observation of the breakpoint region suggests the excitation of the longitudinal plasma wave in the mesa.

$\omega_J = 2\omega_p$ ⇨ $f_p = 1.97$ THz

Experimental results: Utsunomiya university

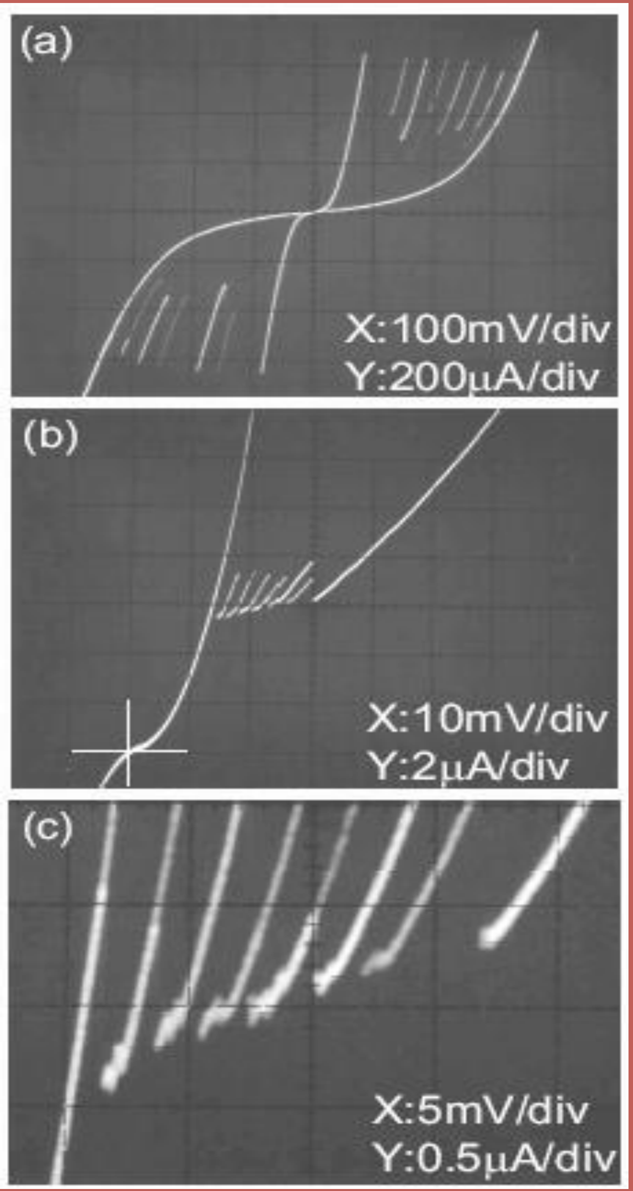

Experimental results: Utsunomiya university

Lecture 3

1. Fine Structure of the Breakpoint Region.
2. Temperature Dependence of the Breakpoint Current

Yu.M.Shukrinov

BLTP, JINR, Dubna, , Russia

CCJJ+DC model

$$\frac{d^2}{dt^2}\varphi_l = (I - \sin\varphi_l - \beta\frac{d\varphi_l}{dt})$$

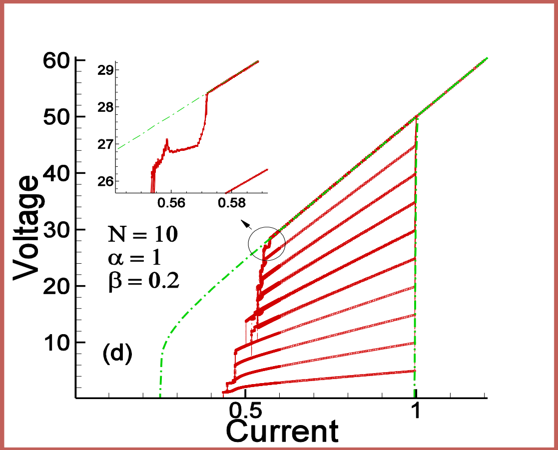

$$+\alpha(\sin\varphi_{l+1} + \sin\varphi_{l-1} - 2\sin\varphi_l)$$

$$+\alpha\beta(\frac{d\varphi_{l+1}}{dt} + \frac{d\varphi_{l-1}}{dt} - 2\frac{d\varphi_l}{dt})$$

Yu.M.Shukrinov, F.Mahfouzi.
- Supercond.Sci.Technol. 20 (2007) S38-S42

Time dependence

- div $(\varepsilon\varepsilon_0 E) = \rho$

$Q_l = Q_0\ \alpha\ (V_{l+1} - V_l)$

$Q_0 = \varepsilon\ \varepsilon\ _0\ V_0/r_D^2$

- The "time dependence" actually consists of time and bias current variation.
- We solve the system of dynamical equations for phase differences at fixed value of bias current I in some time interval $(0, T_m)$ of dimensionless time $\tau = t\omega_p$ with the time step $\delta\ \tau$, where t is a real time. This interval is used for time averaging procedure.
- Then we change the bias current by δ I, and repeat the same procedure for the current I+δ I in new time interval $(T_m, 2T_m)$. In our simulations we put T_m=250, $\delta\ \tau$=0.05, δ I=0.0001 and total recorded time was calculated as $\tau + T_m(I_0 - I)/\delta I$, where I_0 is an initial value of the bias current for time dependence recording.

Time dependence of charge oscillation on the layers at periodic boundary condition at I = 0.575 (breakpoint)

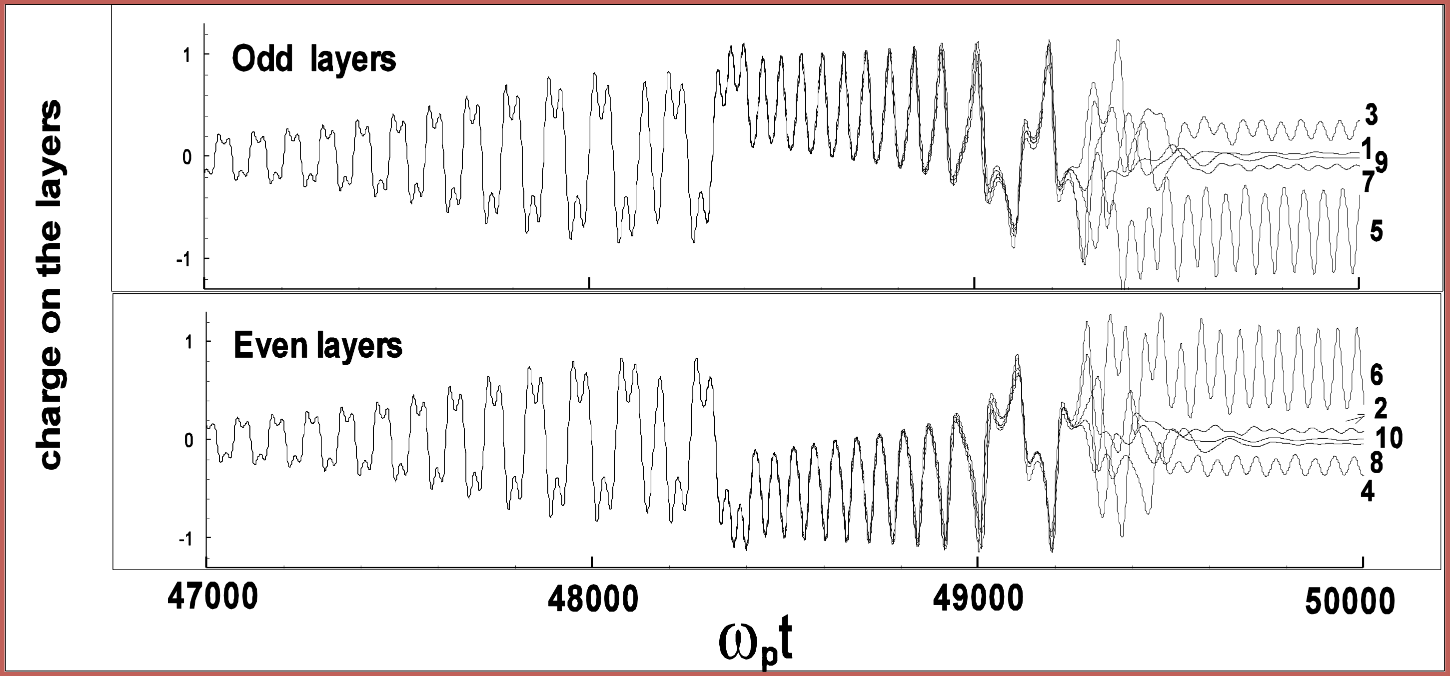

IVC of the stack of 11 IJJ and beta dependence of the BPC

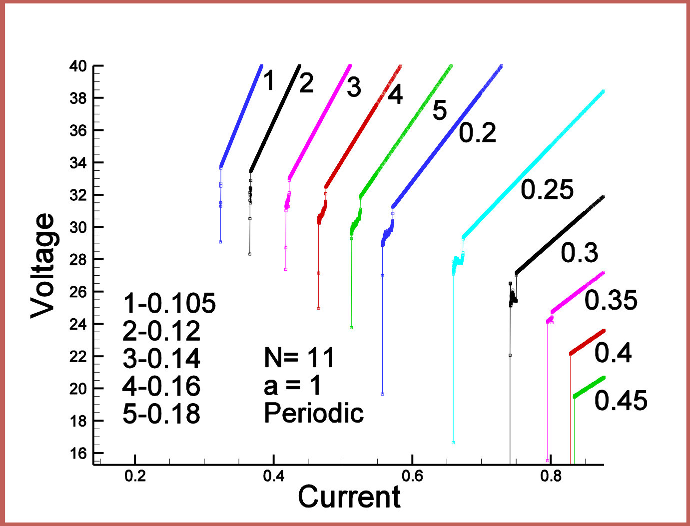

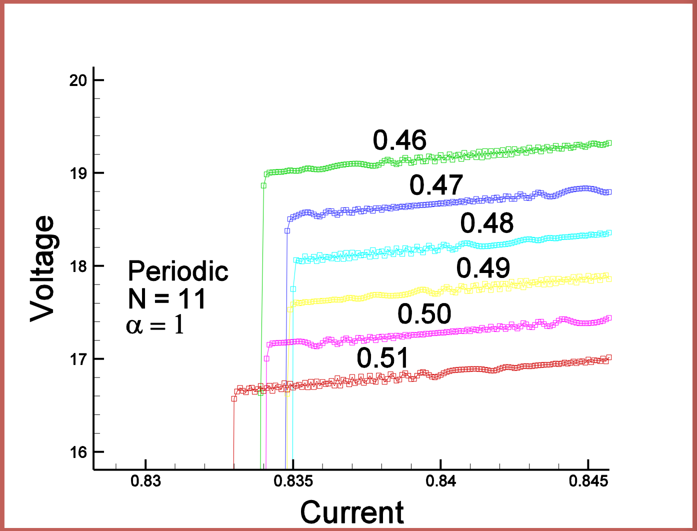

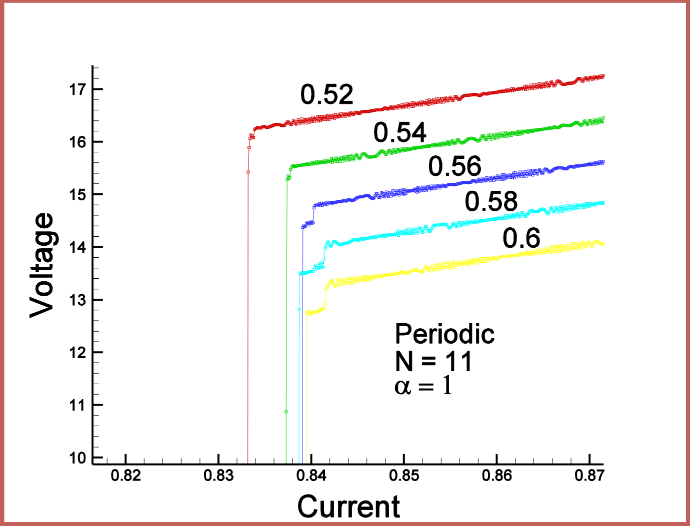

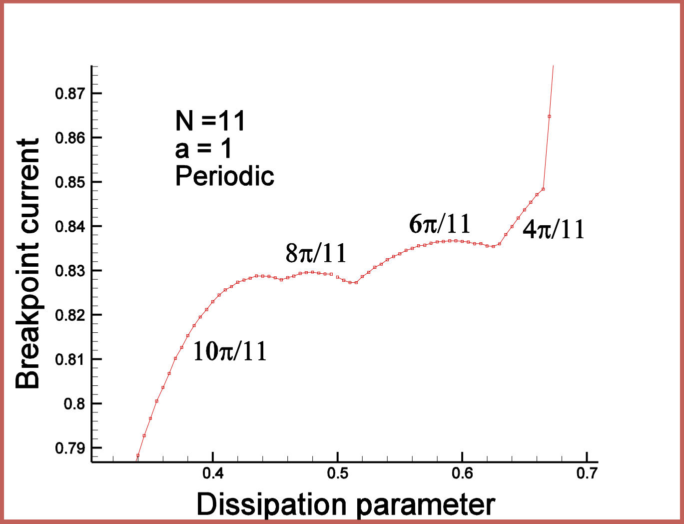

BPR

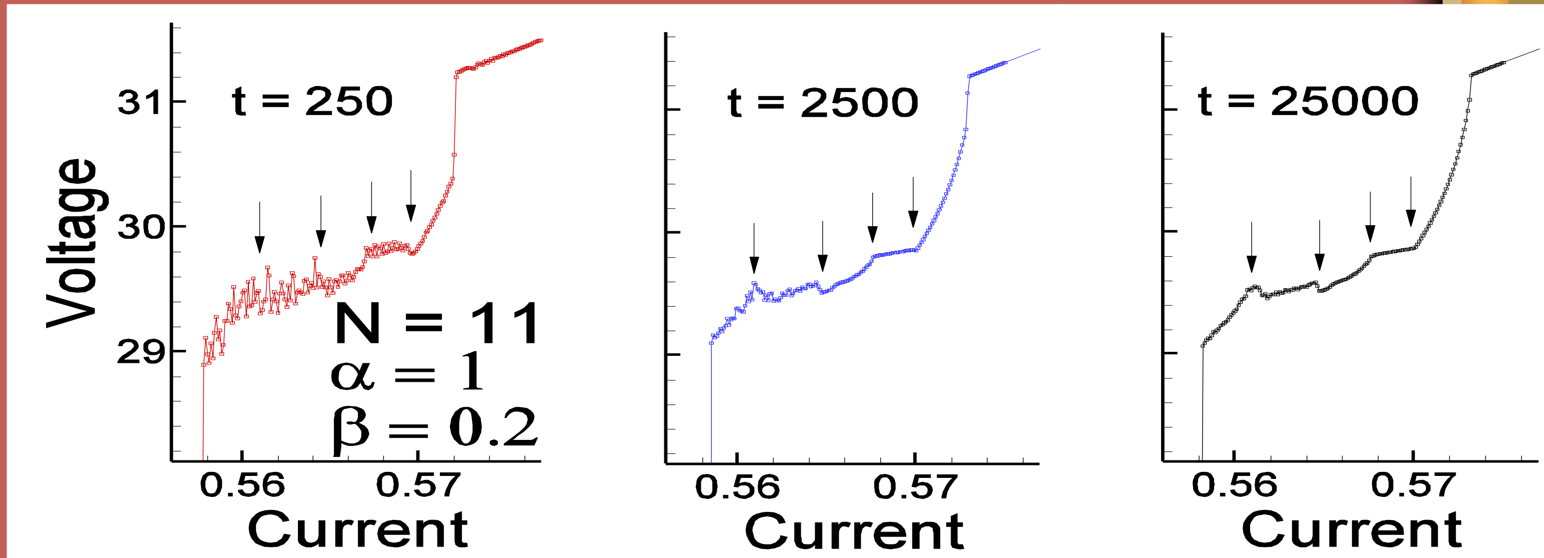

Voltage
31
30
29
t = 250
N = 11
α = 1
β = 0.2
0.56
0.57
Current
t = 2500
0.56
0.57
Current
t = 25000
0.56
0.57
Current

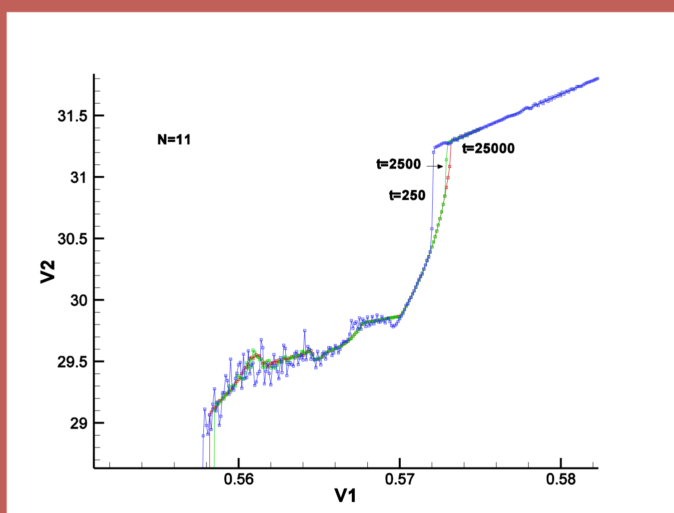

N=11
t=2500
t=25000
t=250
31.5
31
30.5
30
29.5
29
V2
0.56
0.57
0.58
V1

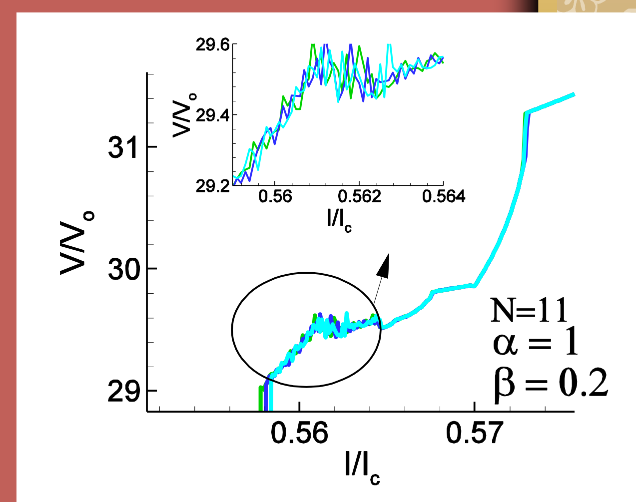

V/V_o
31
30
29
0.56
0.57
I/I_c
N=11
α = 1
β = 0.2
29.6
29.4
29.2
0.56
0.562
0.564

Fine structure in BPR

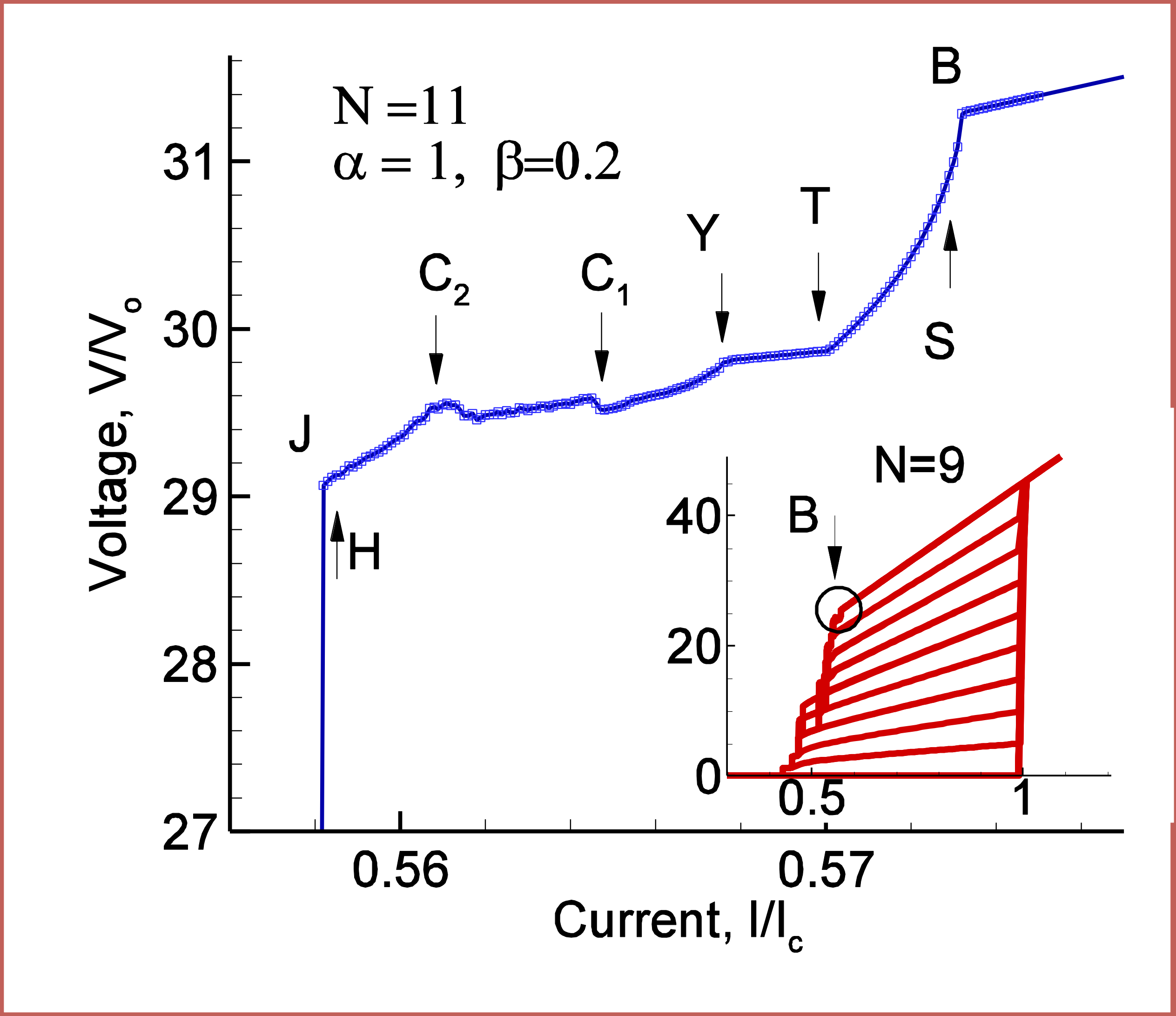

Yu.M.Shukrinov, F.Mahfouzi, M.Suzuki Phys.Rev.B 78, 134521 (2008).

Creation of LPW with k=$10\pi/11$ at the breakpoint for N=11, α=1, β=0.2 and periodic BC

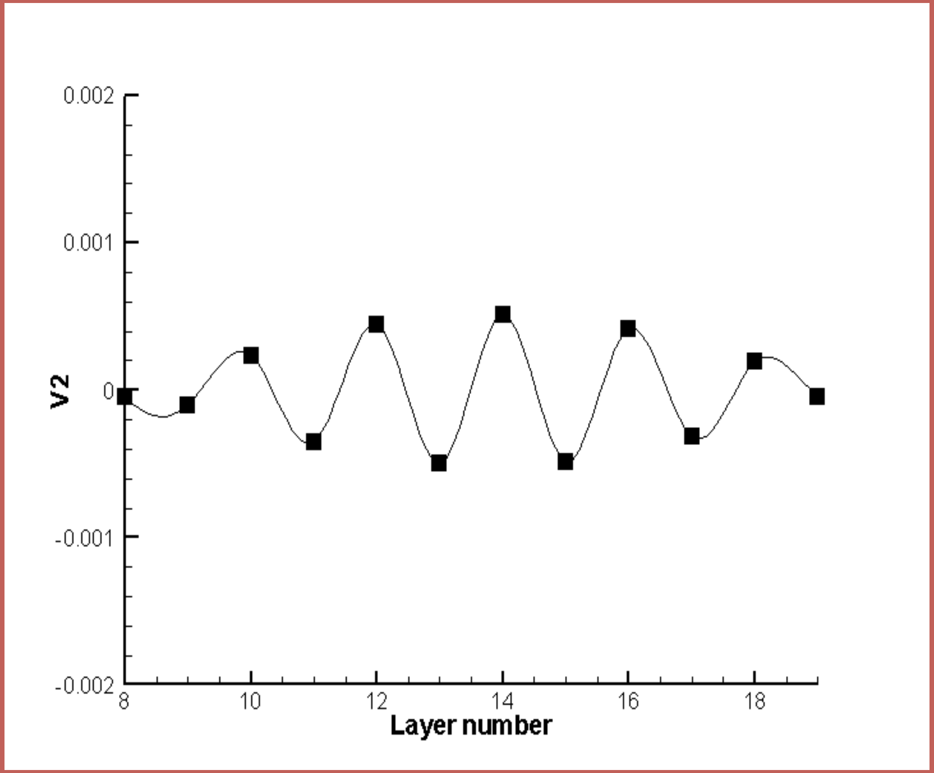

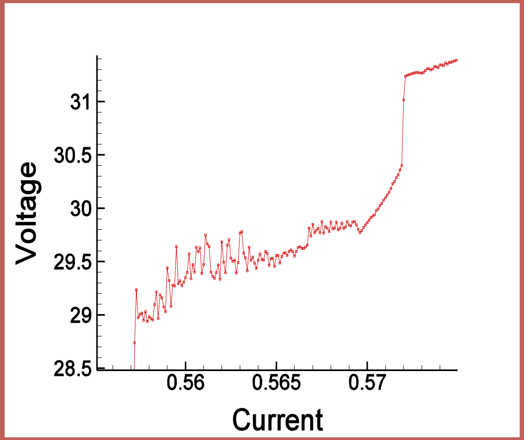

LPW in the breakpoint region for N=11, a=1, b=0.2 and periodic BC

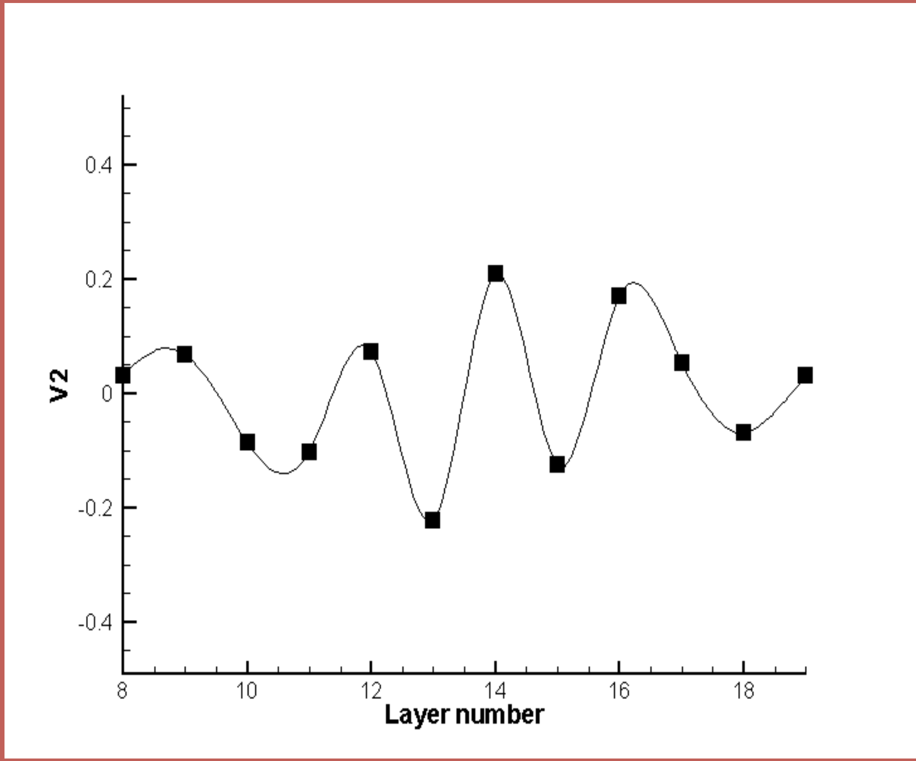

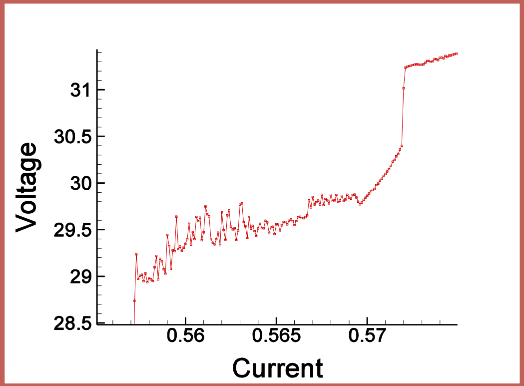

LPW in the breakpoint region for N=11, a=1, b=0.2 and periodic BC

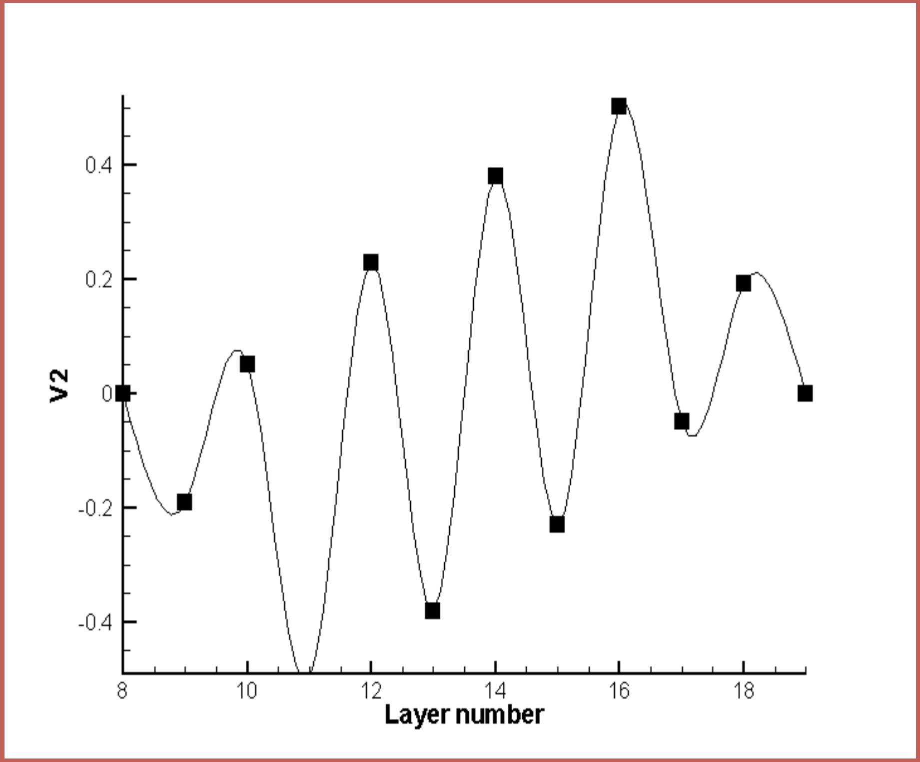

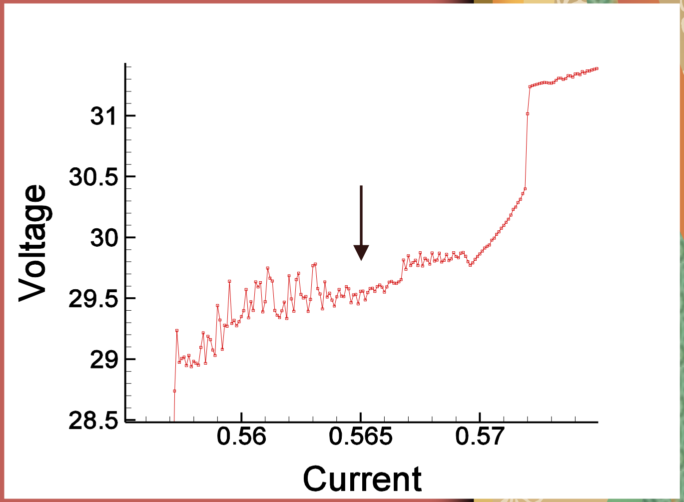

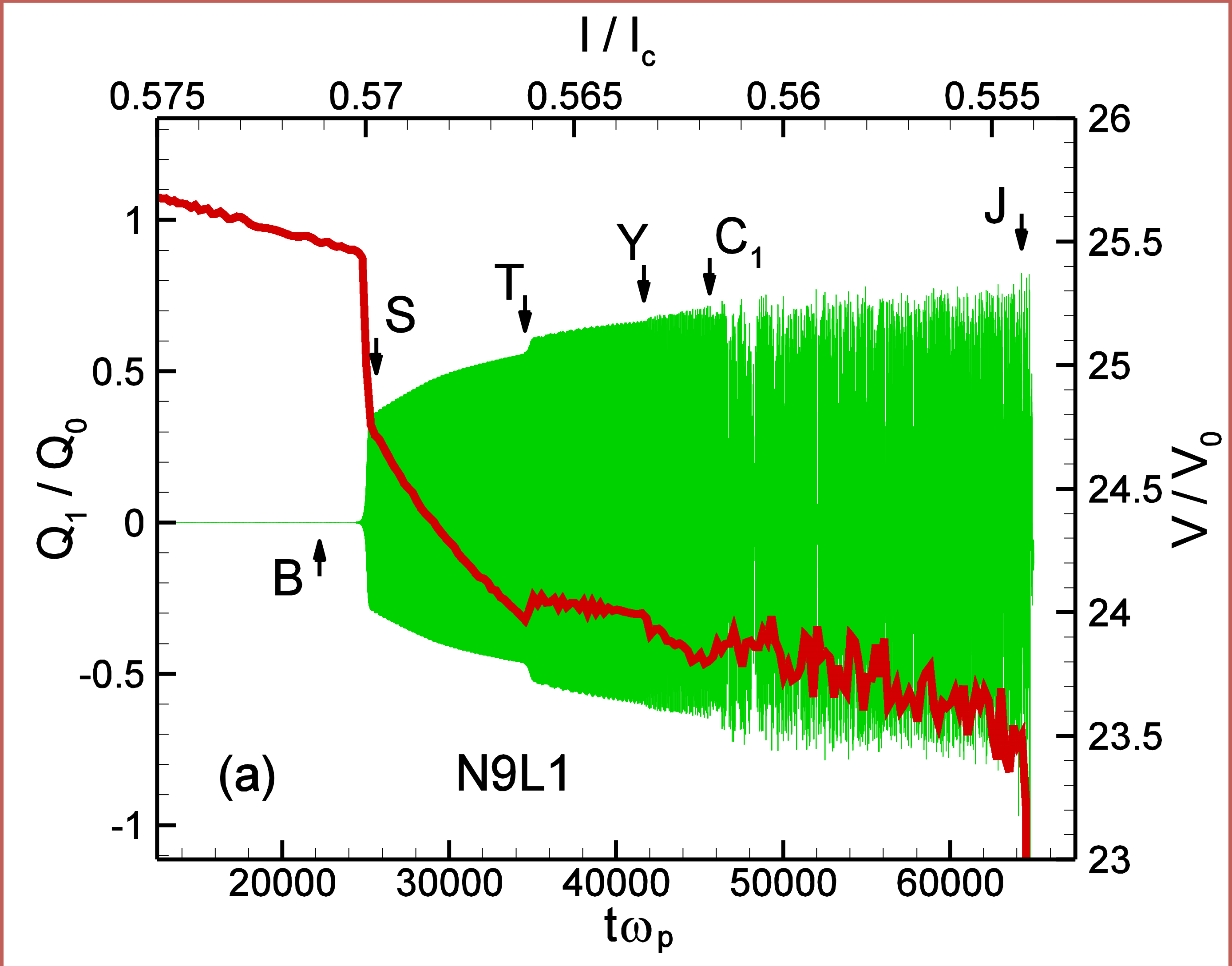

Yu.M.Shukrinov, F.Mahfouzi, M.Suzuki Phys.Rev.B 78, 134521 (2008).

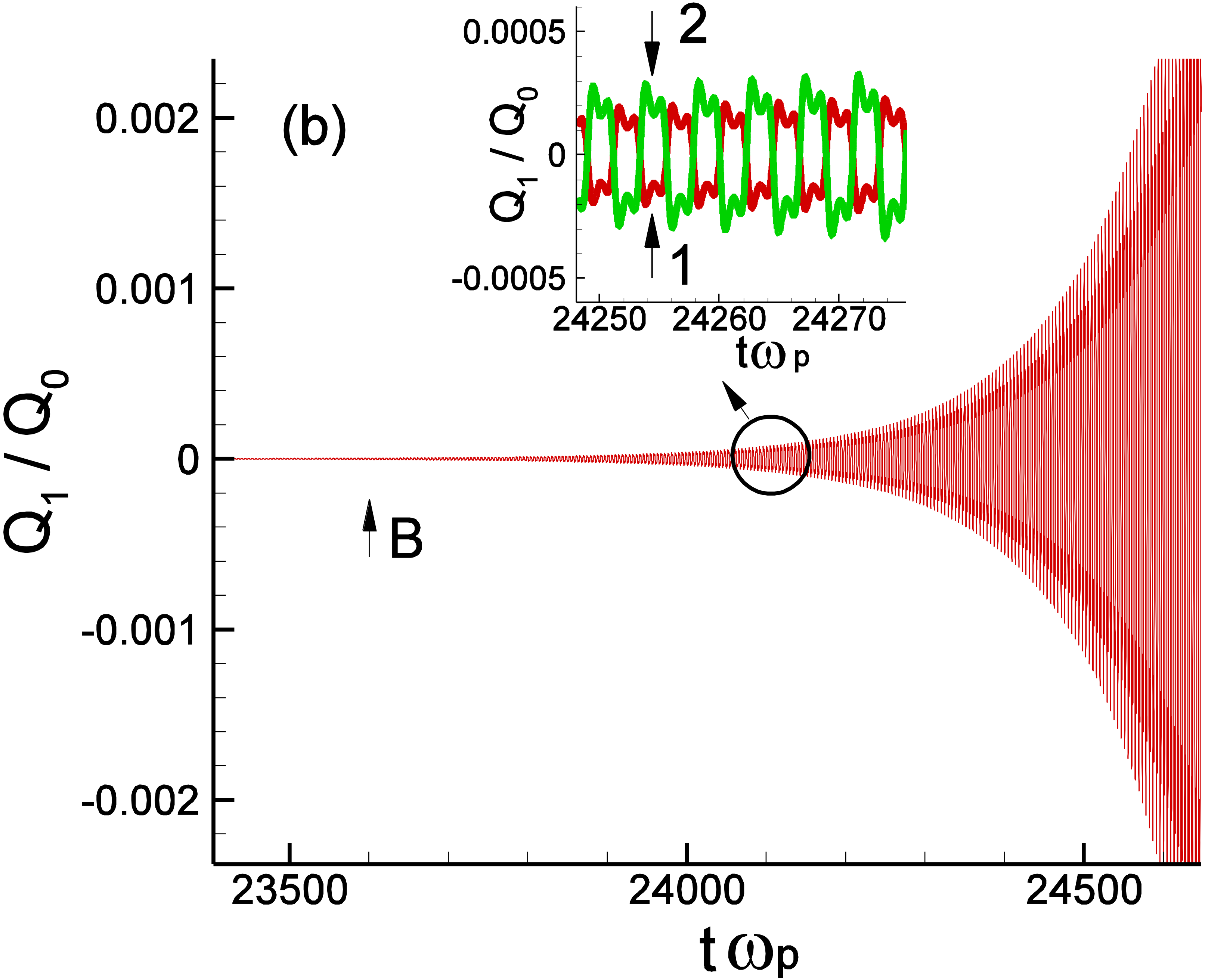

(b)
0.002
0.001
0
-0.001
-0.002
Q1 / Q0
23500
24000
24500
t ωp
B
0.0005
0
-0.0005
24250
24260
24270
tωp
2
1

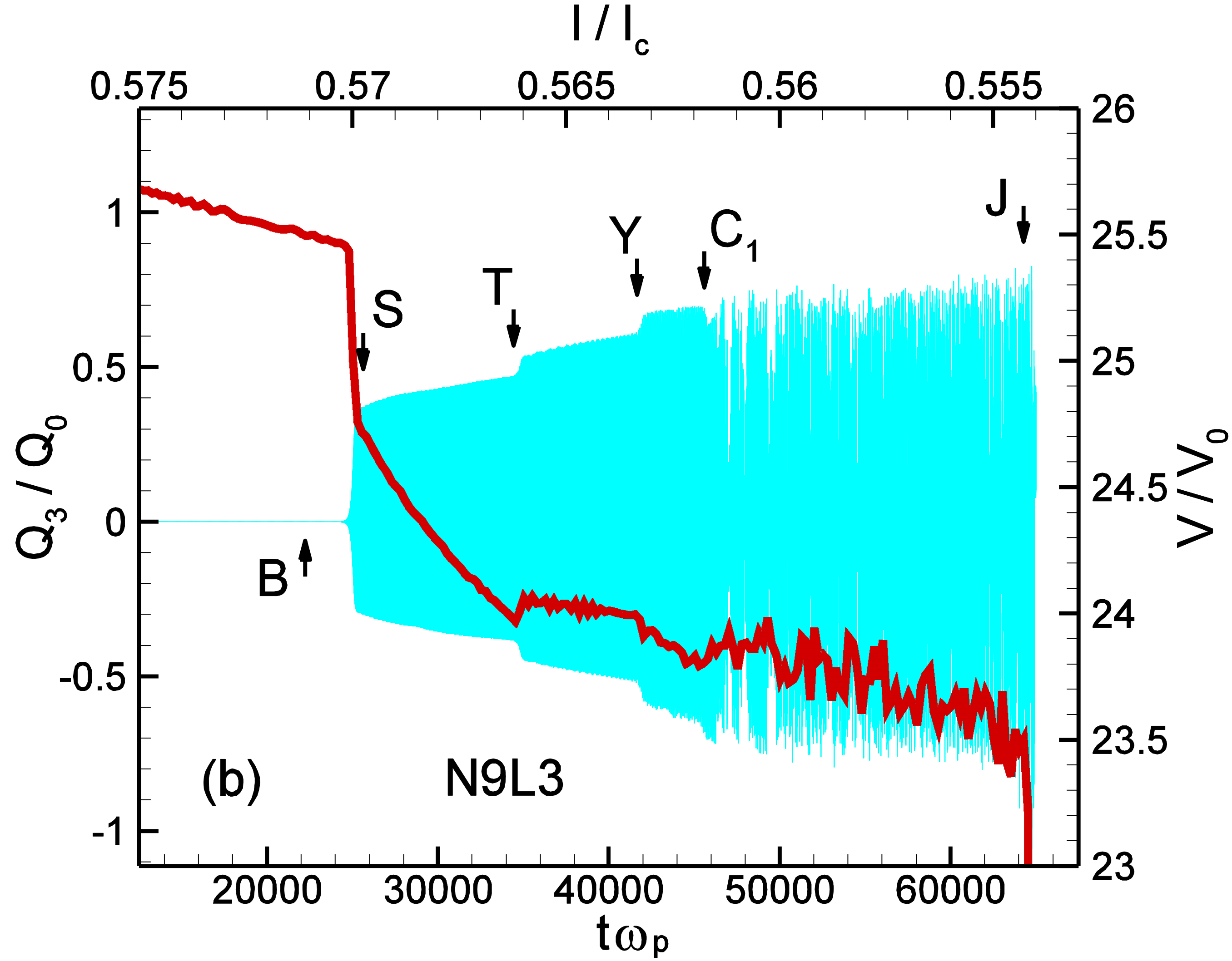

I / I_c
0.575
0.57
0.565
0.56
0.555
26
25.5
25
24.5
24
23.5
23
1
0.5
0
-0.5
-1
Q_3 / Q_0
V / V_0
S
T
Y
C_1
J
B
(b)
N9L3
20000
30000
40000
50000
60000
tω_p

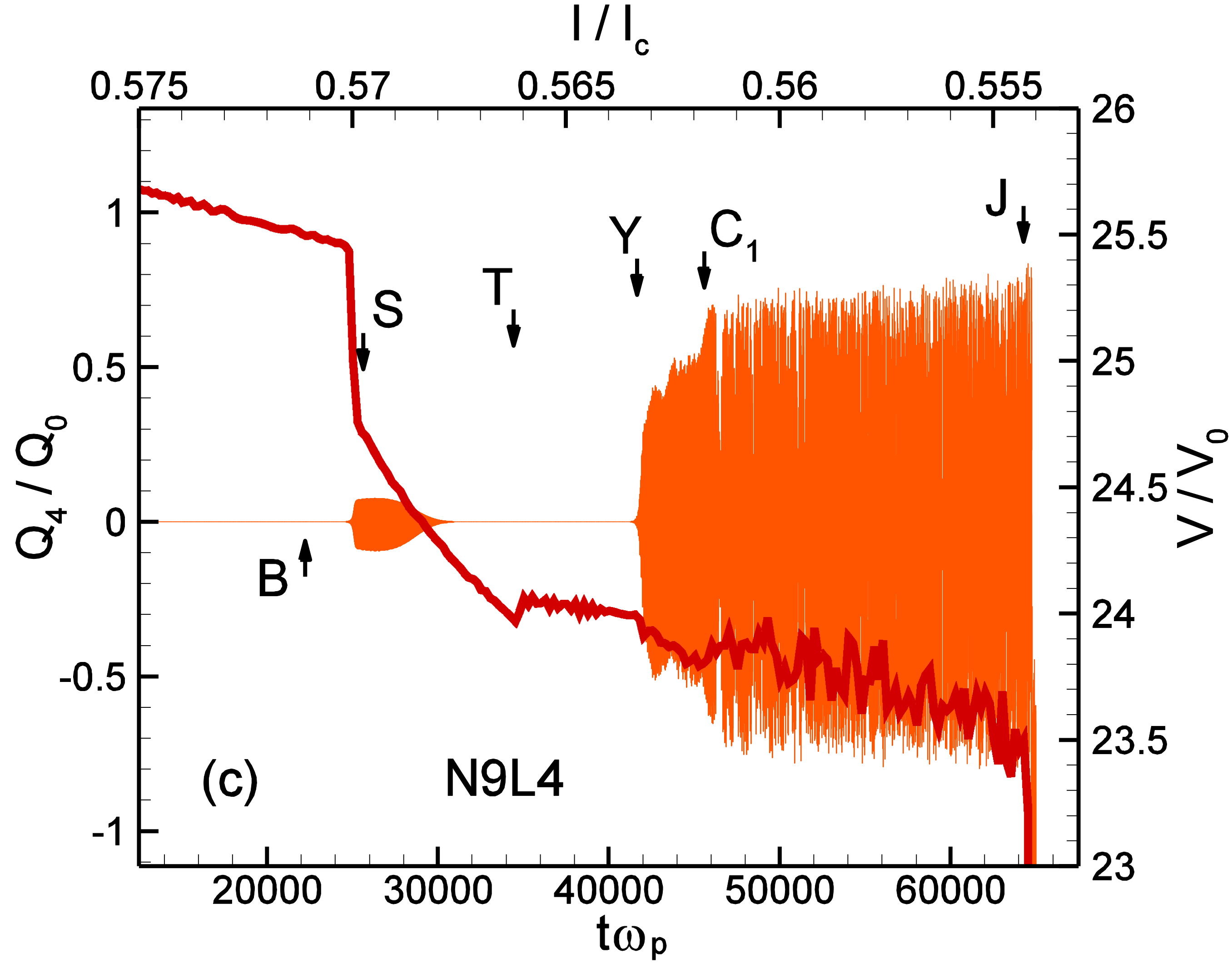

I / I_c
0.575
0.57
0.565
0.56
0.555
26
25.5
25
24.5
24
23.5
23
V / V_0
1
0.5
0
-0.5
-1
Q_4 / Q_0
J
Y
C_1
T
S
B
(c)
N9L4
20000
30000
40000
50000
60000
tω_p

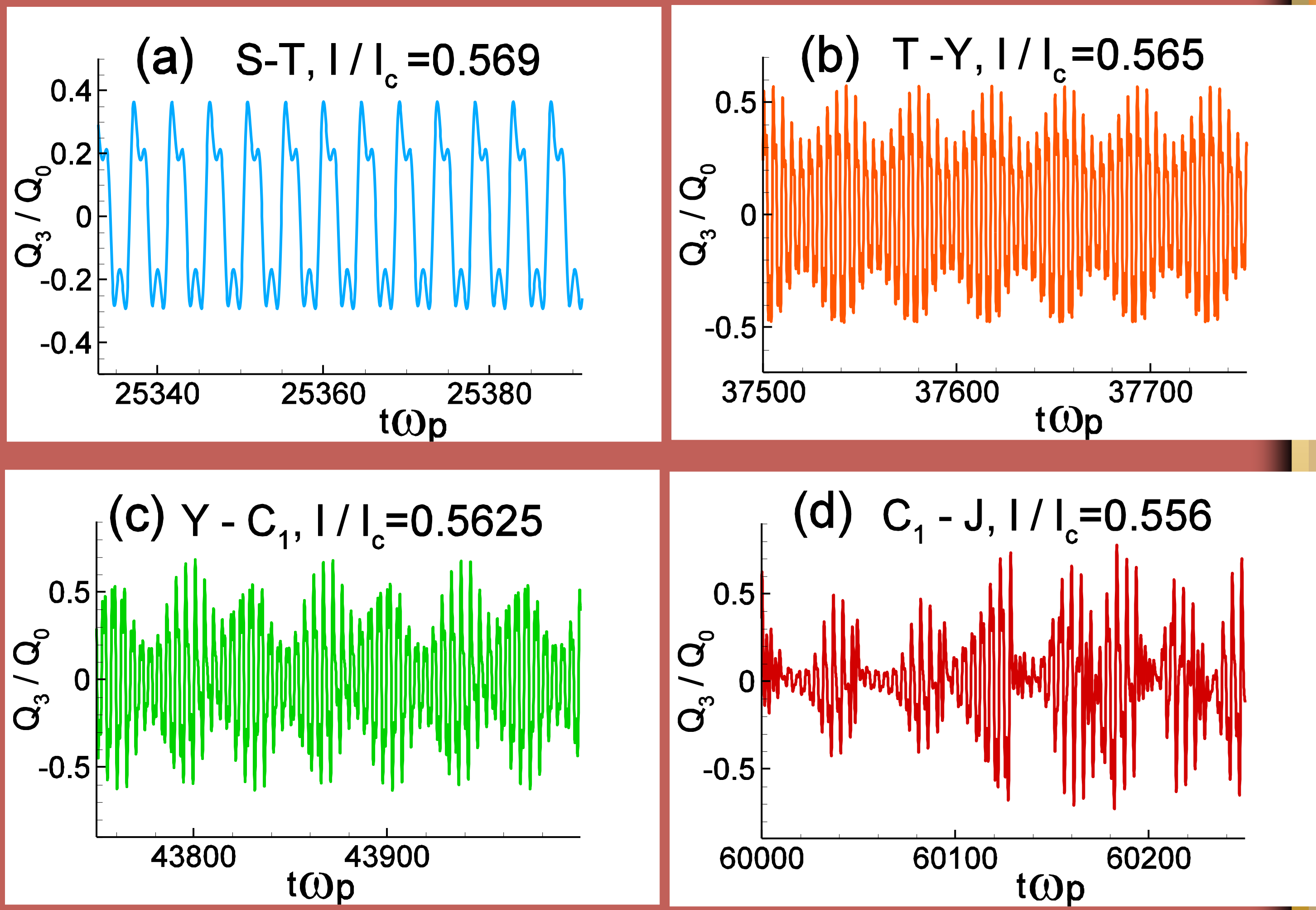

(a) S-T, I / I_c =0.569
Q_3 / Q_0
0.4
0.2
0
-0.2
-0.4
25340
25360
25380
tωp
(b) T -Y, I / I_c =0.565
Q_3 / Q_0
0.5
0
-0.5
37500
37600
37700
tωp
(c) Y - C_1, I / I_c=0.5625
Q_3 / Q_0
0.5
0
-0.5
43800
43900
tωp
(d) C_1 - J, I / I_c=0.556
Q_3 / Q_0
0.5
0
-0.5
60000
60100
60200
tωp

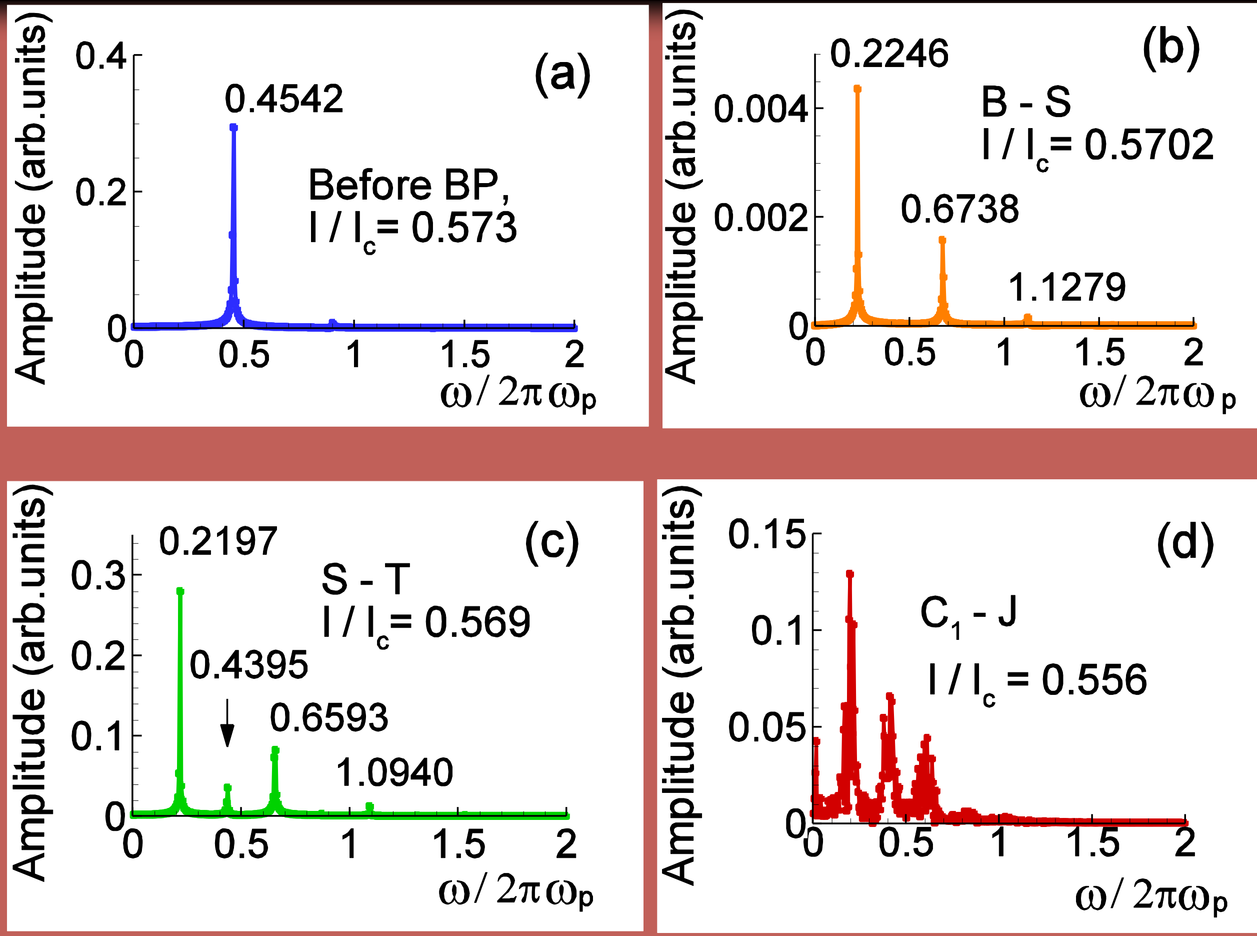

Before the BP at I/I_c=0.573 the Josephson frequency ω_J=0.4542*$2\pi\omega_P$ =2.8538ω_p

- In the B-S region
  ω=0.2246*$2\pi\omega_p$=1.4112ω_p corresponding to the LPW frequency ω_{LPW}
  ω=0.6738*$2\pi\omega_p$=4.2336 corresponding to sum of the Josephson and LPW frequencies $\omega_J+\omega_{LPW}$

- The S-T part shows the additional peak 0.4395*$2\pi\omega_p$= 2.7615ω_p, which value approximately equal to $2\omega_{LPW}$.

Temperature dependence of the breakpoint current

Temperature dependence 1

- In the simple parallel resistance model a single junction resistivity $\rho_J(T)$ at subgap voltage region is given by
- $\rho_J^{-1}(T)=\rho_{sg}^{-1}+\rho_C^{-1}(T)$
- where ρ_{sg} is the temperature independent tunnel resistivity of the junction, and
- $\rho_C(T)= a \exp (b/T)+cT+d$ is the empirical Heine formula of the c-axis resistivity with a,b,c,d as fitting parameters.

Temperature dependence 2

Estimating the tunnel resistivity by $\rho_{sg} = \Delta(0)S/eDI_c(0)$, the energy gap Δ from the expression $2\Delta(0)/kT_c = 6$

$$R_J = \frac{\rho_{sg}\rho_c}{(\rho_{sg}+\rho_c)}\frac{D}{S}$$

$$I_c = \frac{\pi\Delta(T)}{2eR(T)} tanh \frac{\Delta(T)}{2T}$$

$$I_c(T) = I_c(0)\sqrt{\cos\frac{\pi}{2}(\frac{T}{T_c})^2}\tanh(0.88\sqrt{\cos\frac{\pi}{2}(\frac{T}{T_c})^2}\frac{T_c}{T})$$

$$C_J = \varepsilon_r\varepsilon_0 S/D$$

$$\beta^2 = 1/\beta_c = \hbar/2eC_J R_N^2 I_C$$

- In our simulations we chose $S=2.32*10^{-10}$m for the area, T_c=90K for the critical temperature, $j_c(0)=9*10^6$ A/m^2 for the density of critical current at T=0.
- The fitting parameters were chosen as $a=6*10^{-4}\Omega$ m, b=273K, $c=24*10^{-6}\Omega$ m/K, $d=1.23*10^{-2}\Omega$ m.

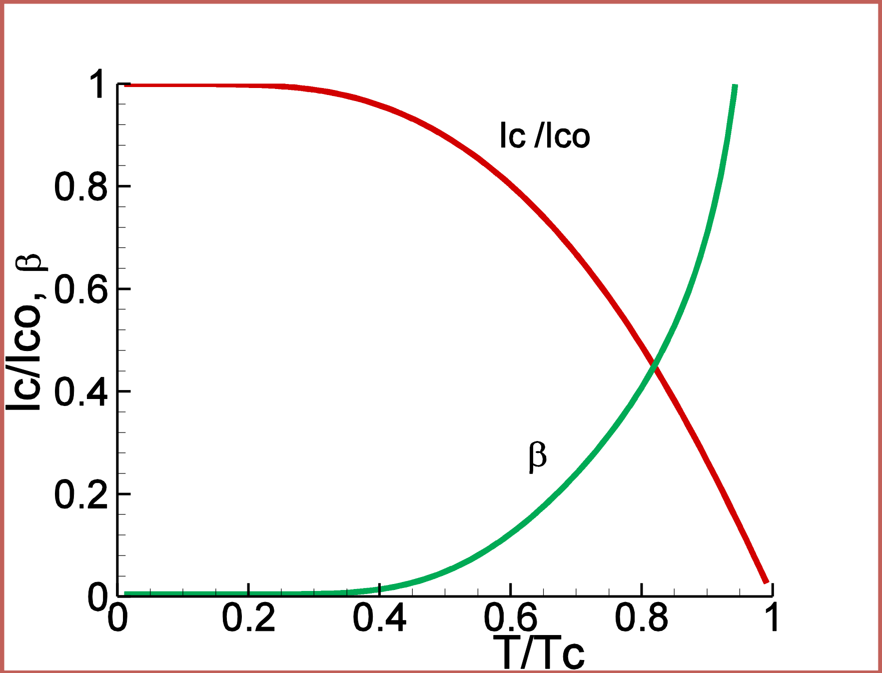
1
0.8
0.6
0.4
0.2
0
0
0.2
0.4
0.6
0.8
1
Ic /Ico
β
Ic/Ico, β
T/Tc

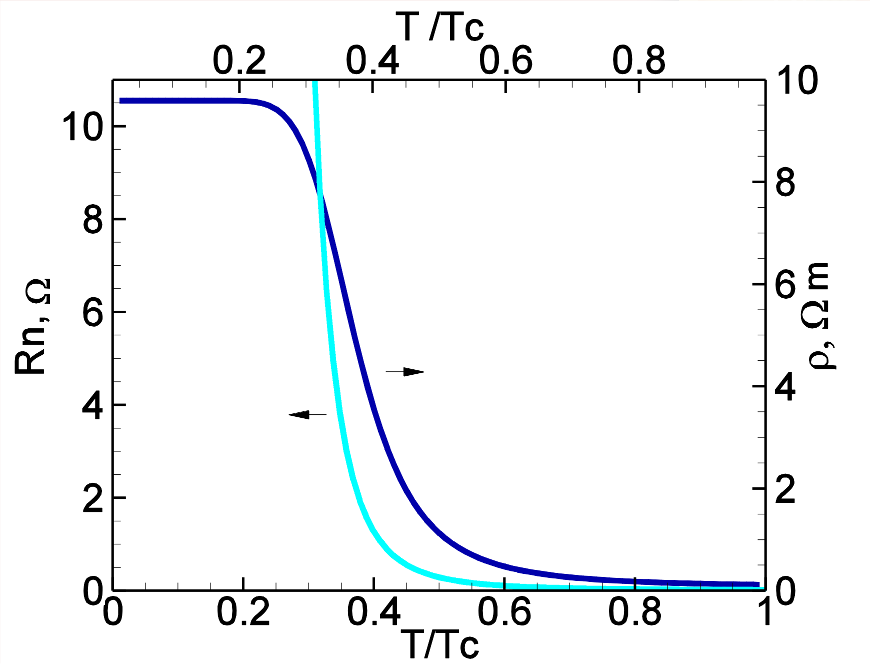
T /Tc
0.2
0.4
0.6
0.8
10
8
6
4
2
0
Rn, Ω
ρ, Ω m
0
0.2
0.4
0.6
0.8
1
T/Tc

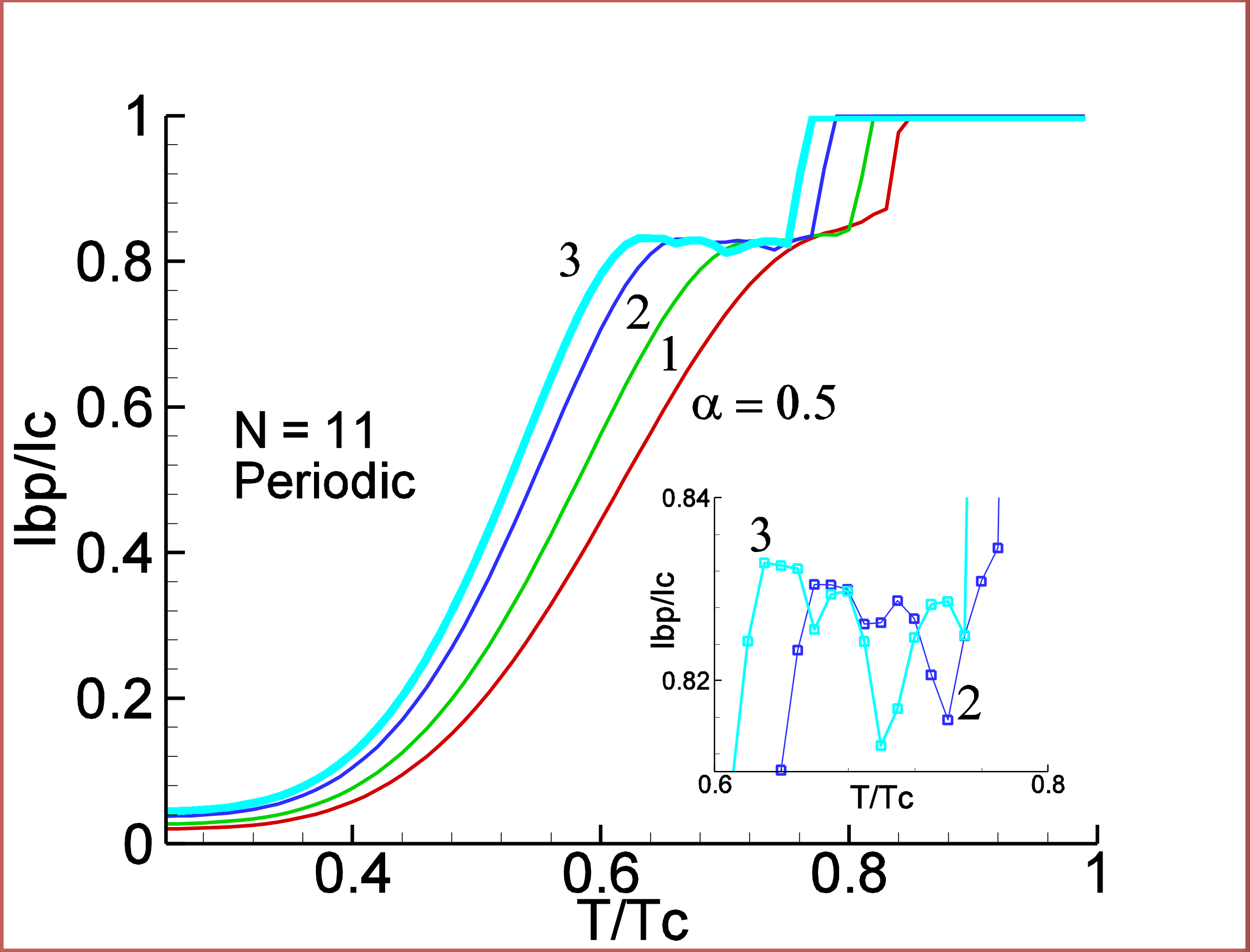

1
0.8
0.6
0.4
0.2
0
Ibp/Ic
0.4
0.6
0.8
1
T/Tc
N = 11
Periodic
3
2
1
α = 0.5
0.84
0.82
Ibp/Ic
0.6
0.8
T/Tc
3
2

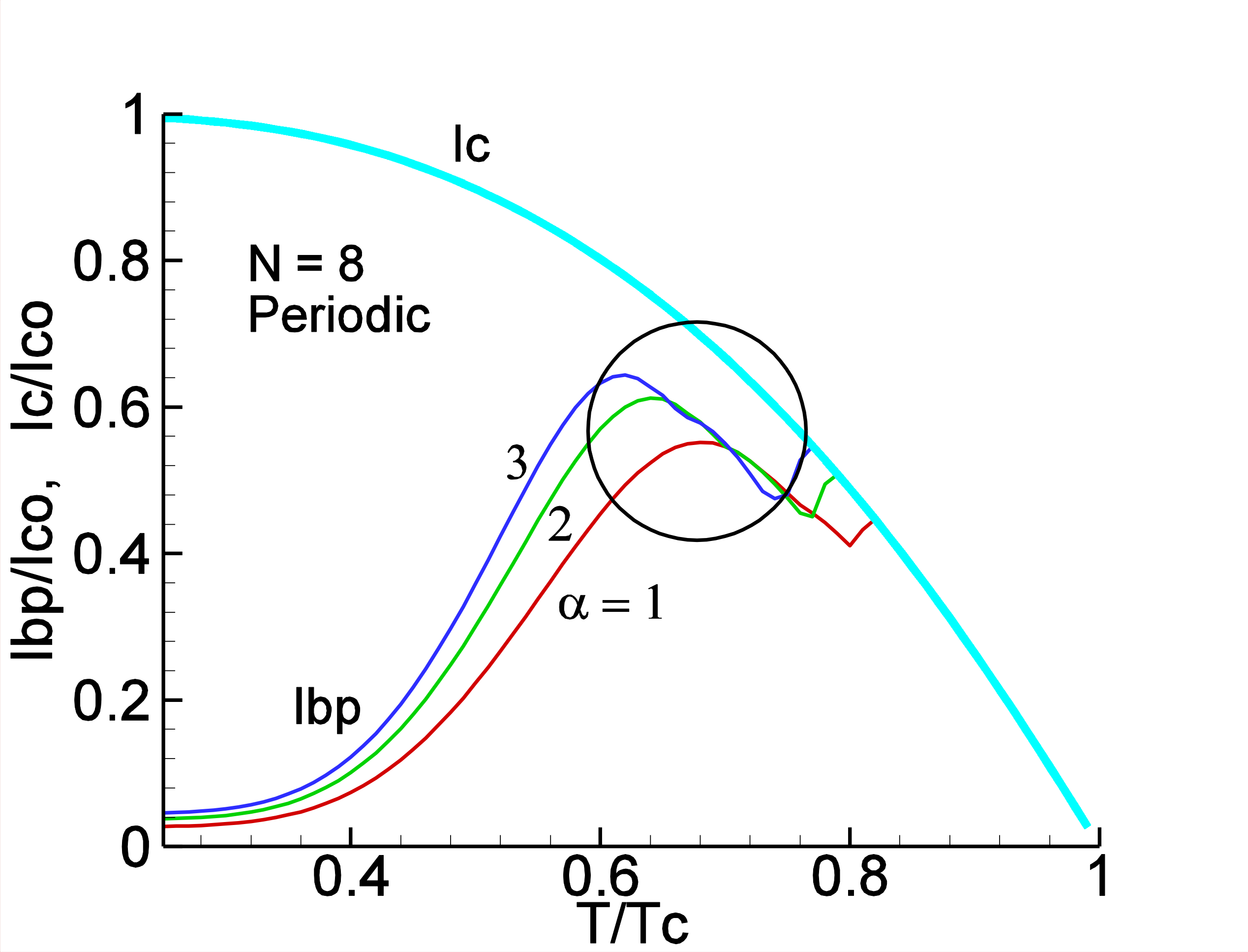
Ic
N = 8
Periodic
3
2
α = 1
Ibp
Ibp/Ico,   Ic/Ico
T/Tc
1
0.8
0.6
0.4
0.2
0
0.4
0.6
0.8
1

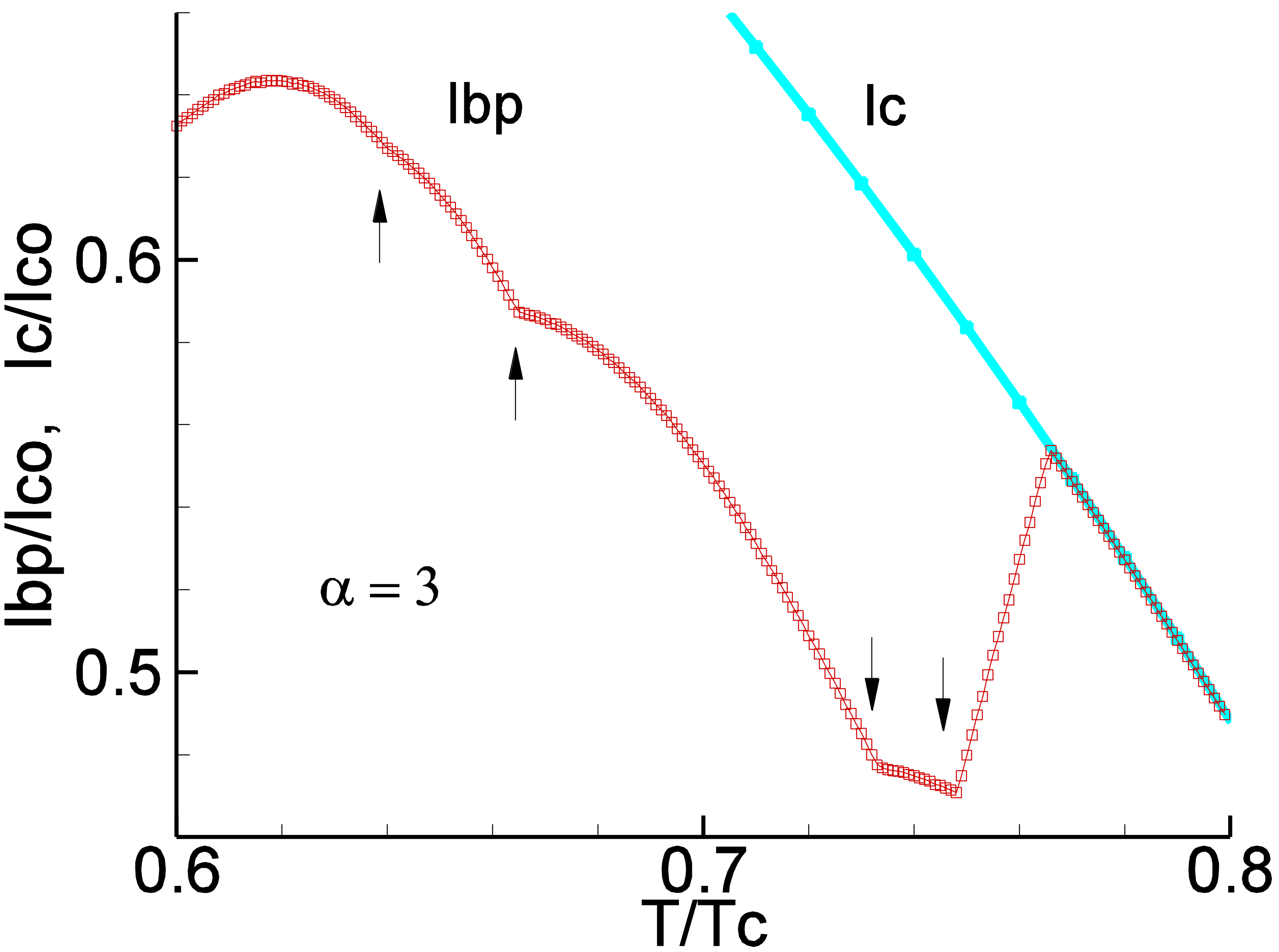
Ibp
Ic
α = 3
0.6
0.5
0.6
0.7
0.8
Ibp/Ico, Ic/Ico
T/Tc

Thank

you

for

your

attention!

Mechanical analog of a Josephson junction: driven underdamped pendulum

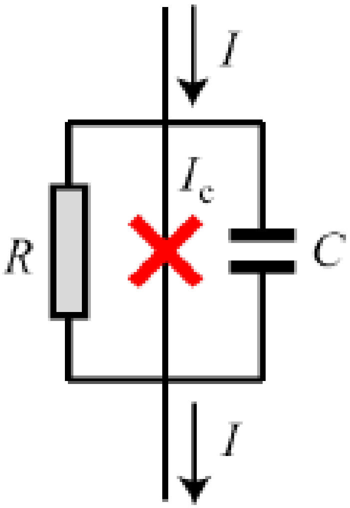

$$I = I_c \sin\varphi + \frac{V}{R} + C\frac{\mathrm{d}V}{\mathrm{d}t}$$

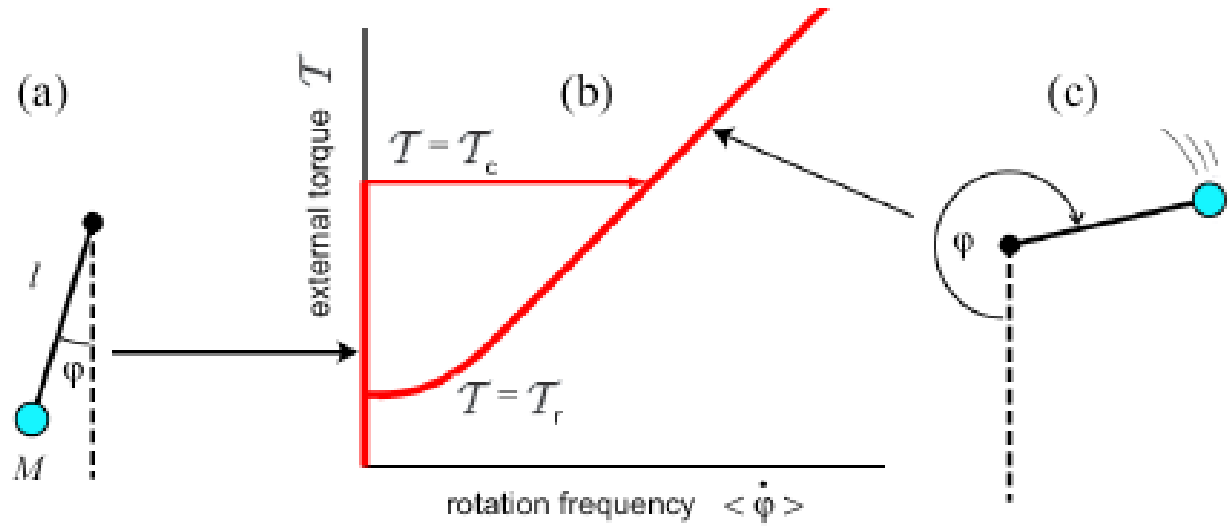

$$\Theta\ddot{\varphi} + \zeta\dot{\varphi} + Mgl\sin\varphi = \mathcal{T}$$

Mapping between Josephson junction and mechanical pendulum

Josephson junction	mechanical pendulum
phase difference φ	angle from vertical φ
voltage $V = \Phi_0 \dot{\varphi}/(2\pi)$	angular velocity $\dot{\varphi}$
critical current I_c	restoring constant Mgl
conductance R^{-1}	damping coefficient ζ
capacitance C	moment of inertia Ml^2
bias current I	external torque T
Josephson plasma frequency f_p	oscillation frequency $f_0 = \sqrt{g/l}/(2\pi)$

Один контакт

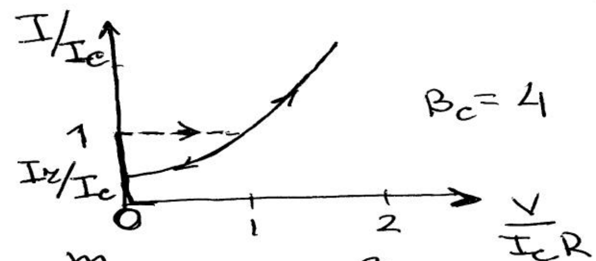

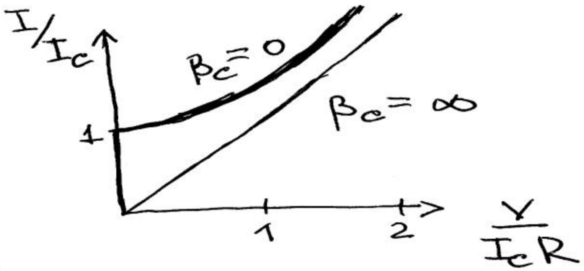

$$\overbrace{\left(\frac{\hbar}{2e}\right)^2 C}^{m}\ddot{\varphi} + \overbrace{\left(\frac{\hbar}{2e}\right)^2 R^{-1}}^{\eta}\dot{\varphi} + \overbrace{E_J}^{E_J(1-\cos\varphi)}\sin\varphi = \overbrace{E_J\frac{I}{I_c}}^{F} \qquad \frac{mv^2}{2} = \frac{CV^2}{2}$$

J - момент инерции

η - вязкость

$mg\ell$ - max. грав. момент

вращ. момент

$$\omega_p = \left(\frac{E_J}{J}\right)^{1/2} \text{ - плазм. частота}$$

$$E = E_J(1-\cos\varphi) - \frac{\Phi_0}{2\pi} I\varphi$$

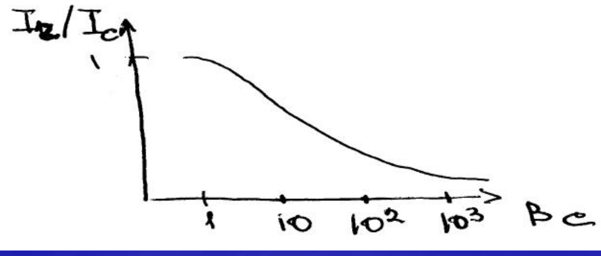

$$\beta_c = \left(\frac{2e}{\hbar}\right) I_c C R^2$$

$$\beta^2 = \frac{1}{\beta_c}$$